Wave impacts on a vertical breakwater

Graduation report
Januari 1999

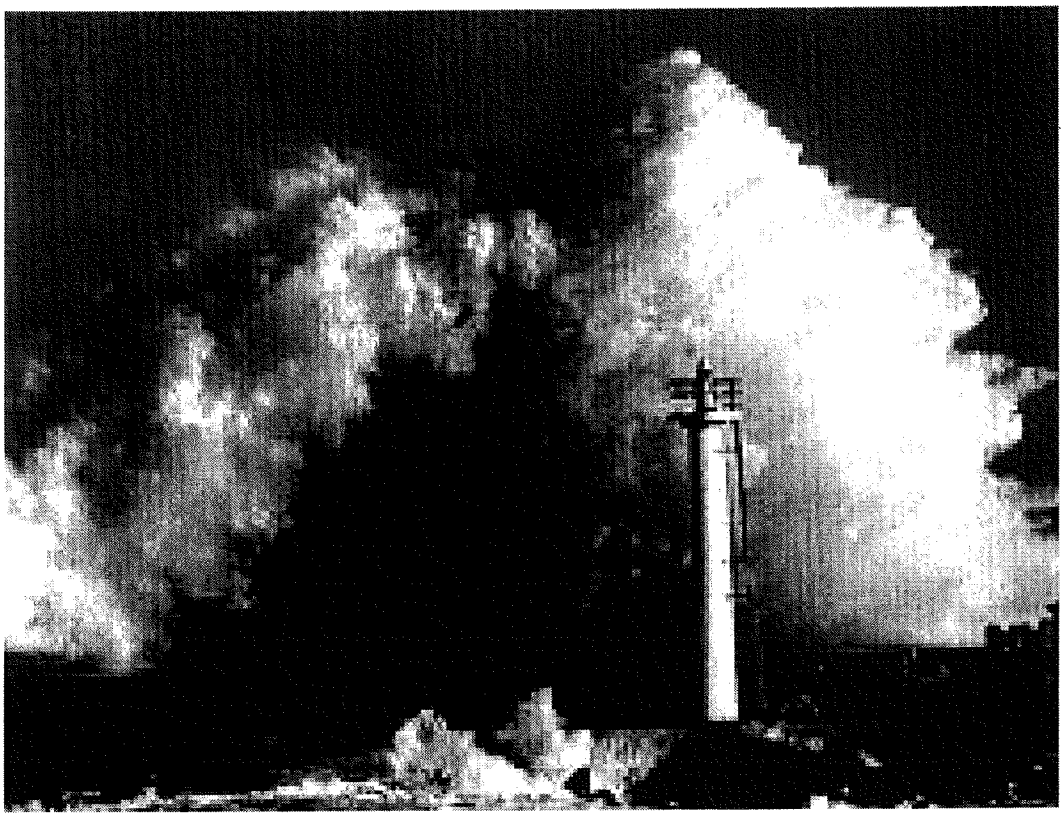

T.M.G. Schaap

Under supervision of :

Prof. drs ir J.K. Vrijling
ir E.C. Klaver
ir H.G. Voortman

Preface

This is the final report of the graduation project of T.M.G. Schaap. Writing this Master's thesis has been a part of my study Civil Engineering at the Delft University of Technology, Hydraulics and Geotechnical Engineering Division of the Hydraulic Engineering Group.

I would like to thank the chairman of my graduation committee, prof. drs ir J.K. Vrijling, ir E.C. Klaver and ir H.G. Voortman for their support and time during my graduation.

I hope you will enjoy reading this report.

Thomas Schaap

Summary

Since waves have enormous power the design of structures to withstand this power is not easy. The history of breakwaters is one of many failures and damages. This has lead to continuously improving technology in marine construction. Over the years men made it possible to construct breakwaters with high stability against waves.
The vertical breakwater is an ideal solution in deep water and in areas where the use of rubble stones is expensive or environmentally less acceptable.

Furthermore a vertical breakwater with smooth vertical walls can be exposed to high wave loads, such as impulsive wave impacts. These impacts are characterised by very high pressure and a short duration time. It is believed that these impacts could well be essential to the failure of vertical breakwaters.
The duration time of the wave impact is essential for the (dynamic) response of the caisson. For example if the wave impact duration is about the eigenfrequency of the vertical breakwater the response will reach a maximum, and the vertical breakwater could collapse.

The objective of this graduation report is to investigate the assumption that wave impact is important with regard to failure of vertical breakwaters. Research has been carried out to investigate the time impact duration for vertical breakwaters and an analogy has been made of wave impacts with impulsive wave load on ships.
Also, in order to investigate the (dynamic) response of vertical breakwater a computer model has been designed. With this model the response to the wave impact loads upon the Genoa Voltri breakwater can be estimated.

The results of this graduation study is that wave impact do occur, but that the impact duration is much shorter than assumed in the past. The impact forces during these short duration result in little response of the vertical breakwater, since the impact duration is not in the range of the eigenfrequency of the vertical breakwater. It can therefore be concluded that wave impacts are not important for the stability of the Genoa Voltri breakwater.

Contents

List of Tables

List of Figures

List of Symbols

Symbol	Unit	Description
L	m	Length (meter)
M	kg	Mass (kilgram)
T	s	Time (seconds)
a	rad	Angle (radial)
P	Pa	Pressure (pascal)
F	N	Force (newton)
α	-	proportionally constants [Tanizawa & Yue]
a	L	vertical distance COG to bottom (i.e. $\frac{1}{2}\ h_c$)
α^*	-	the largest of α_1 and α_2(Goda et al)
$\alpha,\ \delta$	-	dimensionless constants (Goda formulae)
B	L	width of the foundation
B_b	L	berm length
B_{BH}	L	length of soil pressure (Brinch Hansen)
B_c	L	width of the caisson
B_{eff}	L	effective width of the foundation (caisson)
c	-	proportionally constants [Tanizawa & Yue]
c	P	cohesion of soil
C_{mk}	-	impact coefficient for conversion to SI units(C_{mk} =*202*)
D	L	waterdepth at a wavelength from the wall
d	L	waterdepth from top layer rubble mound foundation
d	L	waterdepth in front of the wall
D	-	internal damping parameter
d_ϕ	F×L×T	rotational damping constant
D_ϕ	-	geometrical rotational damping parameter
d_x	F×T	horizontal damping constant
D_x	-	geometrical horizontal damping parameter
e	L	eccentricity of the vertical force
F	M×L/T^2	force
ϕ	a	internal friction of the soil
$F(t)$	F	horizontal wave load
g	L/T^2	gravitational acceleration
γ	-	specific heat ratio (1.405 adiabatic, 1.0 isothermic)
G	P	shear modulus of the soil
γ_s	F×L^3	weight of soil (kN/m^3)
h	L	water depth
h'	L	waterdepth bottom foundation of the vertical breakwater
$H_{0.1\%}$	L	wave height exceeded by 0.1% of waves
$H_{1\%}$	L	wave height exceeded by 1% of waves
h_b	L	waterdepth at $5\times H_s$ from the wall (Goda formulae)
h_b	L	height of the berm
H_b	L	breaker height
h_c	L	height of the caisson
H_i	L	wave height (incoming wave)
H_{max}	L	design wave height, corresponding to the 0.1% exceedence value for Rayleigh distribution of waves (roughly $1.8\times H_s$)
h_s	L	water depth in front of sill
h_s	L	water depth in front of the structure

H_{so}	L	deep water significant wave height
i_c	-	inclination factors, reduction related to the direction of the load
i_γ	-	inclination factors, reduction related to the direction of the load
i_q	-	inclination factors, reduction related to the direction of the load
k	-	wave number ($=\frac{2\pi}{L_i}$)
k	-	constant for impulsive wave formulae (KO&K)
K_ϕ	-	parameter for determining rotational spring element
k_r	-	reflection doefficient
k_x	F/L	horizontal spring constant
K_x	-	parameter for determining horizontal spring element
L	L	wave length
L	L	length of the foundation
L_b	L	wavelength at peak period of waves
L_c	L	length of the caisson
L_{eff}	L	effective length of the foundation (caisson)
L_o	L	wavelength at deep water
L_p	L	wavelength at peak period of waves
m	-	slope angle
M	M	mass breakwater
$M(t)$	F×L	rotational wave load
$m_{hyd,\ hor}$	M	the hydrodynamic mass for horizontal oscillations
M_{max}	F×L	maximum rotational force
M_{tot}	M	total mass of caisson (with added masses)
ν	-	Poisson's ratio (0.2-0.4)
N_c	-	dimensionless constant
N_γ	-	dimensionless constant
N_q	-	dimensionless constant
p	P	maximum bearing pressure of the foundation
p_{atm}	P	atmospheric pressure
p_{max}	P	maximum soil pressure (Brinch Hansen)
p_{peak}	P	impact pressure
Θ	$M\times L_2$	inertia of breakwater
q	P	pressure next to the foundation
Θ_{tot}	$M\times L^2$	total inertia of caisson
R_c	L	crest freeboard
r_ϕ	F×L	rotational spring constant
ρ_s	M/L^3	mass density of the soil
ρ_w	M/L^3	density water
s	-	wave steepness
s_c	-	reduction factors related of the shape of the foundation
s_γ	-	reduction factors related of the shape of the foundation
s_q	-	reduction factors related of the shape of the foundation
$T_{½}$	T	impact duration at ½ peak pressure value (Naval Architecture)
T_p	T	peak wave period
T_{peak}	T	rise time impact duration (Naval Architecture)
ξ	-	Iribarren parameter
ζw	L	Wave height amplitude ($½\times H$)

1. Introduction

In the last decade the need for land recalmation and harbour expansion has increased. The construction of the airport at Singapore, Chek Lap Kok, the discussion about an airport in the North Sea and the discussion about expansion of the harbour of Rotterdam are only examples of this trend. And most reclamation projects are situated in deep waters. For example an airport in the North Sea would be in a water depth of approximately 20 m. At this depth the conventional methods are relative expensive. The vertical breakwaters could make a difference.

The history of breakwaters is one of much failures and damages. This has progressed construction technology in marine construction. Throughout the years man made it possible to construct breakwaters having high stability against waves.

Breakwaters and related marine structures can have several functions. They are primarily built to give protection against wave attack on:

1. Ship moorings and manoeuvring areas
2. Port facilities
3. Adjacent areas of land (coastal protection)

Breakwaters can also influence currents and tides to reduce the dredging costs of an entrance channel to a port or to reduce the currents to ensure safer navigation.

Breakwater can roughly be divided into two categories:
- rubble mound breakwaters
- vertical breakwaters

Rubble mound breakwaters
The rubble mound breakwater is constructed out of rubble stone - a natural material - of different gradation and different sizes (see figure 1-1). The smallest stones are used for the inner slopes and gradually - when moving towards the outer slope - the stones will become much larger in size and weight, and therefore they will be able to withstand the enormous power of the waves.
The rubble mound breakwater is usually the first and the most economical option to use if a breakwater is constructed in shallow water - i.e. water depths of approximately 10 meters. Rubble mound breakwaters use more material per cross section, but due to the simple construction method costs can be kept to a minimum.

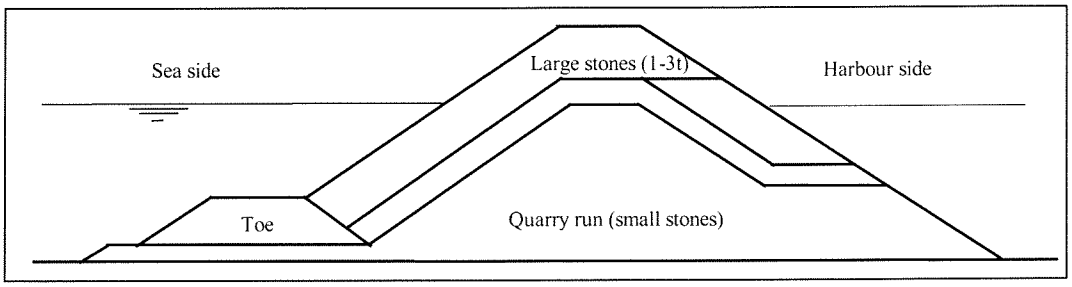

Figure 1-1 Cross-section of a rubble mound breakwater

Vertical breakwaters
Because of the increased draught of vessels and the expansion of the shore and harbours the breakwater has to fulfil its functions in deeper water. This yields to different approaches for

the breakwaters. The vertical and composite type are relatively expensive in construction costs, but with the increasing depth the rubble mound breakwater is becoming more expensive due to increasing material costs. Therefore the vertical breakwater can compete economically with the rubble mound type.
In figure 1-2 a few different types of vertical breakwaters are shown.

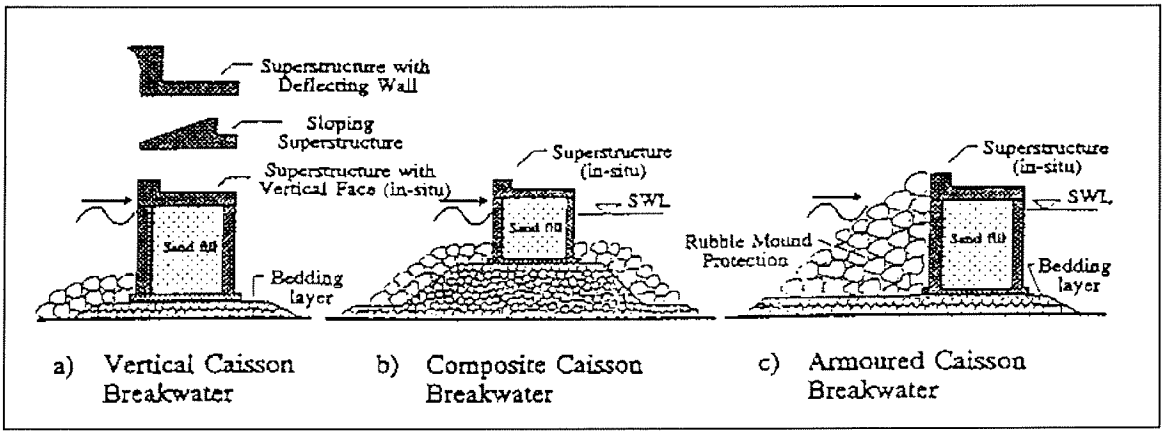

Figure 1-2 Examples of vertical breakwaters [Oumeraci 1994]

The original concept of the vertical breakwater is to reflect waves, while that for rubble mound breakwaters is to break them. This is visualised in Figure 1-2 vertical breakwater (a) and composite caisson breakwater (b).
To reduce reflection and the wave force on the construction, heavy concrete or rubble units are placed in front of the caisson breakwater. The units will dissipate the wave energy and thus reduce the wave impact on the structure. This type of breakwater is called the armoured caisson breakwater (c). The armour layer in front of the caisson often use specially shape designed concrete units such as tetrapods.

To avoid using rather expensive concrete blocks while reducing the wave impact on the caisson, special breakwaters are designed, such as the perforated wall breakwater. The wall of the caisson will allow the wave to enter a front chamber in which the wave energy is dissipated, and thus the wave action will be reduced.

The advantages of vertical breakwater are :

1. The breakwaters occupy less seabed, hence a reduction of environmental impact and area usage
2. The construction of caissons can take place elsewhere, which results in less environmental disturbance in the area
3. The actual construction at the site takes less time, which result in less disturbance to the area (for example harbour) activities
4. Reduction of material quantities (stones), preferred when acquiring quarry stones is economical or environmentally criticised
5. Saver and closer navigation possible due to better visibility of the breakwater

Vertical breakwaters are becoming more popular because of better design methods. In the past several damages and failures prevented the construction of vertical breakwaters in many countries. A number of important (scientific) developments in the last decades the vertical breakwater becomes more interesting. Not in the least on account of off-shore land reclamation in deep waters.

2. Scope of graduation project

Wave loads on vertical breakwater have been a subject of research for quite some time. A wave breaking onto a vertical wall, which brings the water mass to a sudden and complete stop, could make the caisson respond in an on-safe manner, and may even result in failure. The importance of these wave impact loads is often exaggerated or diminished. The truth is still to be found.

2.1 Problem description

Through recent research of wave impacts it is believed that wave impacts are important to the overall stability of vertical breakwaters. The overall stability is constituted by the wave load - i.e. wave load formula - and the (dynamic) response of the breakwater to the wave load.

Throughout the years formulae have been derived in order to estimate the wave impact forces upon the vertical breakwater. The most recent wave load formulae are based upon model tests, although it is not clear if model tests provide enough information to be able to draw final conclusions, such as an impact load formulae. The problems involve upscaling of impact pressure, force and impact time duration.

On the other hand, the exact influence of impact wave loads on vertical breakwaters has still to be proved. The response of the breakwater to impact wave forces is unknown, and therefore the influence of the impact wave forces to the overall stability is also unknown.

2.2 Objective of graduation project

The objective of this graduation project is:

"To gain more insight in the time duration of wave impacts and investigate whether these wave impacts have a significant influence on the overall stability of the vertical breakwater."

2.3 Method of approach

The objective of this report will be achieved on the basis of a true case, the Genoa Voltri breakwater. The calculations made are specific for this case. More detailed information about the Genoa Voltri breakwater can be found in the annexes.

The objective will be achieved in three stages.

1. A study of current used formulae
2. Investigation of the time duration of wave impacts on a vertical breakwater
3. Calculation of the response of the Genoa Voltri breakwater to wave impacts

2.4 Framework

This graduation report has been written as a part of the study Civil Engineering at the Delft University of Technology. The subject, *"wave impacts on a vertical breakwater"*, fits within the framework of an European research programme Marine Science and Technology (MAST). This research programme is sponsored by the European Union.

3. Waves

In this chapter the origin, definition and the classification of waves are described. Waves can be generated by different forces, such as wind blowing along the water surface, gravitational forces, induced by the moon and sun and even by earthquakes. Every force will generate its own type of wave.
When a wave reaches the shore, it will be stopped by a nature element, such as a beach, or an artificial object, such as a (vertical) breakwater. The wave will apply a force onto the structure. In this graduation project wind waves are considered to be generating the whole of wave loads.

3.1 Different types of waves

The movement of waves in water with a free fluid surface are dominated by gravity. To create these waves energy is added to the water mass. In nature wind supplies this energy, but also waves induced by ships can supply this energy. When the waves are created, the wave crests and wave troughs have higher respectively lower potential energy. Within the area of high and low potential energy a continuous exchange of energy takes place by transforming potential energy into kinetic energy.

A wave field or wave group looks like a complete mess of waves of different shapes and directions. Still we can define specific constants and formulate a (approximate) mathematical model to describe the wave field. Individual waves can be characterised by period (T), wave height (H), wave propagating velocity (c) and wave direction or angle of attack in case of wave impacts on vertical breakwaters. When looking at the wave period as classifying measure a rough classification of waves can be made.

Wind waves
Wind waves are created by the wind striking along the water surface. Wind-strength, duration, fetch and (the variation of) the wind direction dominate the wind waves. The period of the wind wave at sea is usually 10 s, inshore the period is not higher than 3 to 5 s due to a short fetch.

Swell
Swell are waves with a length from 30 to over 500 times the wave height. They are generated by a distant storm and they may travel over hundreds of kilometres of calm seas before reaching the shore. Under these conditions waves decay, hence short and steep waves become long and low waves. This is caused by frequency dispersion and direction dispersion. The wave period is about 30 seconds.

Seiches
Seiches are oscillations caused by some exciting mechanism and trapped by a susceptible bathmetry, e.g. a harbour basin. Seiches are water surface variations on shore with relatively short duration. This can be taken for long waves or temporally water level variations. The exciting mechanisms can be local meteorological phenomena and gusts. Period ranges from 2 - 40 minutes.

Tides
Tides are created by the gravitational force of the moon and the sun. These tidal motions of water mass can be characterised as a long period wave motion. The period varies from ½ to 1 days.

Storm surges
Local depressions cause a corresponding rise of Mean Water Level. Due to the dynamic aspects the water level can be amplified significantly. The period of these waves may be in the order of days

Tsunamis
Tsunamis are seismically induced waves, characterised by wave periods that are in the order of minutes to hours. They occur in seismic areas. They often originate from earthquakes, where the water depths are 1000 meters with no noticeable wave height. When reaching the shore the height may increase considerably. The wave period differ from 10 to 100 minutes.

3.2 Wave breaking

Wave breaking occurs due to two criteria; depth and steepness, each limiting the maximum wave height. While depth induced breaking is usually determining factor in shallow water, the limit of steepness (s), should still be considered.
The steepness of a wave is defined as wave height divided by wave length ($s=H/L$).

3.2.1 Breaking of single wave

Breaking due to exceedance of steepness criterion is the main limiting factor in deep water. The steepness criterion is influenced by water depth and for regular waves where the water depth is not deep given as [Miche 1944],

$$H_b = 0.14 \cdot L_b \tanh\left(2\pi \cdot \frac{h}{L_b}\right) \qquad 3\text{-}1$$

with,

H_b = breaking wave height
L_b = breaking wave length
h = water depth

3.2.2 Breaking of reflected wave

The breaking of a wave near an obstruction can be influenced by the reflectionof waves of that obstruction. Calabrese & Allsop have written a paper which describes the derivation of an estimate for the wave breaking near an obstruction - i.e. vertical of composite breakwater. They assume a Raleigh distribution of the waves near the breakwater. The procedure consists of 6 steps and is written below,

1. Identify the geometry and wave parameters
h_s = water depth in front of the structure
B_b, h_b and α = width, height and slope of front face of the berm
d = depth of water over the berm in design cases

2. Derive the effective berm width (B_{eq})

$$B_{eq} = B_b + \left(\frac{h_b}{2 \cdot \tan\alpha}\right) \qquad 3\text{-}2$$

3. Identify the design wave conditions given by H_{si} and T_p, taking in account the effect on local wave height caused by refraction and shoaling. Derive peak period wave length L_{pi} at the local water depth h_s, using an explicit approximation, such as below.

$$L_{pi} = \left(gT_p^2/2\pi\right)\tanh\left(2\pi h_s / L_{pi}\right) \qquad 3\text{-}3$$

4. Calculate an estimate of the maximum wave height, $H_{99.6\%}$

$$H_{99.6\%} = \left(0.1025 + 0.0217C^*\right)L_{pi}\tanh\left(2\pi\xi h_s / L_{pi}\right) \qquad 3\text{-}4$$

with,

$$C^* = \left(1-k_r\right)/\left(1+k_r\right) \qquad 3\text{-}5$$

$$\xi = 0.0076\left(B_{eq}/d\right)^2 - 0.1402\left(B_{eq}/d\right) + 1 \qquad 3\text{-}6$$

Values of k_r (reflection coefficient) may be estimated for the particular structure combination:

$k_r = 0.95$	= Simple vertical walls and small mounds, high crest
$k_r = 0.8+R_c/H_{si}$	= Low crests
$k_r = 0.5 - 0.7$	= Composite walls, large mounds, heavy breaking

5. Estimate the proportion of impacts $P_{i\%}$.

$$P_{i\%} = \exp\left[-2\left(H_{99.6\%}/H_{si}\right)^2\right] \times 100\% \qquad 3\text{-}7$$

6. Prediction of breaking waves and impacts

For $P_{i\%}<2\%$	little breaking, wave loads are primarily quasi static
For $2<P_{i\%}<10\%$	Breaking of waves give impacts
For $P_{i\%}>10\%$	Heavy breaking and waves may give impacts or broken loads

3.2.3 Different shapes of breaking waves

For wave running up a slope, there is a method to define the different types of wave breaking.

$$\xi = \frac{m}{\sqrt{s}} \qquad 3\text{-}8$$

with,

m	= slope angle
s	= wave steepness (H/L)

The different types of wave are defined by the Iribarren number as can be seen in Figure 3-1.

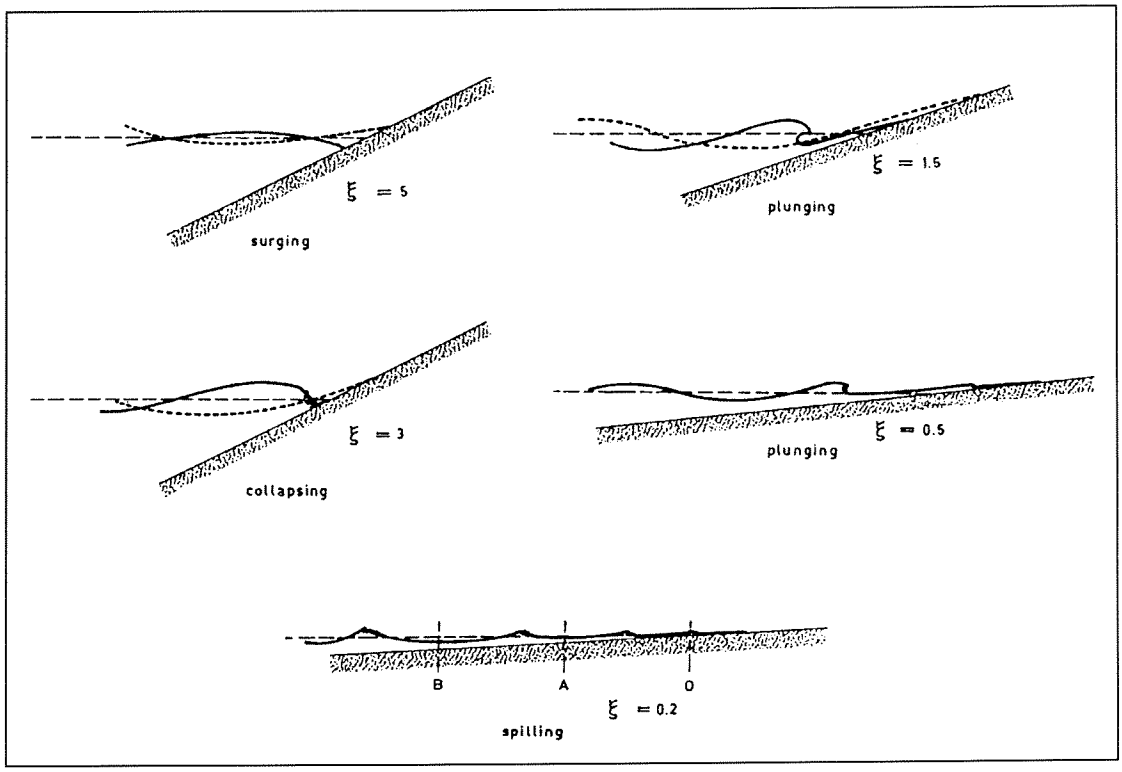

Figure 3-1 Different types of breaking wave [Battjes 1974]

3.3 Extreme wave heights in shallow water

At the front face of the Genoa Voltri breakwater the significant wave height is influenced by shoaling, refraction and maybe even breaking. The significant wave height at sea - off shore - have to be conversed to the wave climate we should expect in nature. Practical relations for extreme wave heights in shallow water are given by Stive (1986). The relations are based upon prototype and laboratory data, and give $H_{1\%}$ and $H_{0.1\%}$ as a function of H_s and local depth h.

$$H_{1\%} = 1.517 \cdot H_s \cdot \frac{1}{\left(1 + H_s/h\right)^{1/3}} \qquad 3\text{-}9$$

$$H_{0.1\%} = 1.859 \cdot H_s \cdot \frac{1}{\left(1 + H_s/h\right)^{1/2}} \qquad 3\text{-}10$$

The coefficients 1.517 and 1.859 represent conversion coefficients to the significant wave height which follow the Raleigh distribution, while the remaining parts reflect the depth limitation.

4. Wave loads

When waves encounter a construction such as a vertical breakwater the wave will be reflected and thus will generate a force to the construction. This load will be varying in time and in force. The magnitude of these loads depends on wave height, wave period, propagation velocity and angle of wave attack onto the structure. The shape of the structure surface and bottom geometry influence the wave load as well.

It can be said that wind waves supply the most important part of the wave loads. However when considering a earthquake-harzard area other waves have to be taken into account with respect to the wave loads. In this study however, it is assumed that wind waves are providing the whole of the wave loads.

In this chapter the main wave load formulae are described, covering the quasi-static wave loads and the impulsive wave loads.
At the end of this chapter the outcome of the wave impact formulae will be evaluated with regard to the Genoa Voltri breakwater and its hydraulic conditions.

4.1 Quasi-static wave load

Quasi-static wave loads change relatively slowly, and vary in the same period as the waves do. Traditionally quasi-static loads were used in the design of the vertical breakwaters by means of a quasi static problem.
The quasi-static wave loads can be divided in two phases :

1. The wave crest encroaches the structure applying a hydrostatic pressure difference. The vertical wall causes the wave surface to rise up the wall, increasing the pressure difference across the wall. The force can be easily determined by using simple methods.
2. The second case is the opposite of above. The wave level decreases (wave trough) leaving a negative force on the vertical wall. Prediction of the negative forces is as stated above.

The term quasi-static wave load suggests that the wave load is static. In nature the quasi-static wave load is a varying load, but the period is large enough (with respect to the eigenfrequency of the vertical breakwater) to assume that the non breaking wave load is quasi-static.

4.1.1 Linear theory

Non breaking wave loads on a vertical wall can be derived from the linear wave theory and its pressure distribution.

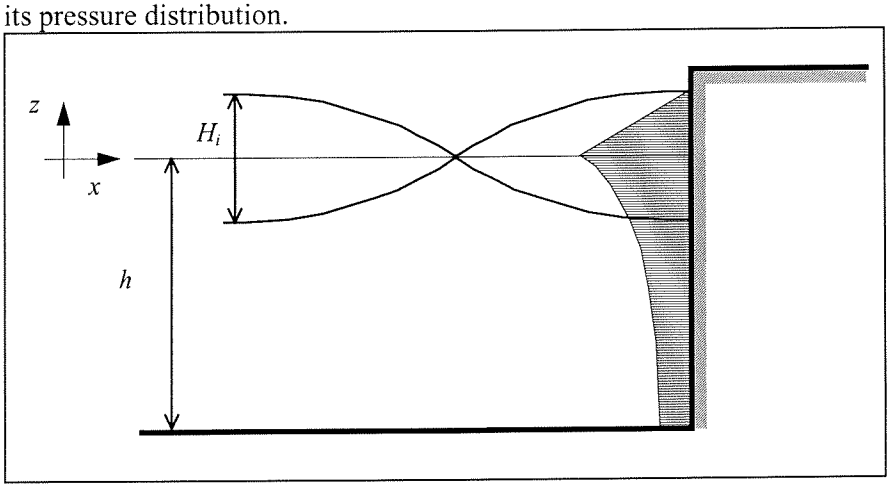

Figure 4-1 Linear wave theory

According to the linear wave theory with full reflection of the incoming wave the maximum pressure is,

$$p = \rho_w g H_i \frac{\cosh(k(h+z))}{\cosh(kh)} \qquad \text{for } -h < z < 0 \qquad 4\text{-}1$$

$$p = \left(1 - \frac{z}{H_i}\right)\rho_w g H_i \qquad \text{for } 0 < z < H_i \qquad 4\text{-}2$$

with,

H_i	=	wave height (incoming wave)
h	=	waterdepth
ρ_w	=	density of water
g	=	gravitational acceleration
k	=	wave number $(= \frac{2\pi}{L_i})$

The force per linear meter of the structure length results from integration to the waterdepth, assumed that $R_c > H_i$,

$$F = \int_{-h}^{0} \rho_w g H_i \frac{\cosh(k(h+z))}{\cosh(kh)} dz + \int_{0}^{H_i} \left(1 - \frac{z}{H_i}\right)\rho_w g H_i = \qquad 4\text{-}3$$

$$F = \rho_w g H_i \left(\frac{\sinh(kh)}{k\cosh(kh)} + \frac{H_i}{2}\right)$$

This formula will usually be replaced by the method of Sainflou. This method applies a wave theory of a higher order.

4.1.2 Method of Sainflou

In this model Sainflou assumes the second order wave theory of Stokes and full reflection of the waves, which have the form of a trochoid .

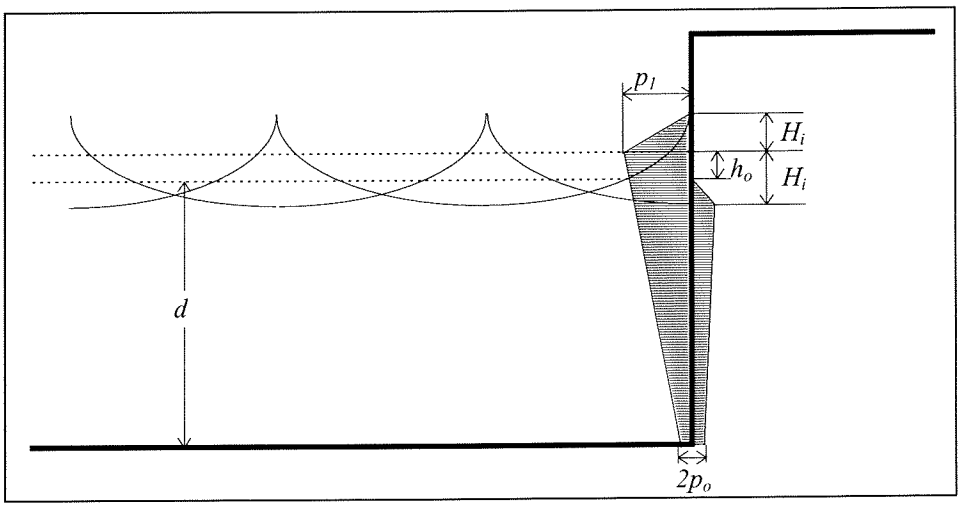

Figure 4-2 The model of Sainflou

In this case the still water level will increase with,

$$h_0 = \tfrac{1}{2} k H_i \coth(kd) \qquad 4\text{-}4$$

with,

h_0 = increase of the still water level
H_i = wave height incoming wave
k = wave number

The maximum pressure at the still water level is,

$$p_1 = \rho_w g H_i \qquad 4\text{-}5$$

and the pressure at the bottom of the structure,

$$p_0 = \frac{\rho_w g H_i}{\cosh(kd)} \qquad 4\text{-}6$$

The pressure distribution is assumed to be linear. For steep wave the method of Sainflou gives an overestimation of the pressure. According to an adjusting and higher wave theory Rundgren adjusted the formula of Sainflou.

4.1.3 The Goda formulae

The Goda formula is derived by Goda from theoretical and laboratory studies in order to establish a comprehensive formula to calculate the design wave forces. The Goda formula has been extensively used throughout the world. The advantage is that the formula can be employed for all wave conditions, i.e. both standing and breaking waves. The formula is based partially on non-linear wave theory and can present wave pressure characteristics by considering two pressure components. Therefore it is relatively easy to extend the Goda formula to apply it to other type of vertical structures.

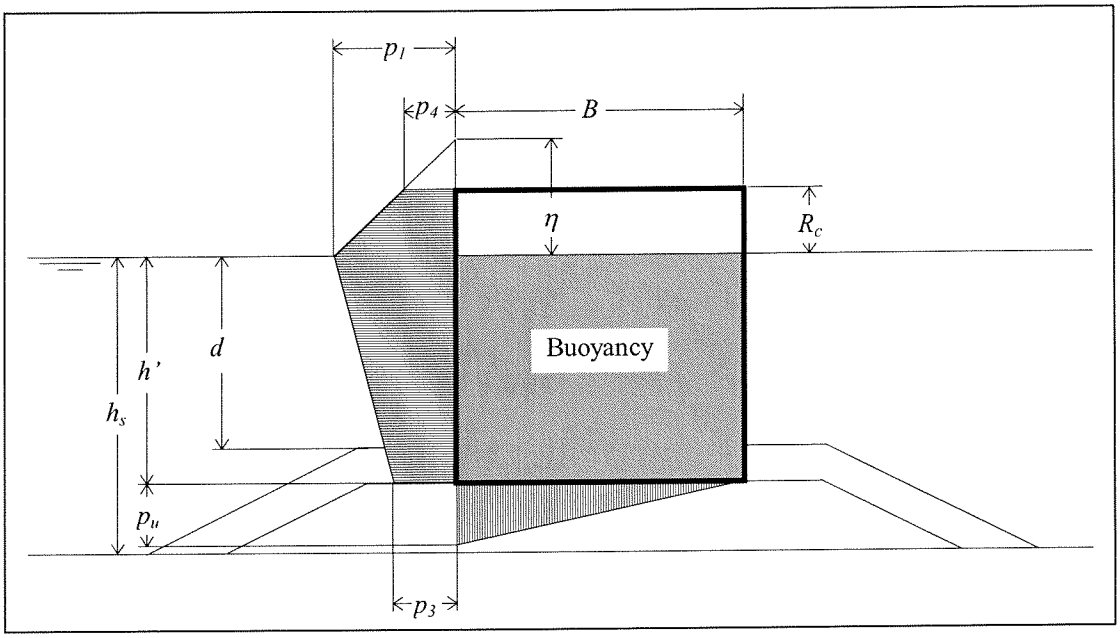

Figure 4-3 Model of non-breaking and breaking waves by Goda

The wave pressure along the vertical wall is assumed to have a trapezoidal distribution above and below the still water level. The uplift pressure has a triangular pressure distribution along the caisson bottom pointed upwards. The buoyancy is calculated according to the still water level.
Formulas,

$$\eta^* = 0.75 H_{\max} \qquad 4\text{-}7$$

$$p_1 = 0.5(\alpha_1 + \alpha_2)\rho_w g H_{\max} \qquad 4\text{-}8$$

$$p_3 = \alpha_3 p_1 \qquad 4\text{-}9$$

$$p_4 = \alpha_4 p_1 \qquad 4\text{-}10$$

$$p_u = 0.5\alpha_1\alpha_3\rho_w g H_{\max} \qquad 4\text{-}11$$

with pressure coefficients,

$$\alpha_1 = 0.6 + 0.5 \cdot \left(\frac{4\pi h_s / L}{\sinh(4\pi h_s / L)} \right)^2 \qquad 4\text{-}12$$

$$\alpha_2 = \min\left(\frac{(h_b - d)}{3h_b} \cdot \left(\frac{H_{\max}}{d} \right)^2, \frac{2d}{H_{\max}} \right) \qquad 4\text{-}13$$

$$\alpha_3 = 1 - (h'/h_s)\left(1 - \frac{1}{\cosh(2\pi h / L)} \right) \qquad 4\text{-}14$$

$$\alpha_4 = 1 - \frac{h_c^*}{\eta^*} \qquad 4\text{-}15$$

$$h_c^* = \min(\eta^*, R_c) \qquad 4\text{-}16$$

with,
h_b = waterdepth at $5 \times H_s$ from the wall

H_{max} = design wave height, corresponding to the 0.1% exceedence value for Rayleigh distribution of waves (roughly $1.8 \times H_s$)
L = wave length
h_s = water depth in front of sill
d = waterdepth from top layer foundation
h' = waterdepth bottom foundation of the vertical breakwater
R_c = crest freeboard

These are the Goda formulae for quasi-static wave loads.

4.2 *Impulsive wave loads*

Impulsive or wave impact forces are caused by wave breaking against the structure. Impact pressures are generally higher than quasi-static wave loads, but are of shorter duration. The difference with the quasi-static load is easily understood. When a dive into the water fails and a person's flat belly encounters the water, the force of the rather 'soft' water on the body is rather severe, and of short duration. A red and painful body is the result.

Modeling the impulsive wave load has found to be very difficult, resulting in a large number of different formulae, approaches and theories.
In general, the impulsive wave load is a wave which breakes just before it hits the construction. When breaking, the shape of the wave changes. When a breaking wave impinges on the construction the pressures - i.e. forces - exaggerated on the construction are higher and shorter in duration than the quasi-static wave loads.
The impact force is usually described by three features, the maximum impact force ($F_{h,max}$), the impact rise time (t_r) and the total impact duration (t_d). In figure 4-4 a scheme of the impulsive wave load is given, and a general description of the wave load.

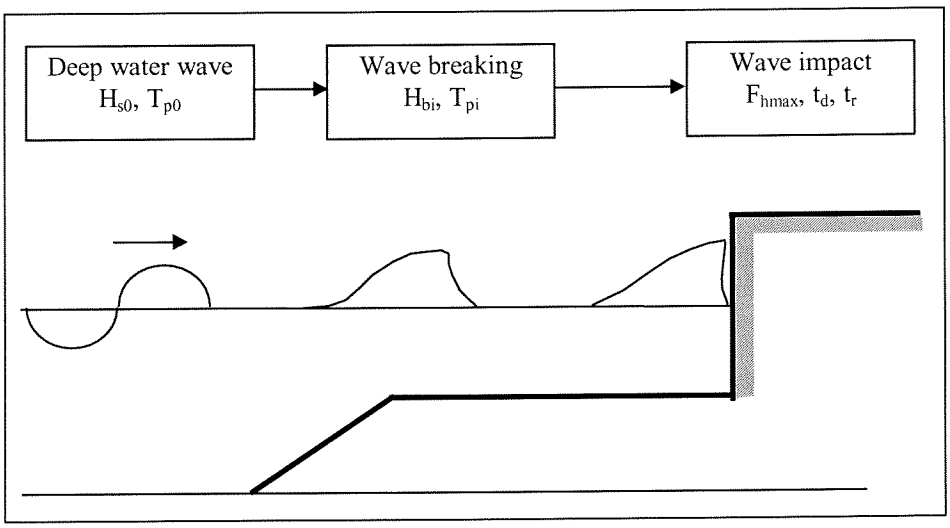

Figure 4-4 Scheme of impulsive wave load

The impulsive wave loads can be defined in three different types of wave impact. The differences are found to what extent the wave is broken or will break when encountering the structure.

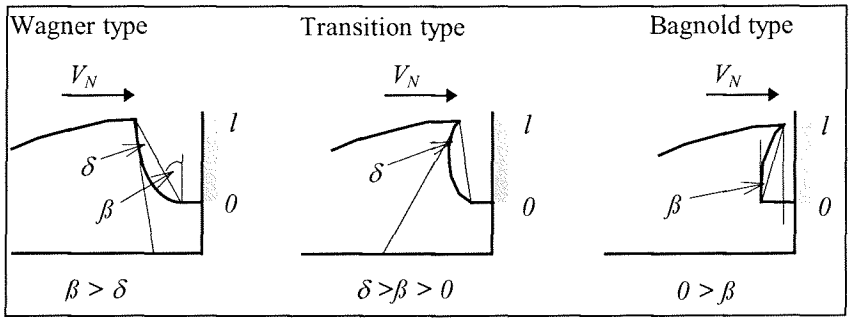

Figure 4-5 Three types of impulsive pressure [Takahashi]

Wagner type impact load
In this case the wave has not broken when it hits the structure. There will be no air trapped between the water surface and the vertical wall. The impact can be described as a sudden rise and exponential decay of pressure. Goda called this type of pressure "single peak pressure" and Lundgren, Horikawa, Noguchi and Kolkman & Jongeling called it "ventilated shock".

Bagnold type impact load
In this case the wave is broken when it hits the structure. There will be (some) air trapped between the water front and the structure. The enclosed air extensively influences the magnitude, duration and the oscillation of the impact pressure and therefore the impact load onto the structure. This type of impact is called the Bagnold type impact load. This type of impact is very popular to represent impulsive wave loads.

Transition type impact load
The largest impact loads on vertical breakwaters occur when plunging waves hits the structure. This type of pressure causes a transition type of impact. This is the classical type of impulsive wave load. The water surface encounters parallel to the construction and the water is unable to flow alongside the construction. No air is enclosed, and , in case air is enclosed the amount will be small and local. The force applied onto the construction will be high, but the duration is very short (in the order of milliseconds). This type is also called the "hammer shock" impact.

Force history of impulsive wave load

The impulsive wave load has been measured in many model tanks and some at protoype scale. The procedure is to measure the wave pressure at strategic places in a vertical line from top to bottom in the vertical wall. After integration of the local pressures over the depth we are able to derive the force history. An example of a force history is visualised in Figure 4-6.

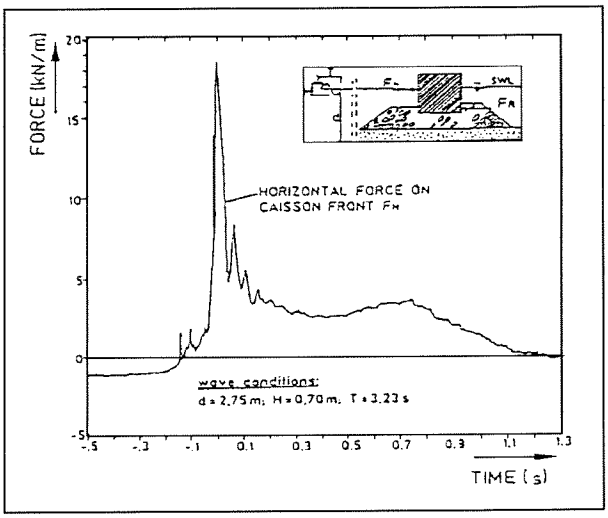

Figure 4-6 Characterisic force history of wave impact [Oumeraci 1991]

Note the short time scale of the increase from *0* to *18.5* kN/m. This is called the rise time of the impulsive wave load. It is obvious that the sample rate of the pressure box must be adequate to enough to register the accurate increase of pressure at the accompaning time scale.

Figure 4-6 visualises also two different components which the wave impact load is build of. An impulsive component (from 0 to 0.1 sec) and a quasi-static component (from 0.1 to 1.2 sec).

The impulsive wave load can be schematised as a triangular wave impact force.

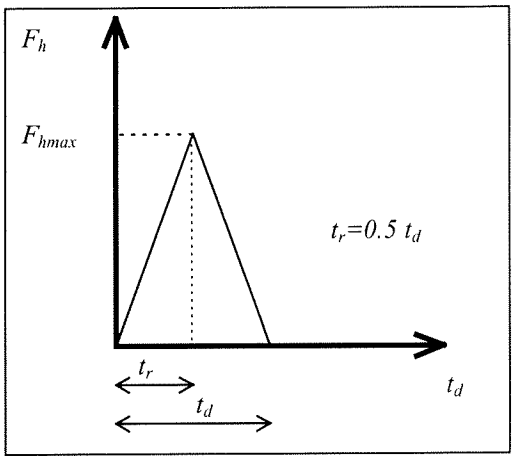

Figure 4-7 Triangular force-time diagram

When the impact load is schematised as visualised in Figure 4-7 above, the wave impact can be defined by a maximum force (F_{max}), impact rise time (t_r) and a total impact duration (t_d).

4.2.1 Model of Minikin

Minikin developed a design procedure based on observations of full-scale breakwaters and the results of Bagnold's study [Bagnold 1939]. The model assumes a maximum dynamic pressure at the still water level and a parabolic decline to zero at the distance $H_b/2$ above and under still water level added by an increased hydrostatic pressure level due to the rise of still water level. See Figure 4-8.

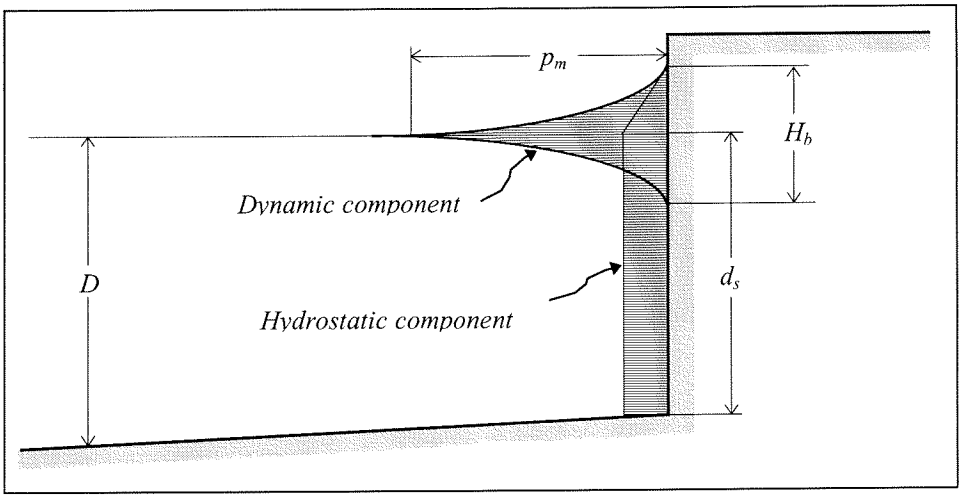

Figure 4-8 Pressure distribution according to Minikin

The maximum pressure is,

$$p_{\max} = \tfrac{1}{2} C_{mk} \rho g \frac{H_b}{L_o} \frac{d_s}{D} \left(D + d_s\right) \qquad 4\text{-}17$$

with,

C_{mk} = impact coefficient (C_{mk} = 202)
D = waterdepth at a wavelength from the wall
d_s = waterdepth in front of the wall
L_o = wavelength at deep water

The resulting force on the structure is,

$$F = \frac{p_{\max} H_b}{3} + \frac{\rho g H_b}{2} \left(\frac{H_b}{4} + d_s \right) \qquad 4\text{-}18$$

4.2.2 Goda formulae - extended by Takahashi

The Goda formula has been extended by Takahashi (in 1996) with impulsive pressure coefficients. This was obtained by reanalysing the results of comprehensive sliding tests. The addition should be regarded as an additional effect to the slowly varying pressure component. According to Takahashi the pressure p_1 at the water surface in the Goda formula can be expressed as (compare with section 4.1.3),

$$p_1 = 0.5\left(\alpha_1 + \alpha^*\right)\rho_w g H_{\max} \qquad 4\text{-}19$$

with,

α^* = the largest of α_1 and α_2 (see section 4.1.3)

Impulsive coefficient α_1 is obtained by reanalysing the results of comprehensive sliding tests (by Takahashi), being a non dimensional value. This coefficient should be regarded as an

additional effect to the slowly varying pressure component. The dynamic effect of impulsive pressures is not always modeled correctly by using α_2.
Figure 4-9 shows a diagram for α_I, in which it is expressed by the product of α_{I0} and α_{I1}, where α_{I0} represents the effect of wave height on the mound. The impulsive dimensional parameters are given in the following formulae,

$$\alpha_I = \alpha_{I0}\alpha_{I1} \qquad 4\text{-}20$$

$$\alpha_{I0} = {}^{H_{\max}}\!/_{1.8 \cdot d} \qquad H_{max} \le 2 \times 1.8d \qquad 4\text{-}21$$

$$\alpha_{I0} = 2 \qquad H_{max} > 2 \times 1.8d \qquad 4\text{-}22$$

and α_{I1} represents the effect of the mound shape (shown by contour lines). This term can be evaluated using,

$$\alpha_{I1} = \frac{\cos\delta_2}{\cos\delta_1} \qquad \delta_2 \le 0 \qquad 4\text{-}23$$

$$\alpha_{I1} = \frac{1}{\cosh\delta_1\left(\cosh\delta_2\right)^{0.5}} \qquad \delta_2 > 0 \qquad 4\text{-}24$$

$$\delta_1 = 20 \times \delta_{11} \qquad \delta_1 \le 0 \qquad 4\text{-}25$$

$$\delta_1 = 15 \times \delta_{11} \qquad \delta_1 > 0 \qquad 4\text{-}26$$

$$\delta_2 = 4.9 \times \delta_{22} \qquad \delta_{22} \le 0 \qquad 4\text{-}27$$

$$\delta_2 = 3 \times \delta_{22} \qquad \delta_{22} > 0 \qquad 4\text{-}28$$

$$\delta_{11} = 0.93\left(\frac{B_b}{L} - 0.12\right) + 0.36\left(\frac{h_s - d}{h_s} - 0.6\right) \qquad 4\text{-}29$$

$$\delta_{22} = -0.36\left(\frac{B_b}{L} - 0.12\right) + 0.93\left(\frac{h_s - d}{h_s} - 0.6\right) \qquad 4\text{-}30$$

with,

B_b	=	berm length
L	=	wave legth corresponding to that of the significant wave
h_s	=	waterdepth in front of sill
d	=	water depth from top layer rubble mound foundation
α, δ	=	dimensionless constants

Please refer also to Figure 4-3.

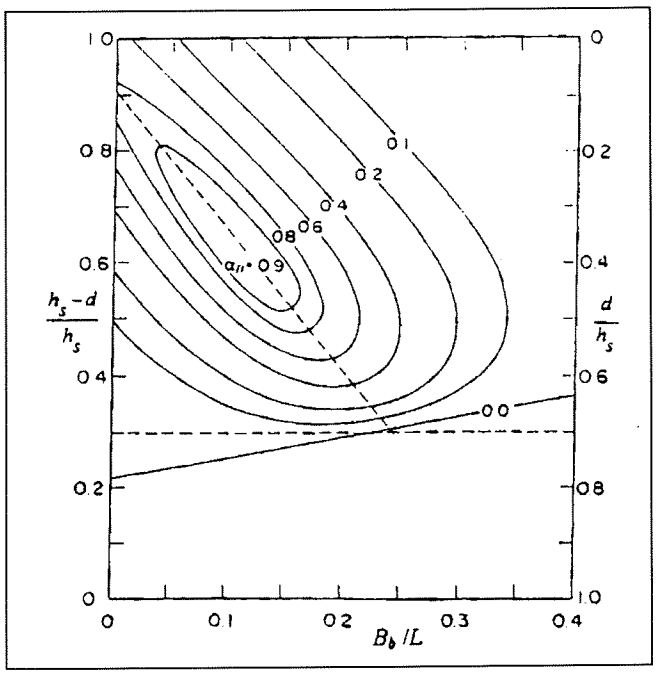

Figure 4-9 Calculation diagram of impulsive pressure coefficient [Takahashi]

The value of α_1 reaches a maximum of *2* at $B_b/L = 0.12$, $d/h_s = 0.4$ and $H/d > 2$. When $d/h > 0.7$, α_1 is always close to zero (*0*) and is less than α_2. It should be noted that the impulsive pressure significantly decreases when the incoming wave is oblique (angle of incidence $\beta > 0$).

4.2.3 Formula by Klammer, Oumeraci and Kortenhaus

From large scale model tests the following relation between t_r and F_{max} has been found by Klammer, Oumeraci and Kortenhaus (KO&K),

$$\frac{F_{h,\max}}{\rho g H_b^2} = k\left(\frac{t_r}{\sqrt{d_b/g}}\right)^{-1} \qquad 4\text{-}31$$

with,

k = 2.24 (suggested by Klammer, Oumeraci & Kortenhaus (KO&K))

This formula is based upon the theory of momentum conservation. At short impact duration the maximum impact force is large, while for the longer impact duration the maximum impact force is smaller. When schematising the impact force history as a triangular load, the area of the triangle will be the same at short and longer impact duration.

The formula of KO&K represents an upper boundary limit for impulsive wave load based upon model scale tests. With $k=2.24$ this formula results in very high impulsive wave forces at impact durations below 1 sec. It seems that this formula has a large overestimation of the impact force. Analising data from scale model tests [Van Gelder 1998] show us that the upperlimit set by $k=2.24$ (KO&K) is very high. Suggested values of k for three different model tests are given in Table 4-1.

Table 4-1 constant k, average and standard deviation

k	Horizontal	Horizontal	Uplift	Uplift
	average	stdev	average	stdev
GWK.IMP	0.086	0.084	0.16	0.17
WKS_U.IMP	0.10	0.20	0.63	0.44
QUB.IMP	0.16	0.38	0.57	0.45

An explanation of the difference of the three model tests can be found in the difference of scale. The GWK test is the largest scale, while the QUB set is the smallest scale. There seems to be a decrease in k at larger (increasing) scale. The reason for the decrease could be found in the increasing aeration of the water at increasing scale.

A more realistic estimate of the constant k (for design purposes) would be $\mu+2\sigma = 0.25$, based upon the results of GWK tests,

$$\frac{F_{h,\max}}{\rho g H_b^2} = 0.25\left(\frac{t_r}{\sqrt{d_b/g}}\right)^{-1} \qquad 4\text{-}32$$

The ratio between t_r and t_d suggested by Klammer, Oumeraci and Kortenhaus is,

$$t_d = t_r + 0.35\left[1-\exp\left(-20\cdot t_r\right)\right] \qquad 4\text{-}33$$

4.2.4 Schmidt et al

In the case of a single peak history the maximum impulsive wave force may be approximated by the following empirical equation which has been determined on the base of large scale model tests performed by Schmidt et al. The formula is,

$$\frac{F_{h,\max}}{\rho_w g H_b^2} = 1.24\left(\frac{t_d}{T_p}\right)^{-0.344} \qquad 4\text{-}34$$

with,

H_b = breaker height
T_p = peak period of the waves
ρ_w = mass density of sea water (1025 kg/m^3)

This equation has a considerable uncertainty because of the large scatter in the test results (linear correlation coefficient = 0.8). The test result forces can be up to twice the force calculated by equation above.
In the same test was found that the point of application of the peak force $F_{h,max}$ is generally located slightly below SWL (Still Water Level) and does not vary significantly during the impact. The ratio of the rise time t_r to the total peak duration t_d has been found to vary between (t_r/ t_d =) 0.3 and 0.65, depending on the amount of trapped air and the magnitude of the force peak. Larger values of t_r/ t_d occur for trapped air volumes and smaller force peaks.

This formula is based on large scale test for a certain amount of parameters. Therefore the formula has some limitations:

- The validity for prototype dimensions is a point of discussion, given the uncertainty of scale laws, although the tests are at large scale.
- The test have been made for a certain group of parameters. The influence of for instance berm width has not been taken into account.
- No restrictions are given for the ratio t_d/T_p.

The theoretical basis of this formula is weak, because there is no mathematical and physical basis to this formula. The formula is based on a fit to data points and, for the scatter of the data point is rather large, the uncertainty is considerable (see Figure 4-10, note the double logarithmic scale). As stated before there are no restrictions for the ratio t_d/T_p.
Through the 'cloud' of scattered data points a line with constant momentum can be drawn, for which a different formula is proposed,

$$\frac{F_{h,\max}}{\rho_w g H_b^2} = 0.06\left(\frac{t_d}{T_p}\right)^{-1} \qquad 4\text{-}35$$

In the test of Schmidt et al the following ratio between rise time and total impact duration was found,

$$0.3 \le \frac{t_r}{t_d} < 0.65 \qquad 4\text{-}36$$

The ratio of rise time to the total peak duration depends on the amount of trapped air and the magnitude of the force peak. The larger values of t_r/t_d occur for large trapped air volumes and smaller force peaks. According to Walkden et al [1995] the reduction of the impact force and the associated increase of impact duration are due to the combined influence of the increase in compressibility of the air/water mixture and the observed change in the wave profile at the impact.
In Figure 4-10 the formulae by Schmidt are shown. Note that both axis are logarithmic and dimensionless. The force is made dimensionless by $\rho g H_b^2$ and the impact duration by T_p.

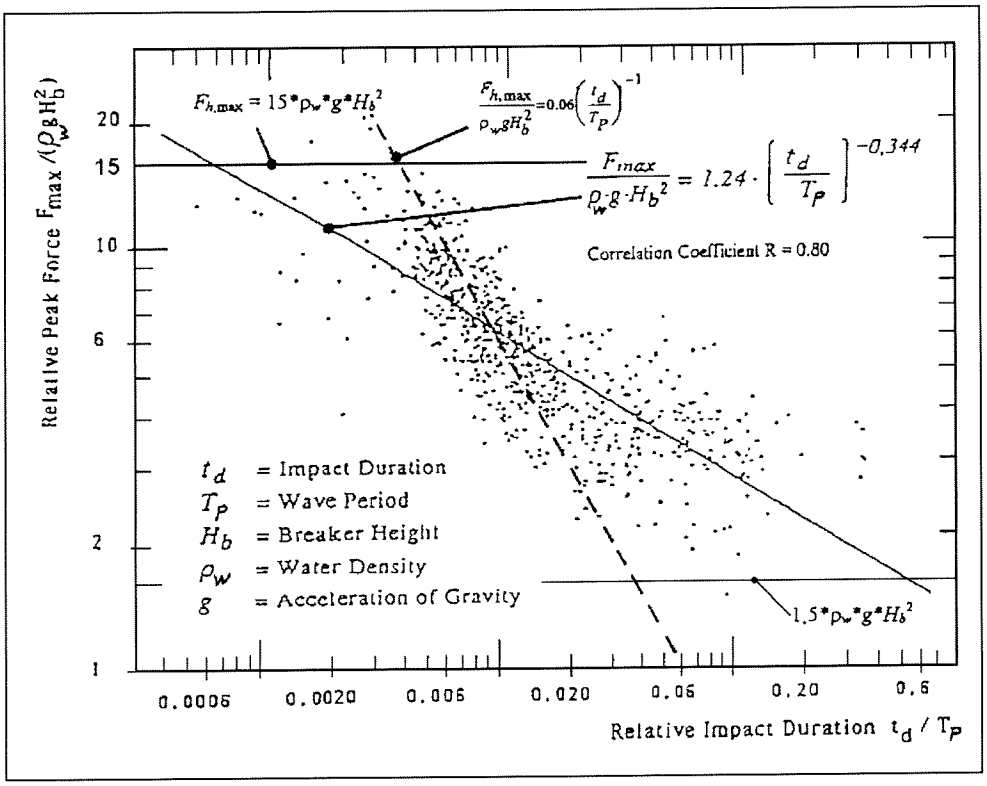

Figure 4-10 Maximum impact force vs. impact duration [Schmidt et al 1992]

4.3 *Wave loads at Genoa Voltri breakwater*

The investigation of wave loads in this report is made for a particular case, the Genoa Voltri breakwater.The wave loads at the Genoa Voltri breakwater will be calculated, with help of the formulae stated earlier. The essential part of the impulsive wave load, breaking, will also be investigated here.

The results of this method is shown in Table 4-2.

Table 4-2 Outcome of impact prediction method

H_{si} (m)	$P_{i\%}$	outcome
5.50	0.015	*no impact*
6.50	0.083	*no impact*
8.40	0.712	*no impact*

The conclusion can be drawn that at the Genoa Voltri breakwater the waves will not break according to this method, thus resulting in only quasi static loads upon the breakwater. These loads can easily be derived by the linear wave theory or the Goda formula.

Wave breaking at Genoa Voltri breakwater

The breaking limit of the wave field at Genoa Voltri breakwater is defined by the formulae by Miche, derived in chapter 3. The estimation of breaker height with respect to the waterdepth is given in figure below.

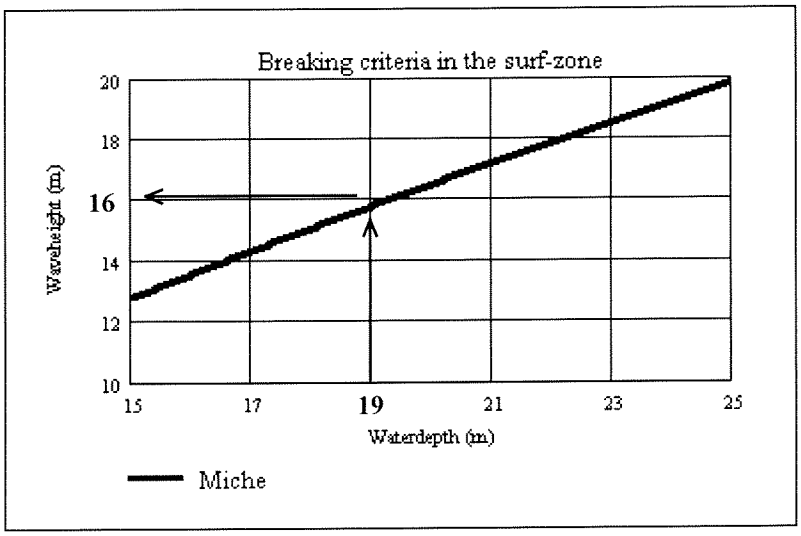

Figure 4-11 Wave breaking in the surf zone

The water depth in front of the Genoa Voltri breakwater is $d = 19.05\ m$. The wave height is *15.86 m* (Figure 4-11). The maximum wave height at the Genoa Voltri breakwater is about *11* meters. Therefore it can be concluded that there will be no wave breaking at the Genoa Voltri breakwater.

General conclusions

Based upon the paper written by Calabrese and Allsop and the breaking limit of Miche, it can be concluded that there is no wave breaking at the Genoa Voltri breakwater. If there is no wave breaking, the impulsive weave loads cannot occur. For stability calculations the wave load can be modeled as a quasi static wave loads.

However, for the purpose of this graduation report the *assumption* will be made that the waves **will break and that the wave impacts do occur**.

4.4 Comparison different impulsive wave load formulae

In the previous sections we have seen five different wave load formulae, which model the impulsive wave load on a vertical wall. The differences between these formulae are remarkable.
The hydraulic conditions and the geometry of the breakwater can be found in the annex Genoa Voltri breakwater.

4.4.1 Differences of impulsive wave load formulae

The force scale is made dimensionless by $\rho g H_b^2$. The time scale has kept its dimension (s), giving a good insight in the duration time and the related impact force.
The upper limit given by Goda and accepted by a large number of scientists, has a non-dimensional value of $F / 15 \cdot \rho g H_b^2$. The quasi-static load gives the 'minimum' of the wave load and is given by the Goda forces.

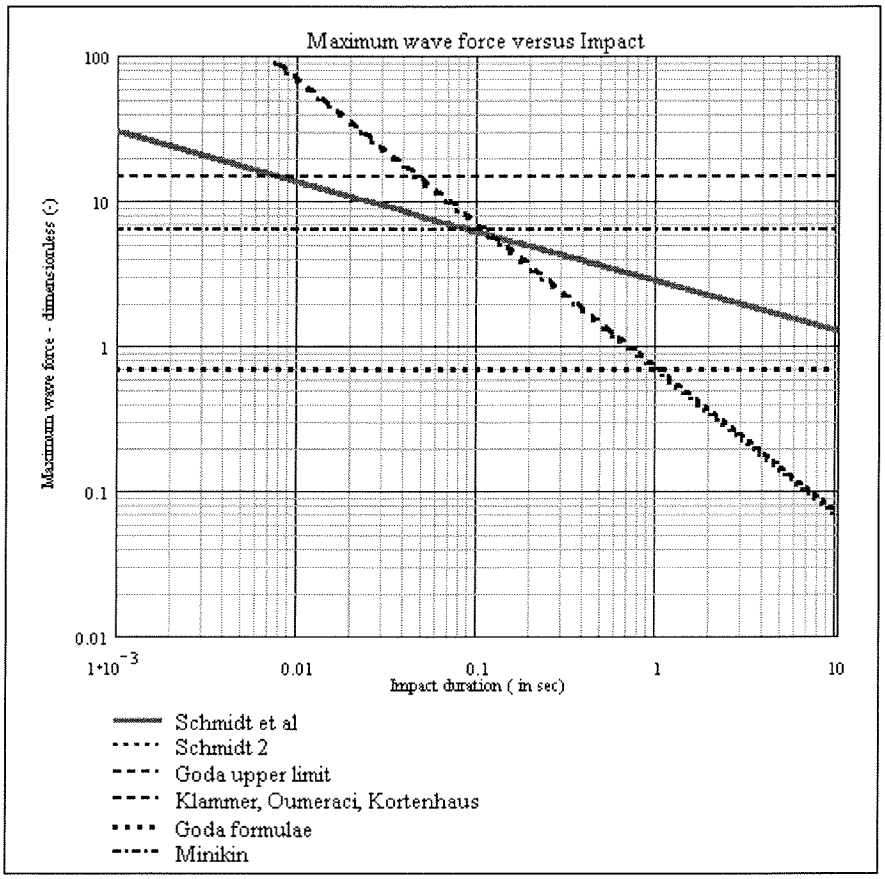

Figure 4-12 Comparison wave impact formulae (double logarithmic scale)

From Figure 4-12 we can see the difference between the slanted lines and the horizontal lines. The slanted lines represent the latest formulae, which are related to the impact duration, derived by Klammer, Oumeraci & Kortenhaus (KO&K) and Schmidt et al. These formulae are based upon model tests.
The horizontal lines represent the upper and lower boundaries (Goda upper limit and Goda formulae) and the formula of Minikin, which is not related to the impact duration.

At first we can see (in Figure 4-12) that the formulae of KO&K and Schmidt et al vary significantly. The formula of Schmidt is purely based upon data from model tests, while the formulae of KO&K and Schmidt2 are based upon a data fit and the theory of momentum conservation.
The second observation is that the two parallel slanting lines, formulae of KO&K and Schmidt 2 are almost similar. Both formulae are based upon the theory of momentum conservation, which yields to the parallel lines in the graph (see the dotted slanting lines).

The following figure shows us the formulae at linear axis (not logarithmic), thus removing any optical distortion or confusion.

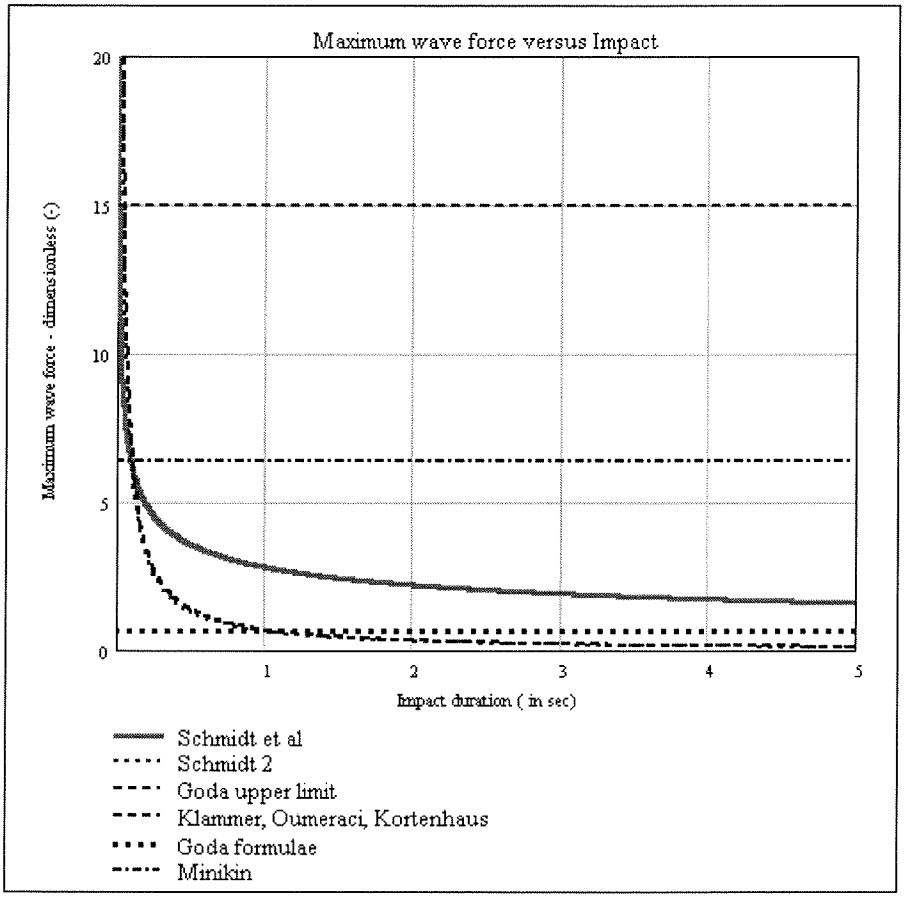

Figure 4-13 Comparison wave impact formulae (linear scale)

In Figure 4-13 above large differences between the Schmidt formulae and the 'momentum conservation' formulae at eigenfrequency of the caisson (about 0.8 sec) are observed. Furthermore we can see that for the longer impact durations (> 1 sec) the formulae based upon the theory of momentum conservation looses its validity as the value of the force is below the quasi-static force (represented by the Goda formula).

Summarised the following observations have been made,

1. Klammer, Oumeraci & Kortehaus and the formula of Schmidt 2 (momentum conservation) obtain high impact forces at short impact duration times
2. Large differences at eigenfrequency of the caisson (about 0.8 sec)
3. At longer impact duration (> 1 sec) the wave impact force results in forces lower than the (quasi-static) Goda forces.
4. The formulae of Klammer, Oumeraci & Kortenhaus and Schmidt 2 are almost similar.

4.4.2 Remarks about latest formulae, which are derived from model tests

In relation to the comparison some remarks should be made about latest (three) formulae, derived by Schmidt et al. and Klammer, Oumeraci & Kortenhaus.
Within the framework of the MAST project, three formulae have been derived, based upon model tests. These tests result in remarks that should be noted before using the formulae in a design process of a vertical breakwater.

1. The tests were aimed at very short impact durations (<0.1 sec).
2. The tests were applied at model scale. None of the tests were verified at prototype level. This is a problem since the effect of scaling from model to prototype measurements hasn't been solved.
3. The definition of the impact duration (rise time and total duration, t_r & t_d) is not standarised, and still open for discussion. It is not clear to what extend the definition of impact duration will influence the impact force.
4. Measurements of wave pressures along the breakwater has not been measured in model tests. Local high pressure can occur, but integrated of a longer breakwater section the mean pressure could be reduced significantly.

Ad 1.
As the model tests were aimed at the very short impact durations and impact pressures, the validity of the longer impact durations and the accompaning impact pressures can decrease significantly. This should be mentioned when using the formulae for design purposes.

Ad 2.
Because the effect of scaling from model to prototype measurements hasn't been solved the use of formulae based upon model tests can be very dangerous, especially when the differences between model tests and prototype measurements can be rather large. The problem of scaling involves correct scaling of impact duration and impact pressure (i.e. force).

Ad 3.
This will be further explained in the next chapter.

Ad 4.
The 'scatter' of the wave impact pressure has not been accounted for, nor measured. The wave impact pressures can reach very high values, but these pressure can be very locally. It is very likely that there is a correlation between the occurrence of high impact pressures and the 'spread' of the impact pressure (i.e. the width of the impact). For example, the higher the impact load, the more local it occurs (i.e. the shallower the impact load is).
When using the formulae in a spring-dashpot model to calculate the response of a vertical breakwater it is crucial for the stability to know the width of the load appied on the breakwater.

5. Impact duration and impact pressure

The previous chapters emphasised the importance of the impact duration in relation to the response of the caisson. The calculations of the dynamic behaviour of the Genoa Voltri breakwater also states the influence of the impact duration in relation to the amplitude of excitation.
In this chapter the impact duration of a wave impact on a vertical structure is examined. The goal is to find an analogy in a different technology, Maritime Engineering.
Further the available time impact histories of model tests and full scale measurements are compared.

5.1 Impact loads on ships

The wave impact caused by slamming can be roughly classified into four types (Figure 5-1). Bottom slamming (1) occurs when emerged bottoms re-enter the water surface. Bow-flare slamming (2) occurs for high relative speed of bow-flare to the water surface. Both slamming types occur in head seas with large pitching and heaving motions. Breaking wave impacts (3) are generated by the superposition of incident wave and bow wave hitting the bow of a blunt ship even for small ship motion. Wet-deck slamming (4) occurs when the relative heaving amplitude is larger than the height of a catamaran's wet-deck, or an offshore structure with insufficient clearance for high wave.

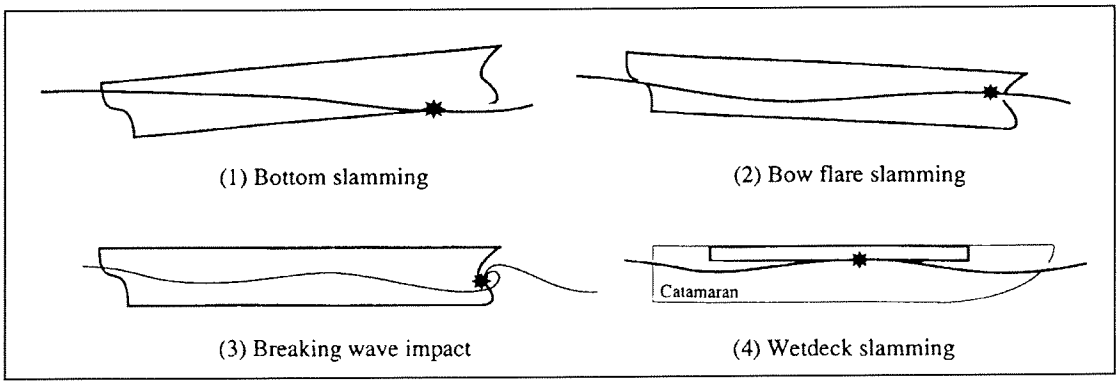

Figure 5-1 Types of slamming impact of a ship

The most important variables of wave impact loads considering vertical breakwaters are force and time duration. Therefore when in search for an analogy with the impact loads of ships the impact duration - i.e. pressure/time history - and pressure are emphasised.

5.1.1 Bottom slamming (model tests)

The wave impact pressure has been a crucial subject to the design of the ship structure since early days of the naval architecture. Naturally, there have been lots of works on this matter. Among them, Von Kármán or Wagner's theories have been used for the forces and the pressure assuming that the impact phenomena are two-dimensional. And their theories are known to give a good estimation for most hull forms if no air entrapping is involved. However, some difficulties arise in calculating impact pressure for the actual cases. Namely, for hull sections with a flat bottom, these theories predict infinite impact pressure because the waterline varies at infinite rate in the two dimensional sense. Of course this is not the case in nature.

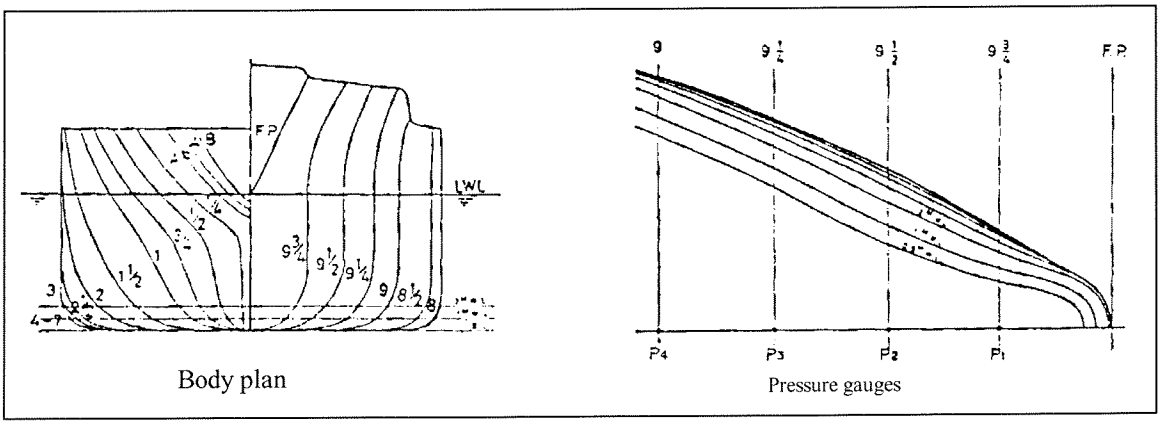

Figure 5-2 Body plan, waterline and location pressure gauges of model [Watanabe 1987]

Theoretical estimations are compared to experimental results in order to check the validity of the present theory of bottom slamming. The model (shown in Figure 5-2) was run in various waves with the different heading and forward velocity. The body plan, waterline and the location of the pressure gauges are visualised in Figure 5-2.

It should be noted that special attention had been paid to recording and analysing the pressure data, because it contains very high frequency components once the impact phenomena occurs. This is done by using an analog equipment instead of the radio telemetry, thus assuring restoration of the high frequency components.

The results of the measurements are shown in Figure 5-3.

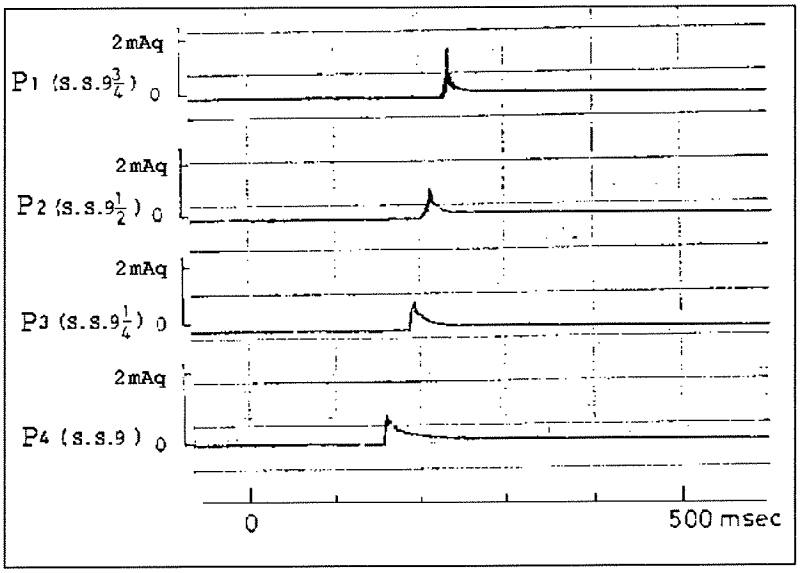

Figure 5-3 Example of magnified measured data (model tests) [Watanabe 1987]

The nature of impact can be characterised by its run, peak, value and duration.
As showed in Figure 5-3 the impact peak shifts from left to right - i.e. from aft to fore. The evaluation of the run is not of interest.

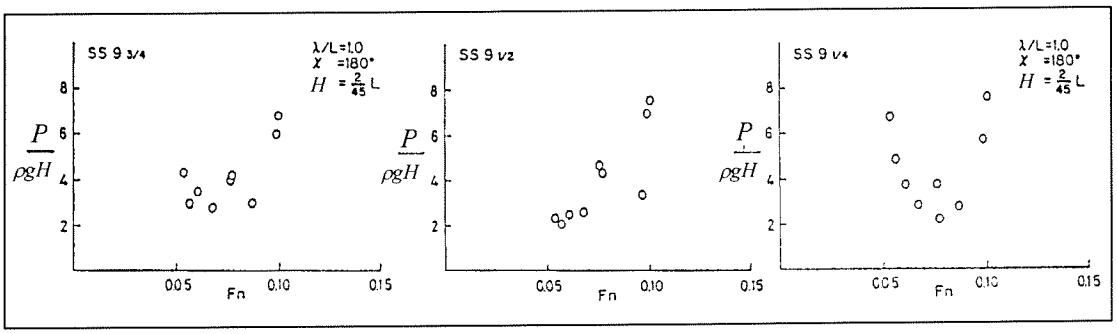

Figure 5-4 Impact pressure vs Froude number (*Fn*) [Watanabe 1987]

The peak value of the bottom impact pressure is showed in Figure 5-4. The pressure is normalised with respect to the wave amplitude (H). It is seen that, despite the scatter of the data, with increasing forward speed (increasing Froude number, Fn) the impact pressure increases.
The measured peak pressure is about 3 to 6 $\times \rho g H$.

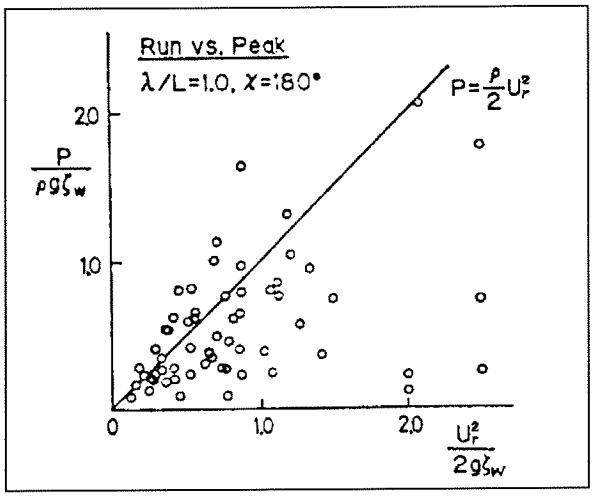

Figure 5-5 Comparison of measured and calculated impact pressure [Watanabe 1987]

The difference between the estimated (i.e. calculated) and the measured peak value is due to the estimation formula of the impact pressure or the estimation of the ship motion, especially of the location of the water line. The difference of time lag - i.e. 'run' - between experiment and calculated is large. Since the travelling speed contributes substantially to the impact pressure, it may be worth to use the measured travelling velocity of the water line, while keeping the present formula for the pressure. It can be seen in Figure 5-5 that the estimation - represented as circles - has been concentrated on the straight line. The vertical axis indicates the estimated values and the horizontal axis the measurements. The peak values are non-dimensionalised with respect to the water head defined by the wave amplitude (ζ_w).

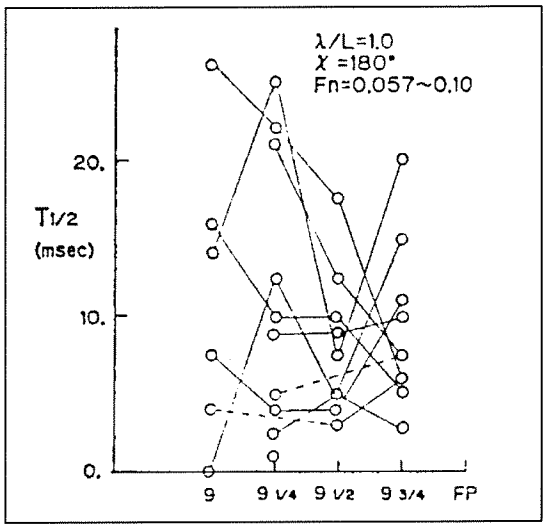

Figure 5-6 Duration of the impact [Watanabe 1987]

The data shown in Figure 5-6 above is taken out of several experiments.
As index of the duration of impact in Figure 5-6 the time of duration ($T_{½}$) during which the pressure stays above a half of the peak value is chosen. At the vertical axis the impact duration is set with respect to the bottom location (horizontal axis).
The lines connecting the different data points represent data from the same run.

The location of the impact peak is of no significance with respect to the impact duration. Although the scattering of the data is apparent, it is seen that the location has little effect on the duration of impact and the average duration is about 5 msec (!!).

Conclusions bottom slamming:

- The average impact duration ($T_{½}$) is about 5 msec. This yields in a total impact duration (t_d) of about 10 msec.
- The measured peak pressure is about 3 to 6 $\times \rho g H$.
- Large random spread of impact pressure along hull.
- Large 'scatter' of impact duration.
- Increase of speed of the ship increases the impact pressure.

5.1.2 Bow flare slamming (model and full scale measurements)

Hydrodynamic impacts on the above water part of a ship occur in waves approximately equal to the length of the ship or in short and steep waves although ship motions may be very small in this case. The slope of the stem and the bluntness of the bow are considered to be the main parameters which govern the magnitude of these impacts. If the angle between the stem and the slope of the short waves is small, large pressures are experienced.

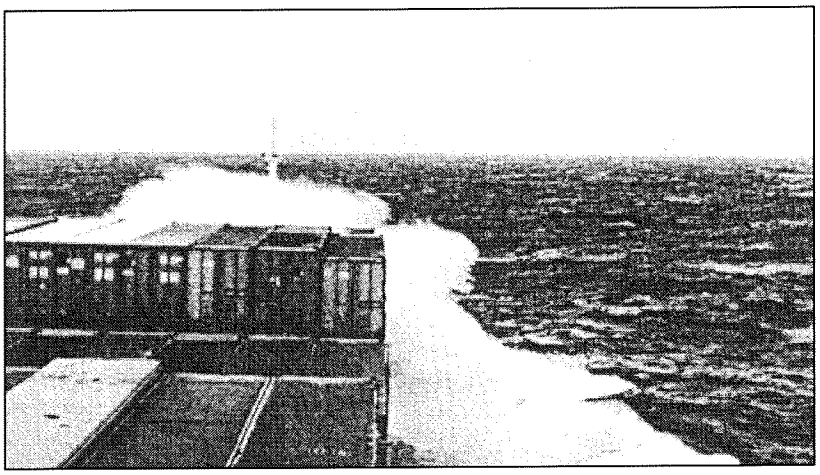

Figure 5-7 Typical example of bow flare slamming

There have been several experimental studies - on scale - and also some full scale tests on ships in rough seas.
H. Fuji & H. Takahashi carried out an experimental (model) study on bow flare impact on two bow forms. The maximum measured pressure observed is about 491 kPa (full scale value). Other model tests obtained a maximum bow flare impact pressure of 61 kPa (full scale value).

Full scale trials to measure impact pressure on the bow flare of a large ore carrier (length of vessel = 247 m, displacement = 135,950 tons) were performed by the Japan Shipbuilding Research Association [SR 124 rep. 140 & 152].
The magnitude of pressures were measured, dynamic as well as non-dynamic, and the duration time of the impact, $\tau_{1/2}$. Throughout the trails the impact duration was less than 0.1 sec. The maximum impact pressure measured was about 570 kPa.
Figure 5-8 shows the relationship between magnitude and duration of the impacts together with the constant impulse curves ($p \cdot \tau_{1/2} = 0.4$ and $p \cdot \tau_{1/2} = 0.6$) for reference. Please note the definition of $\tau_{1/2}$ and remark the shape of the time history of pressure. The impacts were recorded in sea state 6, speed 13 knots, at 7 Beaufort of wind.

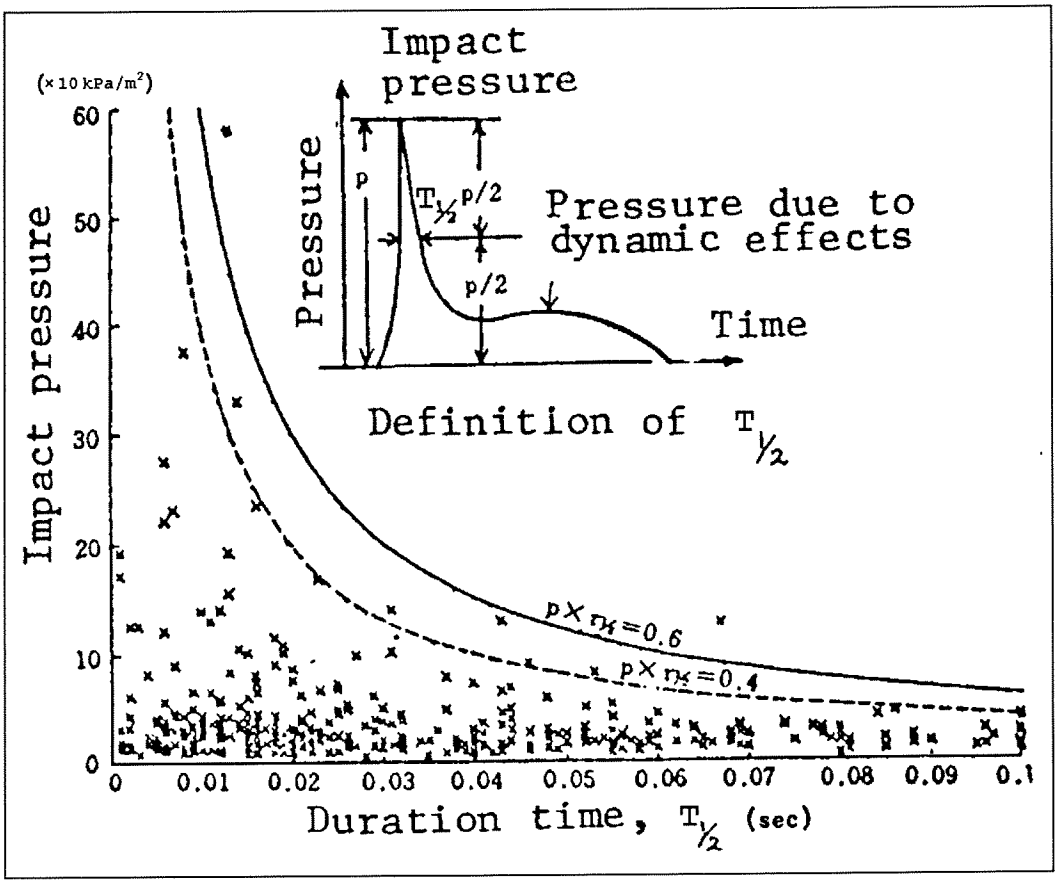

Figure 5-8 Impact pressure vs impact duration, full scale [SR 124 rep. 140, 1971]

As has been visualised in Figure 5-8 the impact pressures occur at very short impact duration times. The duration of the peak pressure was less than 0.1 sec throughout the trail. The maximum impact pressure observed is 570 kPa with corresponding duration of about 12 msec.

In addition to Figure 5-8, probability of impact pressure and impact duration ($T_{1/3}$) are given in Figure 5-9 and Figure 5-10.

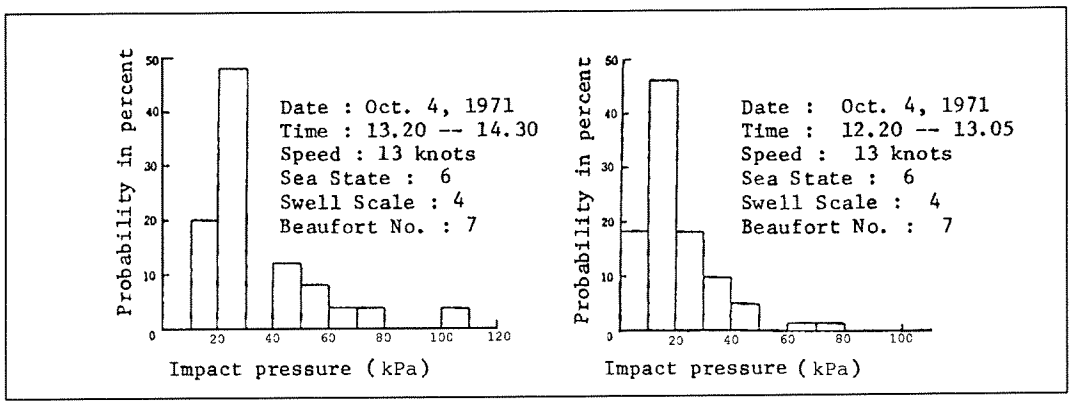

Figure 5-9 Probability of impact pressure, full scale measurements [SR 124 rep.140, 1971]

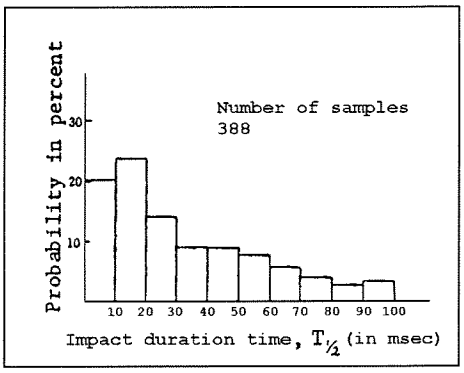

Figure 5-10 Probability of impact duration [SR 124 rep. 140, 1971]

In Maritime Engineering the fierceness of the sea is classified by sea states, numbered from 0 to 9 . The data measurements have been made at Sea State 6, which corresponds to a (significant) wave height of 4 to 6 m. Additional information about the sea states can be found in the Annex Sea States.

From Figure 5-10 above can be concluded that the impact duration ($T_{½}$)is very short, about 20 msec.

Another set of full scale measurements of bow flare impact on a large tanker during several voyages from Japan to the Persian Gulf were carried out by S. Nakashima [1973]. The maximum pressure on the bow flare observed in these trails was about 700 kPa in Sea State 7, and the impact was accompanied by severe shudder through the entire hull length. This is in good agreement with the maximum value obtained by the Japan Shipbuilding Research Association [SR 124 rep. 140, 1971], about 570 kPa.

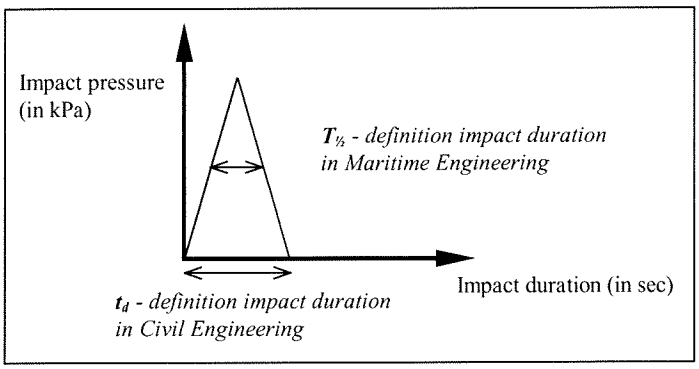

Figure 5-11 Definition of impact duration

The impact duration $T_{½}$ as defined in Maritime Engineering should be converted to the total impact duration as is used in Civil Engineering, and represented by the symbol t_d. This can be done roughly by multiplying the $T_{½}$ by 2,

$$t_d = 2 \times T_{½} \qquad 5\text{-}1$$

Conclusions Bow flare slamming:

- The impact duration ($T_{½}$) is very short, about 20 msec. This yields in a total impact duration (t_d) of about 40 msec.
- The maximum observed impact pressure is 570 kPa. The corresponding impact duration ($T_{½}$) is 12 msec (i.e. $t_d = 24$ msec).
- A relation between pressure and impact duration show very short rise times

- Shape of time histories of pressure is similar to that on a vertical wall

5.1.3 Water jet impinging on elastic plate (model test)

In order to study the fundamental mechanism of bow flare impact, an experimental study was carried out using a water jet impinging on a elastic plate surface [Suhara, Hiyama & Koga 1973], which is contrary to other methods such as wedges dropping on still water. In the tests, a bucket containing water, falling along a guide rail, was arrested at certain level (H). The bottom of the bucket was opened and a block of water impacted the plate surface with high velocity. Figure 5-12 shows examples of the time histories of pressure obtained during the tests. As can be seen in the figure the shape of the pressure has (close) resemblance with the time history observed on bow flare impacts on ships at sea.

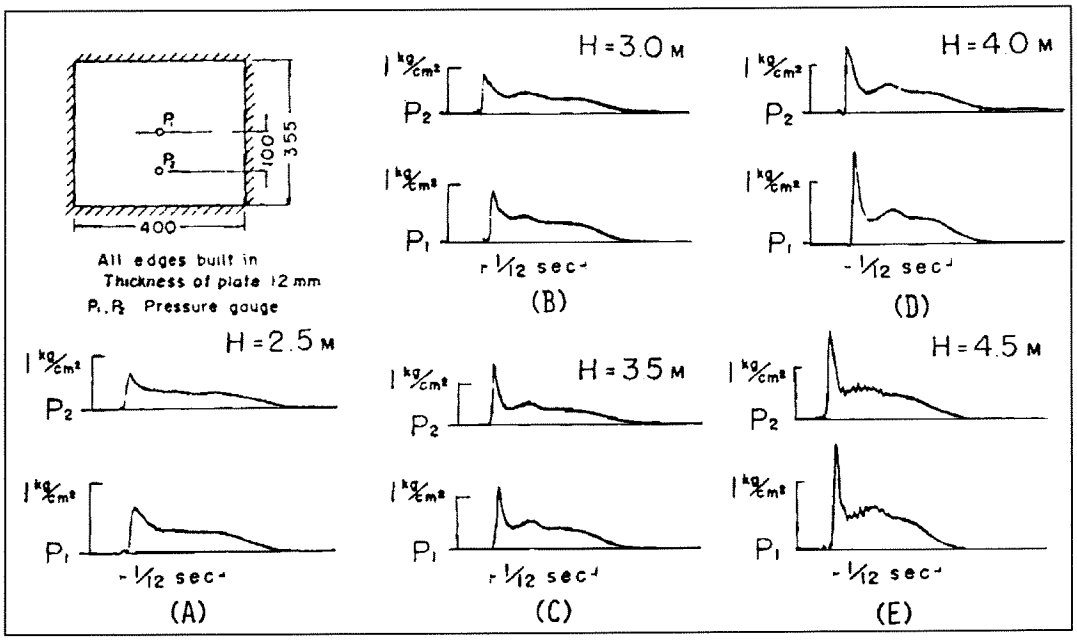

Figure 5-12 Examples of time history of impact pressure [Suhara, Hiyama & Koga]

The maximum impact pressure increases with increasing drop-height, as expected. The pressure box in the centre of the plate (P1) measured a higher pressure than the excentric pressure box (P2), as expected.
As Figure 5-12 above shows, the impact duration is very short (about 10 msec). The maximum pressure is lower compared with the impact of a wedge impact on still water.
At large drop-heights H oscillation in pressure can be identified (Figure 5-12 (E)). Air entrapment can very well cause these oscillations.

5.1.4 Slamming forces on wedges at forward speed (model test)

As a follow up of former research, forced oscillation experiments have been performed by Beukelman (1991) and Radev (1991) to determine peak pressures and rise times for four metal wedges with different dead rise angles. The pressures has been measured as a function of vertical oscillation speed, trim angle and forward speed.
The wedges have been visualised in Figure 5-13 and the measurements are drawn in Figure 5-14.

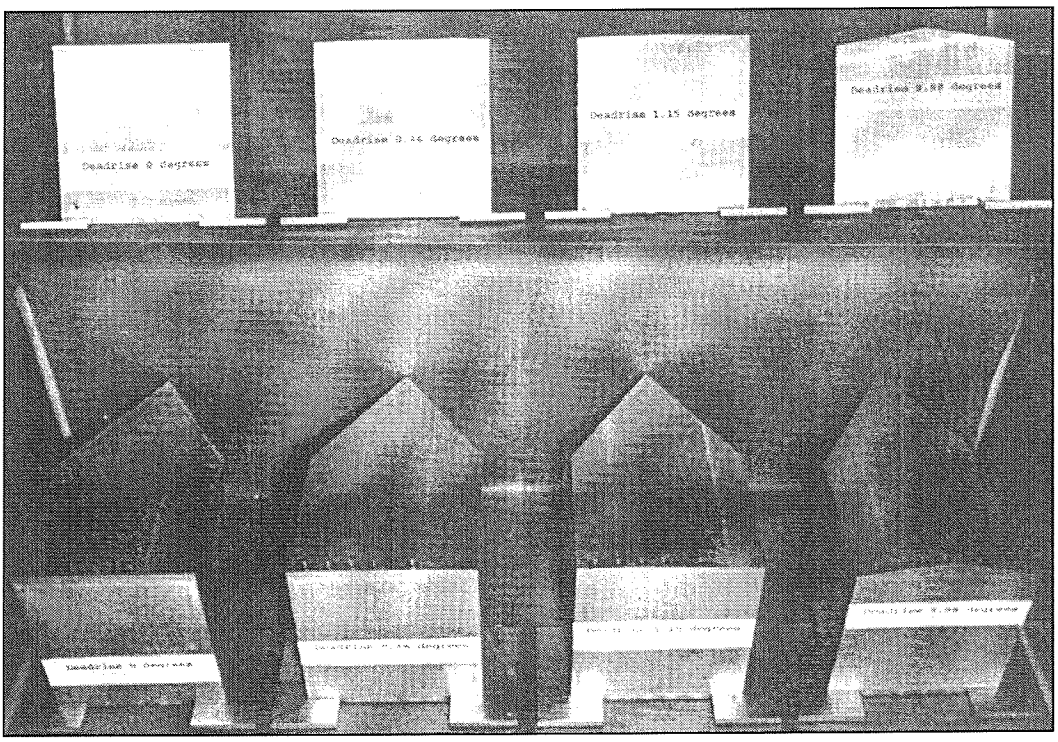

Figure 5-13 The four wedges [Beukelman 1991]

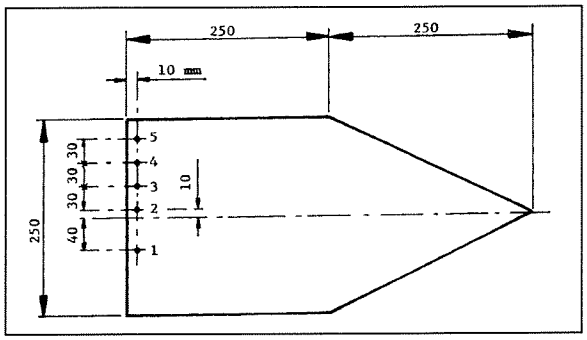

Figure 5-14 Wedge's bottom [Beukelman 1991]

Each wedge was forced oscillated as heaving motion in vertical direction with an adjusted trim angle in such a way that the average position of the transducers was situated in the zero position of the harmonic motion and the still water level. This means that the transducers hit the water surface with maximum oscillation speed.
For all the trim conditions no influence of the forward part of the wedge was present, except for trim angle $\alpha = 0^o$.
The results of the measurements are shown in Table5-1, and in Table 2 to 5 in Annex Wedge impact results.

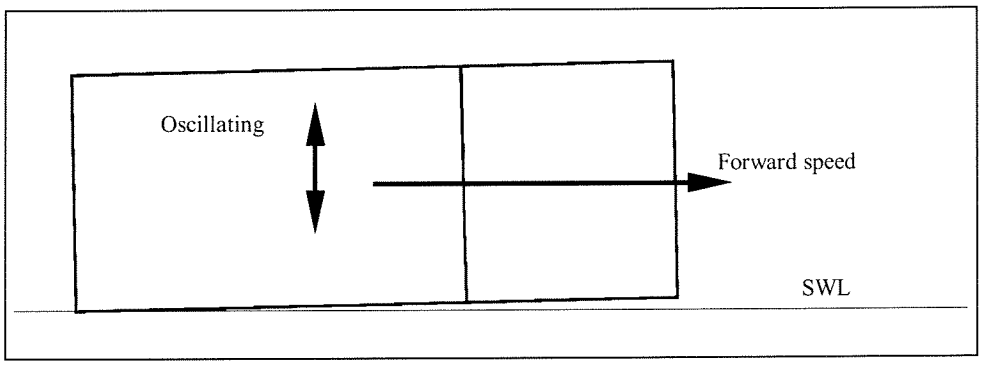

Figure 5-15 Side view of wedge entering the water

Table 5-1 Results wedge tests - flat bottom wedge [Beukelman 1991]

			PRESSURE p kPa					RISETIME t msec				
V	α	U	TRANSDUCER NR.					TRANSDUCER NR.				
M/s	degr	m/s	1	2	3	4	5	1	2	3	4	5
		1	-	-	-	-	-	-	-	-	-	-
	0	2	2.4	2	2.1	2.3	1.5	2.1	2.2	1.7	2	1.7
		3	2.3	14.5	2.5	1.6	1.5	1.6	1.6	1.5	2.3	1.8
		1	-	-	-	-	-	-	-	-	-	-
	0.5	2	2	2.1	2.6	-	1.5	-	-	-	-	-
		3	1.8	1.8	2.3	-	1.7	-	-	-	-	-
		1	-	-	-	-	-	-	-	-	-	-
	1	2	2.2	1.4	2	-	1.7	-	-	-	-	-
0.24		3	1.5	1.4	1.4	1.3	1.2	-	-	-	-	-
		1	2.5	2.2	2.1	0.8	-	-	-	-	-	-
	2	2	5	2.1	3.7	3.5	2.1	-	-	-	-	-
		3	3.3	2.8	4.2	2.2	2.4	-	-	-	-	-
		1	6.2	-	7	2.2	1.5	-	-	-	-	-
	2.5	2	2	3.1	1.9	1.9	2.4	-	-	-	-	-
		3	3.6	2.7	3.4	2.5	2.7	-	-	-	-	-
		1	1.2	-	-	3.4	1.7	-	-	-	-	-
	3	2	1.9	1.6	1.8	1.1	2.2	-	-	-	-	-
		3	4.9	2.3	3.7	1.5	3.3	-	-	-	-	-
		1	-	-	-	-	-	-	-	-	-	-
	0	2	5.5	4.9	5.8	6.5	2.3	1.9	2.2	1.9	2.2	1.9
		3	12.6	10.6	12.8	14.1	4.3	1.1	1.2	1.2	1.1	1.4
		1	-	-	-	-	-	-	-	-	-	-
	0.5	2	4.4	4	4.1	1.9	2.4	1.3	1.3	1	1.2	1
		3	5.1	5.4	4.9	-	3.9	1.1	0.9	1	-	1.3
		1	-	-	-	-	-	-	-	-	-	-
	1	2	5.5	5.7	6.3	9.8	3.4	12.9	10.2	12.7	10.4	7.8
0.48		3	7.6	5.6	7.5	5.9	4.5	7.2	7.5	7.5	6.4	-
		1	2.1	1.5	2.2	3.5	1.3	-	-	-	-	-
	2	2	13	6.2	12.9	12.5	4.1	6.9	7.1	7.4	6.1	-
		3	13.3	10	11.3	1	2.2	5.8	5.8	5.6	-	-
		1	4.6	2.4	4.1	2.1	-	-	-	-	-	-
	2.5	2	12.7	6.7	8.8	8.4	6.3	5.3	5.2	6.1	4.4	-
		3	13.9	9.2	15.4	12.1	6.1	5.6	5.7	5.5	4.6	4.6
		1	4.5	3.1	5.7	2.6	-	-	-	-	-	-
	3	2	11.7	10.6	11	10.2	7.5	6	6.5	6.7	5.5	5.1
		3	12.5	8.9	10.8	11.2	6.7	5.7	6.6	5.9	5.9	4.4
		1	-	-	-	-	-	-	-	-	-	-
	0	2	7.9	7.2	6.3	6.5	7.3	1.9	2.5	2	1.8	0.8
		3	28.4	33.1	32.9	31.9	29.8	0.6	1.1	0.6	0.7	0.8
		1	-	-	-	-	-	-	-	-	-	-
	0.5	2	9.3	9.1	9.4	7.3	10.4	14.5	12.3	14.1	8.3	5
		3	-	-	-	-	-	-	-	-	-	-
		1	-	-	-	-	-	-	-	-	-	-
	1	2	8.9	15.3	11.1	12.4	4.9	2.6	2.3	2.4	1.2	1.1
0.72		3	-	-	-	-	-	-	-	-	-	-
		1	-	-	-	-	-	-	-	-	-	-
	2	2	17.5	15.5	18.3	9.3	11.7	0.5	0.8	0.6	0.4	0.7
		3	22.6	18.1	20.7	14.9	12.3	0.3	0.6	0.3	0.5	0.6
		1	2.9	2.8	2.5	3.8	2.3	3.4	2.7	3.7	3.3	2.3
	2.5	2	21.3	27.7	23.4	10.1	12.6	0.9	0.7	0.4	0.6	1.1
		3	34.1	35.2	33.1	23.8	23.7	0.2	0.4	0.2	0.2	0.3
		1	1.5	2	2.2	2.3	1.4	8.8	3.1	4.7	5.3	5.1
	3	2	22.2	29.7	21.9	15.2	12.6	0.2	0.2	0.2	0.2	0.2
		3	29.4	29.5	31	24.3	22	0.2	0.3	0.3	0.1	0.2

Remark the same distance to the centre line of the wedge of pressure gauge 1 and 3 (Figure 5-14).

Table 5-2 Evaluation results wedge tests

	PRESSURE p kPa						RISETIME t msec					
	TRANSDUCER NR.						TRANSDUCER NR.					
	1	2	3	4	5	Δ (1-3)	1	2	3	4	5	Δ (1-3)
Average	*9.00*	9.00	*9.20*	7.58	5.98	***12.6 %***	*3.79*	3.5	*3.66*	3.11	2.24	*13.0 %*
Stdev	*8.48*	9.54	*8.81*	7.28	6.63	***9.9 %***	*3.90*	3.29	*3.79*	2.87	2.10	*19.0 %*

From the table above can be concluded that the difference between the peak pressures and rise times of gauges 1 and 3 differ significantly. The difference is 12.6 % and 13.0 % respectively.

In the transverse line of the wedges (from gauge 2 to 5) reduction of the peak pressures to the edge could be observed, as expected.

5.1.5 Numerical estimation of Bagnold's type impact pressure

Tanizawa and Yue (1992) used a boundary element method to simulate a plunging wave impact on a vertical wall. Simulated results agree well with the experimental (model) data of Chan and Melville (1983). Taking advantage of the numerical simulation, they changed the scale of impact from the experimental tank to the real ocean and derived the following scaling law :

$$p_{peak} / p_{atm} = 1 + aH^{0.6} \qquad 5\text{-}2$$

$$T_{peak} = c\sqrt{\rho_w / \gamma\, p_{atm}}\, H \qquad 5\text{-}3$$

with,

p_{peak} = impact pressure
p_{atm} = atmospheric pressure
T_{peak} = rise time
H = wave height
γ = specific heat ratio
a, c = proportionally constants obtained from simulations

According to their study, a is a function of relative position between the vertical wall and wave breaking point. Its maximum value is a_{max} =*5.0*. c is a constant value c=*0.1*. The free surface motion is not accounted for in Bagnold's model. The trapped air compression ratio rises to this proportional relation because of free surface motion.

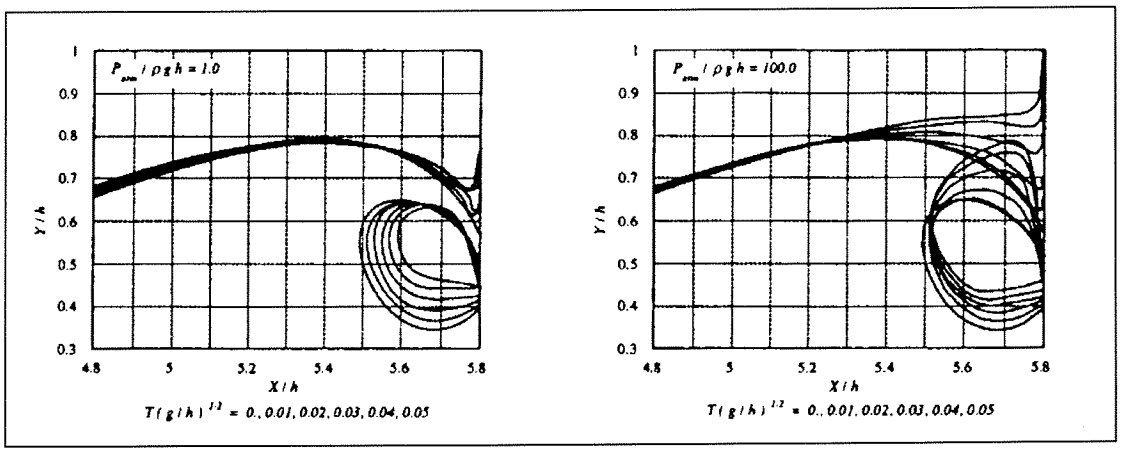

Figure 5-16 Free surface profiles of simulated plunging wave impact [Tanizawa & Yue]

Unfortunately, there are no more data or graphs available on this subject as is mentioned by Tanizawa & Yue (1992) and Chan and Melville (1983).

5.2 Impact load on a vertical wall

This section discusses full scale measurements and a brief attention to the reduction of wave impact pressure due to air entrapment. It is not the intention to review the earlier presented formulae and theories. Only additional data will be presented.

5.2.1 Full scale impact loads on a vertical wall

The duration and the magnitude of a wave impact has been examined extensively in model experiments. The scaling is however not fully understood, for there are many different types of wave impact. The problem of scaling is less understood when water/air mixture is involved in the impact. Some suggestions have been made, but no uniform conclusion can be drawn. Therefore to gain more insight in the time duration of the impact, full scale measurements are very useful.
R.A. Bagnold (1939) has examined the problem of wave impact pressure and added some full scale measurements carried out at Dieppe by MM. Rouville & Petry to his paper. Many valuable data were obtained . Unfortunately the period of measurements was too short (from 1933 to 1935) which resulted in inconclusive results.

These measurements, carried out in Dieppe (France), are shown in Figure 5-17 and Figure 5-18. Note that the vertical scale (pressure) is denoted in ton/m^2. Converting 68 ton/m^2 to SI measures result in,

$$68\frac{ton}{m^2} \cdot 9.81\frac{m}{s^2} = 677\ kPa \qquad 5\text{-}4$$

The maximum observed pressure at Dieppe, according to Bagnold (1939), is 68 ton/m^2 (677 kPa).

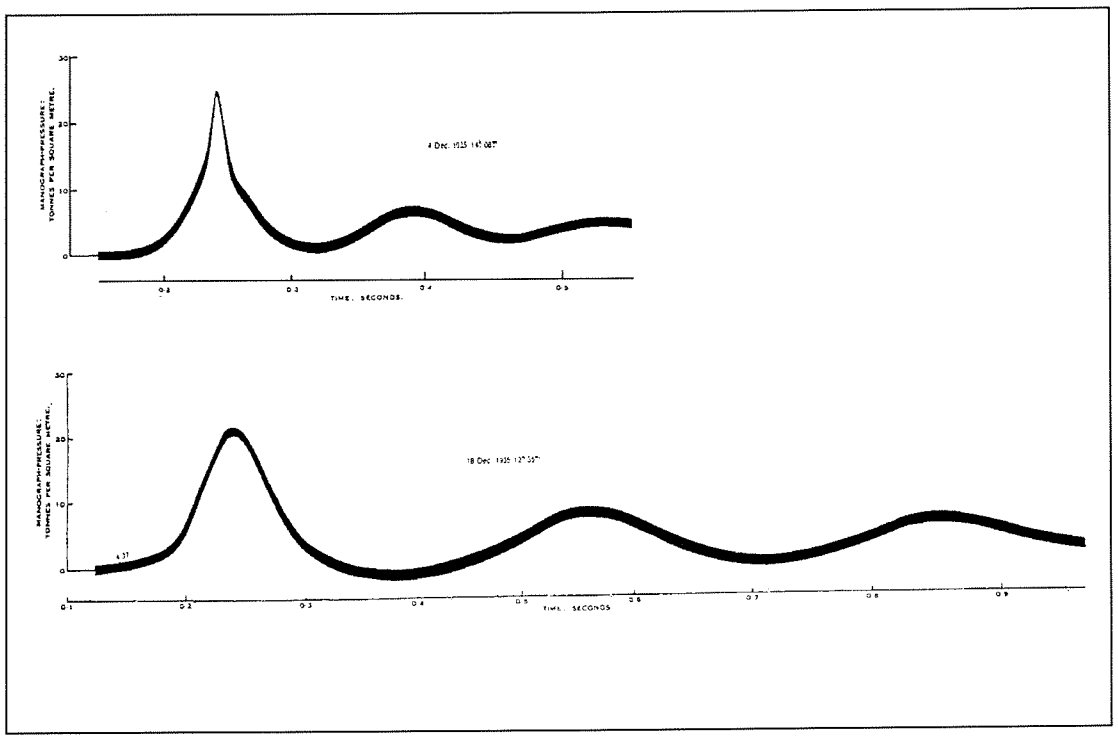

Figure 5-17 Full scale waves pressure impulses, Dieppe [Bagnold 1939]

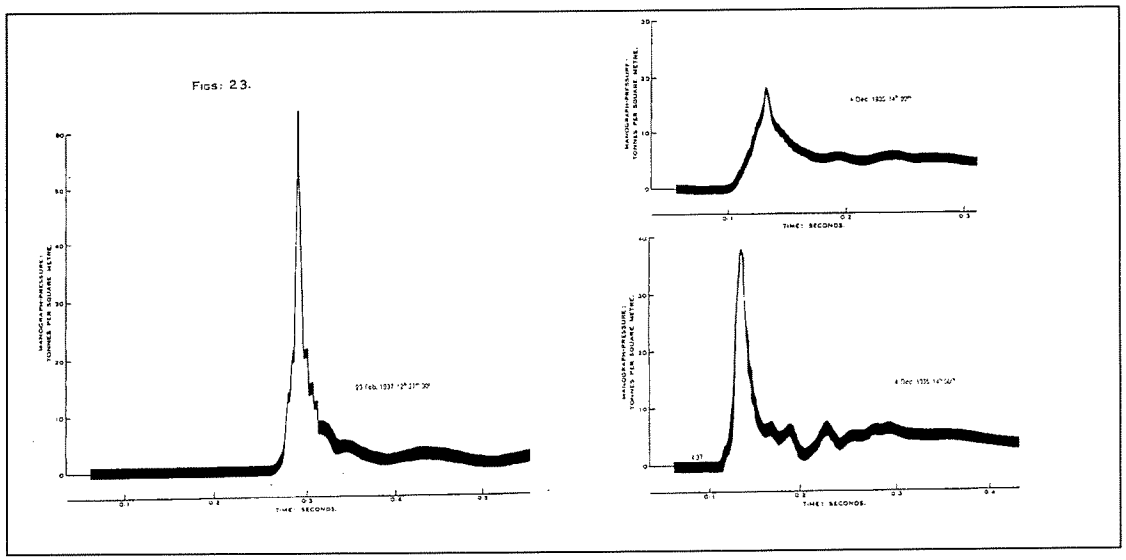

Figure 5-18 Full scale waves pressure impulses, Dieppe [Bagnold 1939]

According to the measurements carried out by MM. Rouville & Petry the rise time is about $1/20^{th}$ to $1/40^{th}$ of a second. The highest peak occurs in the shortest time. This yields in rise times (t_r) of 25 to 40 msec, and a total rise time of 50 to 100 msec.

In Table 5-3 a number of measurements are given.

Table 5-3 Peak pressures exerted by waves on Dieppe breakwater [Minikin1950]

Characteristics of Wave					*Vertical velocity (initial)*	Pressure (kPa)	
Open Sea			At shock			Height above base	
L	*H*	*v*	*H*	v_{horz}	v_{vert}	*0.35 m*	*1.35 m*
(m)	(m)	(m/s)	(m)	(m/s)	(m/s)		
40	1.50	6.0	2.0	12.0	77	-	-
"	"	"	"	"	"	177	69
"	"	"	"	"	"	196	186
"	"	"	"	"	"	510	245
"	"	"	"	"	"	226	304
"	"	"	"	"	"	177	265
45	2.50	6.0	3.50	6.50	31.0	157	78
"	"	"	"	7.50	37.0	392	98
40	1.80	6.0	2.50	8.50	23.0	677	69
"	"	"	"	6.80	25.0	608	29
"	2.50	5.50	3.50	11.50	32.0	363	39

Conclusions full scale impact measurements

- The maximum impact pressure measured at Dieppe (677 kPa) has the same order of magnitude as the full scale bow flare impacts (570 kPa, see section 5.1.2).
- The shape of the impact pressure history of Dieppe has close similarity with the Impact history of the bow flare impacts (see section 5.1.2).
- The rise time (t_r) is about 25 msec for high impact pressure, and about 50 msec for the lower impact pressures. The total impact duration will vary between approximately 50 to 100 msec. This is in good agreement with the full scale measurements of bow flare impact (see section 5.1.2).

5.2.2 Effect on air enclosure on impact load reduction

Air entrapment is believed to reduce impact loads and prolong the impact force on the vertical wall. Scale measurements are conducted in order to illustrate the influence of air enclosure not only with respect to the impact height, but also with respect to the time history of the impact pressure. In the figures below two characteristic time histories are shown, in order to illustrate the reduction of impact pressure and time prolongation of the impact pressure.

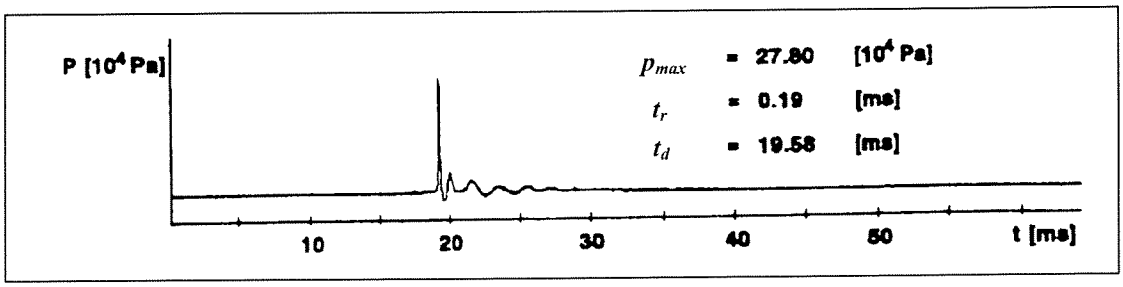

Figure 5-19 Pressure history on smooth wall [Schulz 1992]

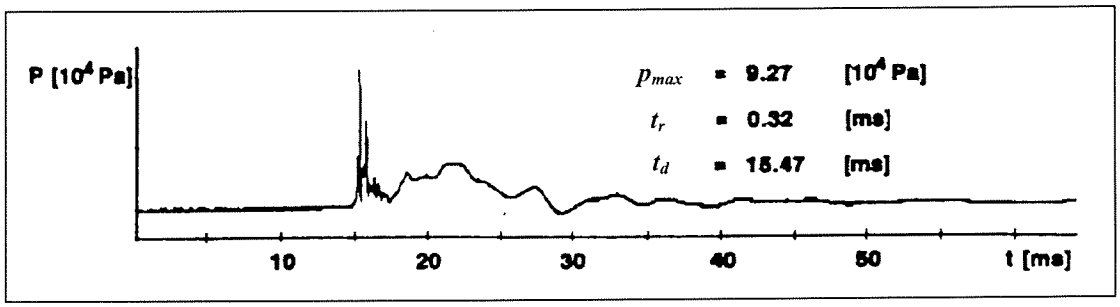

Figure 5-20 Pressure history on wall with air entrapment [Schulz 1992]

As expected the maximum impact pressure is strongly reduced due to air entrapment. The reduction of impact pressure p_{max} is about 1/3rd, the impact rise time (t_r) shows an increase at air entrapment impact. The total impact duration (t_d) has slightly prolonged at air entrapment impact.

5.2.3 Time histories on model scale

In search for formulae to estimate the wave impact load, extensive model tests have been carried out. To gain insight in the impact duration, the time histories are examined. Almost all the time histories show a very short impact duration (order of ms), as can be seen in Figure 5-21. The actual impact duration entered in the formulae is to some authors a matter of opinion. The definition of the impact rise time is not very disputable. The total impact duration however seems to be more difficult. The different views of defining the total impact duration must be understood to avoid misuse in calculation (mostly resulting in overestimation).

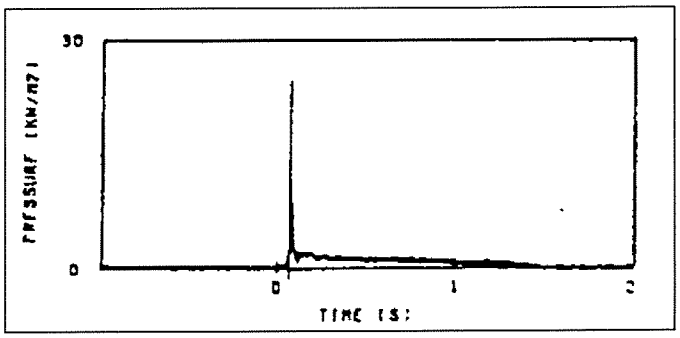

Figure 5-21 Example of time history [Delft Hydraulics 1993]

Two different definitions of wave impact duration are given in the following figures. The influence on the response of the vertical structure, i.e. vertical breakwater, is substantial. When an engineer doesn't reckon with the definition of impact duration, the designer runs the risk of overestimating the wave impact load in a very conservative way.

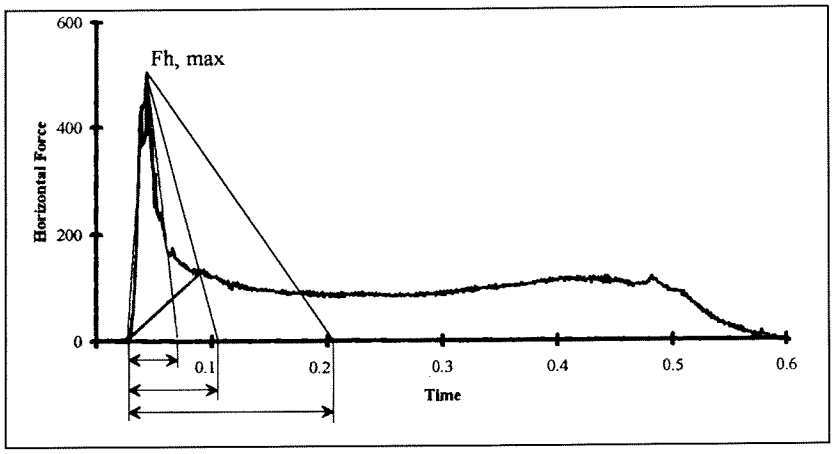

Figure 5-22 Schematising impact duration, method 1

When modelling an impact force on a structure at a different time by way of a simplified triangular load, there will be not much room for mistakes and overestimating due to modelled impact duration. Figure 5-22 visualises three different definitions of the total impact duration.

5.3 Conclusions on impact duration and impact pressure

In search for an analogy of the wave impact load, we have found some valuable examples of wave impact and slamming of ships onto/into waves. When trying to use formulae or theories of maritime engineering we must always bear in mind that the hull of a ship encountering the water can be quite different to a vertical breakwater reflecting a wave.
In quasi-static range the analogy with impacts on ships will not be applicable. For that are the differences between wave impact on ships and vertical walls to large.
However, when considering impulsive impacts on a bow of a ship (bow flare impact) or bottom slamming, the influence of gravity on impulsive (or impact) pressure will decrease, and the applicability will increase.

The following observation has been made :

- The maximum impact pressure is about 500 to 650 kPa, as could be concluded from full scale measurements at a vertical breakwater (Dieppe) and bow flare impacts at a ship.
- The impact rise time (t_r) is approximately 10-20 msec at bow flare measurements and 25-50 msec at Dieppe measurements. Both tests show same order of magnitude. The total impact duration will be approximately 20-40 msec and 50-100 msec respectively.
- The 'scatter' of impact pressure at wedge impact tests is very large. The difference between two pressure gauges, both at the same location is 13%, with an even larger standard deviation (19%). The rise time (t_r) is very short (order of magnitude is 5 msec).

Conclusions:

- The analogy of the bow flare impact and the wave impacts on a vertical wall is justified, for the full-scale measurements of bow-flare slamming and the full-scale measurements at Dieppe [Bagnold 1939] show large similarity in maximum pressure and impact duration.

- The duration of the impact pressure at a vertical breakwater is much shorter than assumed in the latest formulae (Schmidt et al and KO&K). The impact duration is about 20 to 100 msec, with an average of about 20-40 msec.

- The maximum impact pressure is about 500 to 650 kPa. The agreement of bow flare slamming and impacts at Dieppe are very close.

- The scatter of maximum impact pressure found at wedge tests at model scale and bottom slamming tests at model scale show large scatter. Therefore is justified to reduce the width of the wave impact. The high impact pressures do occur, but are local.

6. Dynamic model

In order to determine the influence of the wave impact on the stability of the vertical breakwater a dynamic analysis is required. By deriving a dynamic model and applying a horizontal force upon the caisson the dynamic behaviour can be estimated, and therefore also the forces onto the foundation of the caisson. After the dynamic calculation of the vertical breakwater the influence of wave impact for the stability of the vertical breakwater can be determined.

In this chapter the derivation of the spring dashpot model, spring and dashpot elements and masses are treated. Also the derivation of the maximum forces onto the foundation will be described.

6.1 Spring dashpot model

The dynamic behaviour of a vertical breakwater in nature is rather complex. Besides accurate modelling of the spring and dashpot elements also 3 dimensional effects, such as interaction between caissons, play a significant role.
To gain insight of the dynamic behaviour of the caisson and the related failure modes some assumptions should be made. Some assumptions are very conservative. For example the eigenperiods of the Genoa Voltri breakwater can only be modelled using a very complex 3 dimensional model to correspond with the measurements made by Lamberti and Martinelli (1998).

These assumptions are made to simplify the modelling. These will be,

Assumptions regarding the caisson:
- no interaction between caissons (conservative assumption)
- no 3D influences of soil pressures

Assumptions regarding spring and dashpot elements :
- linear behaviour of the spring elements
- proportional damping of the dashpot elements
- soil pressures calculated directly from the subsoil (conservative assumption)

Assumptions regarding failure modes:
- no uplift considered in first modelling
- no local failure modes considered

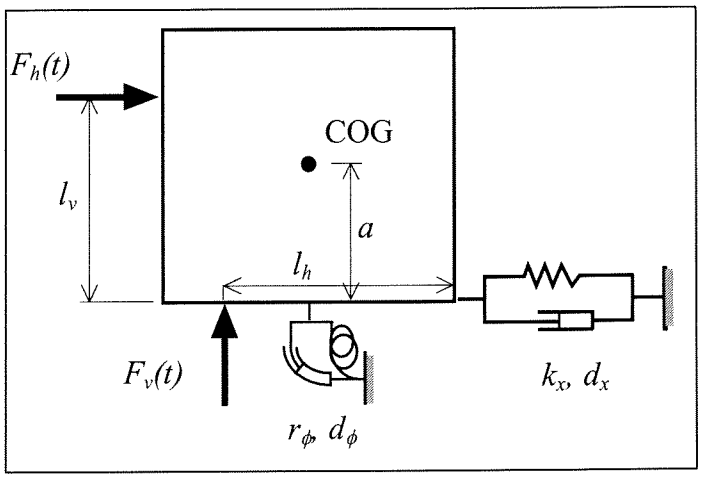

Figure 6-1 Spring dashpot model

With the displacement method the differential equations, which describe the dynamic behaviour of the caisson, can be determined. This results in,

$$\begin{bmatrix} M & 0 \\ 0 & \Theta \end{bmatrix} \cdot \begin{bmatrix} \ddot{x} \\ \ddot{\phi} \end{bmatrix} + \begin{bmatrix} d_x & -d_x a \\ -d_x a & d_\phi + d_x a^2 \end{bmatrix} \cdot \begin{bmatrix} \dot{x} \\ \dot{\phi} \end{bmatrix} + \begin{bmatrix} k_x & -k_x a \\ -k_x a & r_\phi + k_x a^2 \end{bmatrix} \cdot \begin{bmatrix} x \\ \phi \end{bmatrix} = \begin{bmatrix} F(t) \\ M(t) \end{bmatrix} \qquad 6\text{-}1$$

with,

M	=	mass breakwater
Θ	=	inertia of breakwater
a	=	vertical distance COG to bottom (i.e. ½ h_c)
k_x	=	horizontal spring constant
r_ϕ	=	rotational spring constant
d_x, d_ϕ	=	damping constants, horizontal and rotation
$F(t)$	=	horizontal wave load
$M(t)$	=	rotational wave load

$$M(t) = F_h(t) \cdot \left(l_v - a\right) + F_v(t) \cdot \left(l_h - \tfrac{1}{2} h_c\right) \qquad 6\text{-}2$$

This equation can be solved numerically.

6.2 *Added masses*

The caisson is not the only mass that can and will move due to the wave impact. The rubble mound foundation will move if the caisson is rotating or moving in vertical and/or horizontal direction. As for the water surrounding the caisson - despite of the incoming wave - any movement of the caisson will displace water. When considering this in a dynamic calculation, the effect of the foundation and the water has to be added to the calculation. This is named in the description 'added hydro-dynamic mass' and 'added geo-dynamic mass'. The use of the word 'mass' is misleading. It has nothing to do with mass, but everything with a dynamic approach. The influence of the foundation and the surrounding water is simply added in the equations via the masses.
The derivation and the calculation of these added masses is stated in this section.

6.2.1 Hydro-dynamic mass

When the caisson is loaded with periodic or oscillating forces and therefore movements the water surrounding the caisson will have to move also. This amount of water - which is forced to move - is called the "added water mass", or better called the "hydro-dynamic mass".
The theoretical basis of the hydro-dynamic mass is weak, and therefore liable for discussion It is logical that the hydro-dynamic mass is dependent to the frequency of the response of the caisson. This is not true in the equations presented below. A formula that deals with this discrepancy is yet to be found.

On theoretical basis a formula has been derived. Assuming incompressible and irrotational two dimensional potential flow it can be shown that (seaward side of the caisson only),

$$m_{hyd,hor} = L_c \times 0.543 \rho_w d^2 \qquad 6\text{-}3$$

with,

$m_{hyd,hor}$ = the hydrodynamic mass for horizontal oscillations
d = water depth, in front of the caisson

The equation above refers only to the water on the seaward side of the caisson.

Pendulum tests on a caisson have been conducted for different water depths. The results of these tests show that the equation above will underestimate the hydro-dynamic mass. It is better to use the equation (derived for both sides of the caisson),

$$m_{hyd,hor} = L_c \times 1.40 \rho_w d^2 \qquad 6\text{-}4$$

6.2.2 Geo-dynamic mass

When the caisson is forced to move a part of the soil has to move along with the caisson. Therefore we have to add this mass to the differential equations. The added mass of the soil is called the geo-dynamic mass. The geo-dynamic mass is assumed to be the same for horizontal and vertical oscillations. This would not influence the outcome of the calculations anyway, because the wave impacts generally induces horizontal and rotational displacements. The theoretical basis of the geo-dynamic equation is weak. This equation is also independent of the frequency of the caisson.

$$m_{geo} = \frac{0.76 \rho_s R^3}{2 - \nu} \qquad 6\text{-}5$$

with,

ρ_s = mass density of the soil
ν = Poisson's ratio (0.2-0.4)
R = $\sqrt{(B_c L_c / \pi)}$

6.3 *Spring elements*

Spring and dashpot elements will be derived according to Richart, Hall and Woods "Vibrations of soil and foundations" (1970) and the NGI publication nr. 198, volume 1 "Foundation design of vertical breakwaters" (1996), which is partially based upon Richart, Hall and Woods.

The determination of a spring constant, for use with a dynamically loaded foundation, involves essentially the same steps as determination of the load-settlement relationship for a

statically loaded foundation. In each case the key is to subject a small mass of soil to the same initial stresses and stress changes as will be experienced under the actual foundation. In the case of dynamically loaded foundations, this means that the soil should be subjected to an initial static stress equal to the stress expected under the actual foundation as a result of the dead load of the foundation plus geostatic stresses, and to strain changes approximately equal to those expected as the result of the dynamic loading. The frequency with which the stress change is applied to the specimen is relatively unimportant.
The most commonly used approach is to employ formulae from the theory of elasticity.

The spring element can be found from:

$$k_x = K_x B_c L_c \qquad 6\text{-}6$$

$$r_\phi = \tfrac{1}{12} K_\phi B_c^3 L_c \qquad 6\text{-}7$$

with,

k_x	=	horizontal spring element
r_ϕ	=	rotational spring element
B_c	=	width of the foundation
L_c	=	length of the foundation
K_x, K_ϕ	=	parameters for determining spring elements

The parameters K_x and K_ϕ are functions of the shear modulus G, and the Poisson ratio and B and L. It is possible to write non-dimensional parameters in such way that the parameters K_x and K_ϕ depend only from B/L. See Table 6-1 below.

Table 6-1 Parameters for determination of foundation stiffness [NGI 1996]

B/L	K_xB/G	$K_\phi B/G$
0.1	0.00	8.0
0.3	1.75	9.0
1.0	2.75	10.5
3.0	4.50	15.0
10.0	10.50	25.0

with,

B	=	width of the foundation
L	=	length of the foundation
G	=	shear modulus of the soil
K_x, K_ϕ	=	parameters for determining spring elements

The values in this table are mean values from table 6.3.1 found in the NGI rapport.
The values of K_x and K_ϕ are linear interpolated to derive the values for k_x and r_ϕ.

6.4 Dashpot elements

The dashpots of a lumped system represents the damping of the soil. There are two types of damping: loss of energy through propagation of waves away from the immediate vicinity of the foundation, and the internal energy loss within the soil owing to hysteretic and viscous effects.
The use of dashpots in the lumped system does not imply that it is believed that the soil has viscous properties. Rather, dashpots are used in order to derive simple and useful mathematical expressions for the response of the lumped system. Damping rations are chosen to represent a equivalent amount of damping, and not to represent the a particular type of damping.

The damping due to wave propagation is often termed "*radiation damping*" or "*geometrical damping*". Each time that the foundation moves downward against the soil, a stress wave is originated. As this wave moves away from the foundation it carries with it some of the energy put into the soil. Since this energy is then not available to participate in a resonance phenomenon, a damping effect is introduced.
The similar can be said about the interlocking of the caissons. The oscillation amplitudes of the adjacent caissons are about 1/3rd to the excitated (centre) caisson, showing that a large amount of energy is subtracted from the excited caisson by a wave propagating along the breakwater. This energy is not available to participate in a resonance phenomenon, resulting in a damping effect.

6.4.1 Internal damping

The lumped damping parameter for any particular foundation-soil system will include both the effects of geometrical and internal damping. If we take the value of 0.03 to represent a typical internal-damping ratio, then by comparing this value with the geometrical damping (e.g. 0.20) we can estimate the contribution of each.
It is evident from this examination that for vibrations in translatory modes, the geometrical damping overshadows the internal damping to the point where the latter may be disregarded in preliminary analyses.
On the other hand, for the rotary modes of vibration, rocking, the geometrical damping is small and these two damping terms may be of the same order of magnitude. In this case, the internal damping is important and should be included.

Table 6-2 Some typical values of internal damping in soils [RHW, 1970]

Type soil	Equivalent D	Reference
Dry sand and gravel	0.03-0.07	Weissmann and Hart (1961)
Dry and saturated sand	0.01-0.03	Hall and Richart (1963)
Dry sand	0.03	Whitman (1963)
Dry and saturated sands and gravels	0.05-0.06	Barkan (1962)
Clay	0.02-0.05	Barkan (1962)
Silty sand	0.03-0.10	Stevens (1966)
Dry sand	0.01-0.03	Hardin (1965

6.4.2 Geometrical damping - horizontal and rocking

The existence of geometrical damping or radiation damping has been revealed by the theory of half-space (Richart, Hall, Woods, 1970). This theory will be used to evaluate an equivalent value of damping ratio for horizontal and rocking motions only.
The formulae derived by Richart , Hall and Woods are used to derive the values of the dashpot elements. The formulae used are:

$$d_x = 2 \cdot D_x \sqrt{k_x M_{tot}} \qquad 6\text{-}8$$

$$d_\phi = 2 \cdot D_\phi \sqrt{k_\phi \Theta_{tot}} \qquad 6\text{-}9$$

The values D_x and D_ϕ are calculated with,

$$D_x = \frac{0.288}{\sqrt{B_x}} \qquad 6\text{-}10$$

$$D_\phi = \frac{0.15}{\left(1 + n_\phi \cdot B_\phi\right)\sqrt{n_\phi \cdot B_\phi}} \qquad 6\text{-}11$$

The values B_x and B_ϕ are calculated with formulae written below. The value n_ϕ is derived (with linear interpolation) from table below.

$$B_x = \frac{7-8\nu}{32(1-\nu)} \cdot \frac{M_{tot}}{\rho_w R^3} \qquad 6\text{-}12$$

$$B_\phi = \frac{3(1-\nu)\cdot\left(\Theta_{tot} + M_{tot}\cdot a^2\right)}{8\rho_w R_\Theta^5} \qquad 6\text{-}13$$

with,

a	=	vertical distance COG to bottom (i.e. ½ h_c)
d_x	=	horizontal damping element
d_ϕ	=	rotational damping element
M_{tot}	=	total mass of caisson (with added masses)
Θ_{tot}	=	total inertia of caisson
D	=	internal damping parameter
D_x, D_ϕ	=	geometrical damping parameter

Table 6-3 Parameter n_ϕ as a function of B_ϕ

B_ϕ	n_ϕ
5	1.08
3	1.11
2	1.14
1	1.22
0.8	1.25
0.5	1.38
0.2	1.6

The equivalent radius R and R_Θ are derived with formulae below:

$$R = \sqrt{\frac{B_c L_c}{\pi}} \qquad 6\text{-}14$$

$$R_\Theta = \sqrt[4]{\frac{B_c^3 L_c}{3\pi}} \qquad 6\text{-}15$$

6.4.3 Geometrical damping - interlocking

Due to the positioning of the caissons next to each other and the 3 dimensional effect of the soil locking between the caissons is evidently present. The prototype measurements by Lamberti and Martinelli (1998) shows that the extend of interlocking is large. The oscillation amplitudes are about 1/3rd of the oscillation of the excited caisson, showing that a large amount of energy is subtracted. This is visualised in Figure 6-2 below.

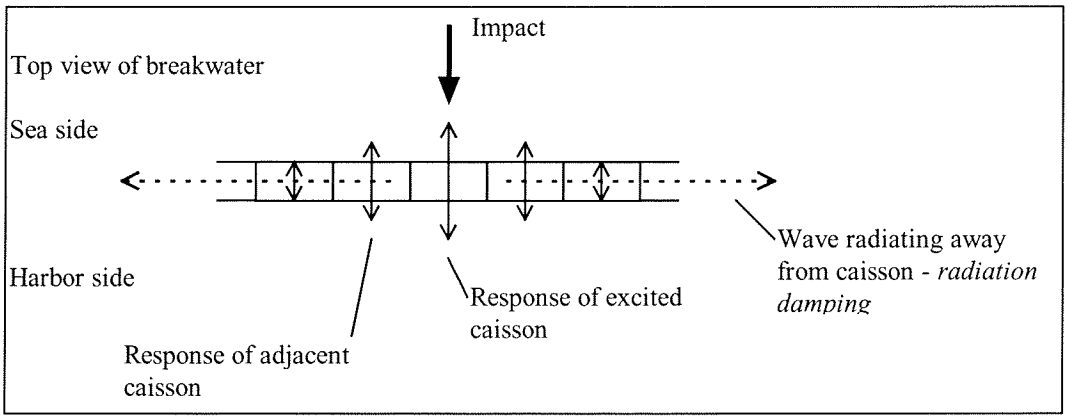

Figure 6-2 Geometrical damping - Interlocking of caissons

This phenomena can be modelled by adding a damping coefficient $D_{interlock}$ or by extending the length (L_c) of the caisson, thus assuming a longer caisson than in nature. This is a more elegant way to model the interlocking of the caisson, but from Table 6-4 it can be concluded that the eigenperiod of the caisson will decrease at increasing effective length of the caisson (L_{eff}).

Table 6-4 Interlocking caisson by L_{eff}/L_c

L_{eff}/L_c		1.0	1.5	2.0	2.5	Measured by Lamberti & Martinelli	
	Unit					mean	stdev
k_x	$\times 10^9$ (N/m)	7.57	9.84	12.1	11.0	..	..
r_ϕ	$\times 10^{11}$ (Nm/rad)	9.49	13.59	17.7	21.4	..	..
d_x	$\times 10^8$ (Ns)	3.80	5.58	7.42	8.13	..	..
d_ϕ	$\times 10^{10}$ (Nms/rad)	2.01	2.97	3.94	4.88	..	..
f_1	(Hz)	*1.374*	*1.311*	*1.275*	*1.165*	*1.5*	*0.24*
f_2	(Hz)	*3.859*	*3.643*	*3.528*	*3.212*	*2.87*	*0.58*
M	$\times 10^7$ (kg)	4.788	7.239	9.716	12.22	..	..
Θ	$\times 10^9$ (kgm^2)	3.424	5.199	6.996	8.812	..	..
a_{max}	m/sec^2					0.018	
a_{min}	m/sec^2					-0.013	

When calibrating the dynamic model according to the prototype measurements the parameter $D_{interlock}$ will be added to the horizontal and rotational damping element to model the response of the Genoa Voltri breakwater nicely.

7. Failure modes and maximum soil pressure

In this chapter the failure modes and an estimation of the maximum soil pressures are given.

7.1 Failure modes of vertical breakwaters.

Extensive studies have been performed in order to investigate the failure modes of the vertical breakwaters. The objective of these studies was to identify the most relevant modes and reasons of failure of vertical breakwaters in subject to breaking wave loads. For this purpose all relevant failures in the past have been analysed.

The main reasons for failure are summarised figure 7-1, showing that there are :

1. reasons inherent to the structure itself
2. reasons inherent to the hydraulic conditions and loads
3. reasons inherent to the foundation and local morphological changes

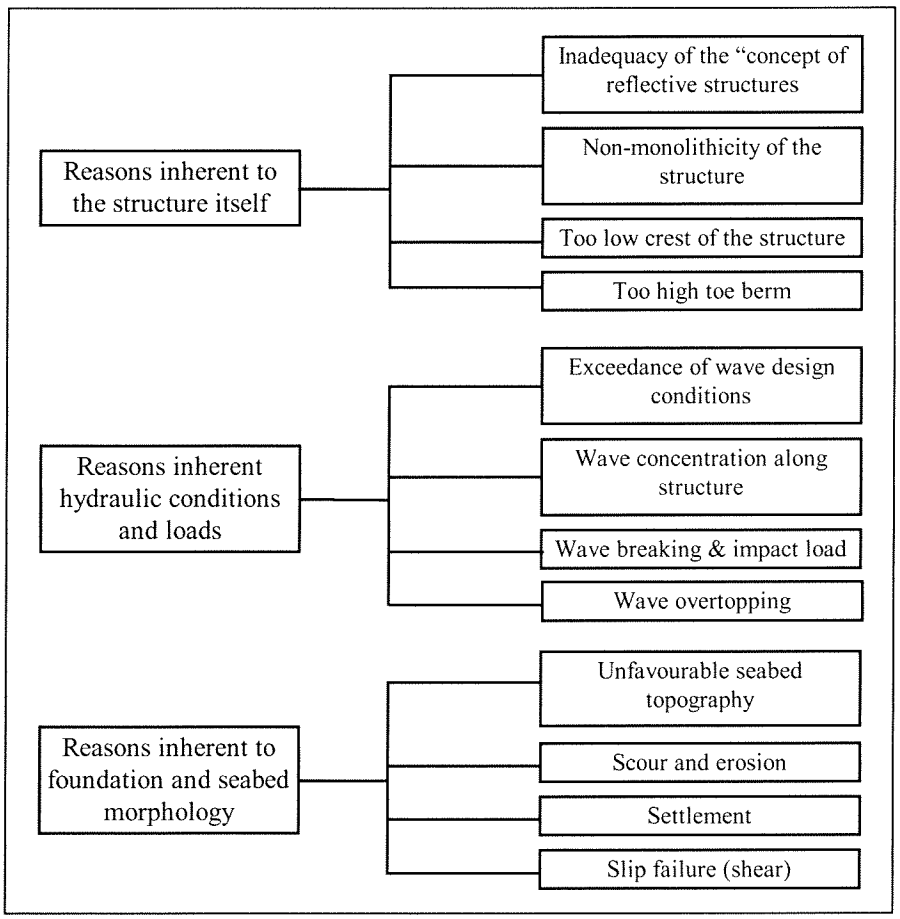

Figure 7-1 Reasons of failure of vertical breakwaters [Oumeraci 1994]

The principal modes of failure showed that various overall and local failure modes may occur. A number of important failure modes is given figure 7-2.
The failure modes which are most important to this graduation study are the overall failure modes;

- sliding of the caisson over its foundation
- overturning of the caisson
- exceeding of the bearing capacity of the foundation subsoil, which leads to settlement and probably to slip failure of the foundation.

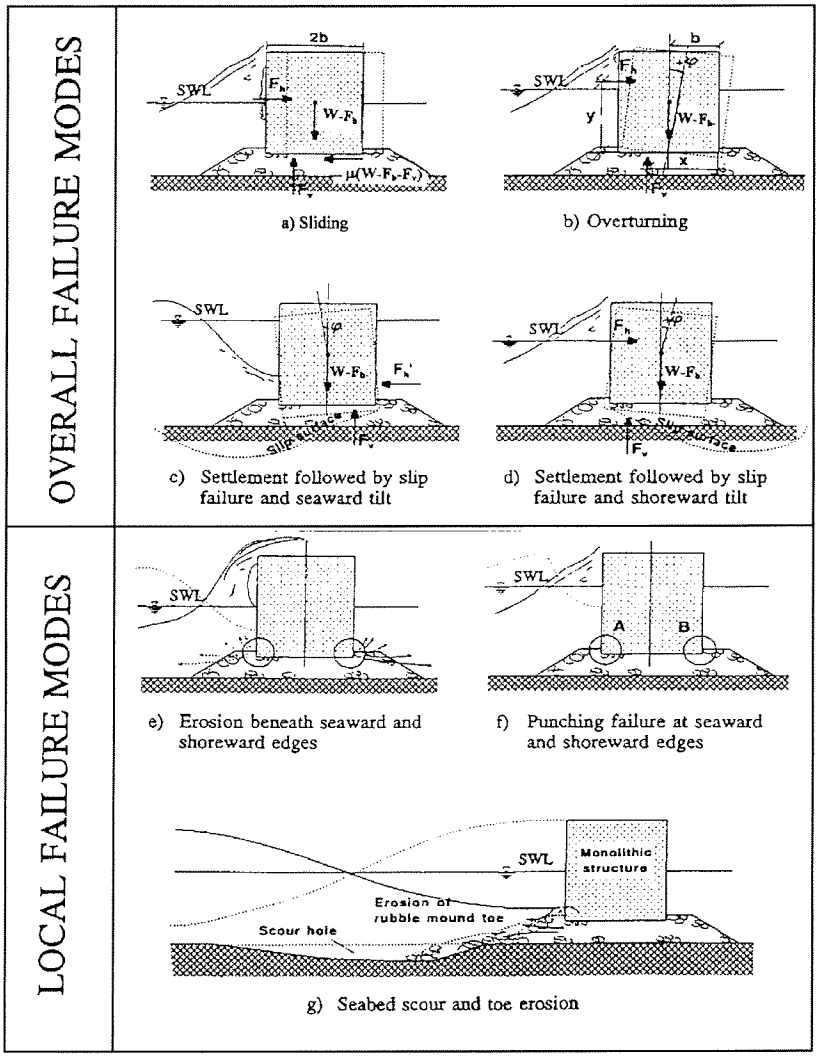

Figure 7-2 Overall and local failure modes [Oumeraci 1994]

Since there is no relevance with the scope of this graduation study, the following failure modes are not taken into account:

- Seaward tilt of the breakwater
- Local failure modes such as scour of the berm or failure of the caisson itself

7.2 Soil pressure

In the scope of this graduation project the failure of the vertical breakwater is considered only by sliding and overturning due to wave impact load. The dynamic model gives the maximum displacement and rotation of the maximum soil pressure gives the upper limit of sliding force and rotation force, thus giving the displacement and rotation capacity of the caisson. The overall failure modes are shown in the figure below.

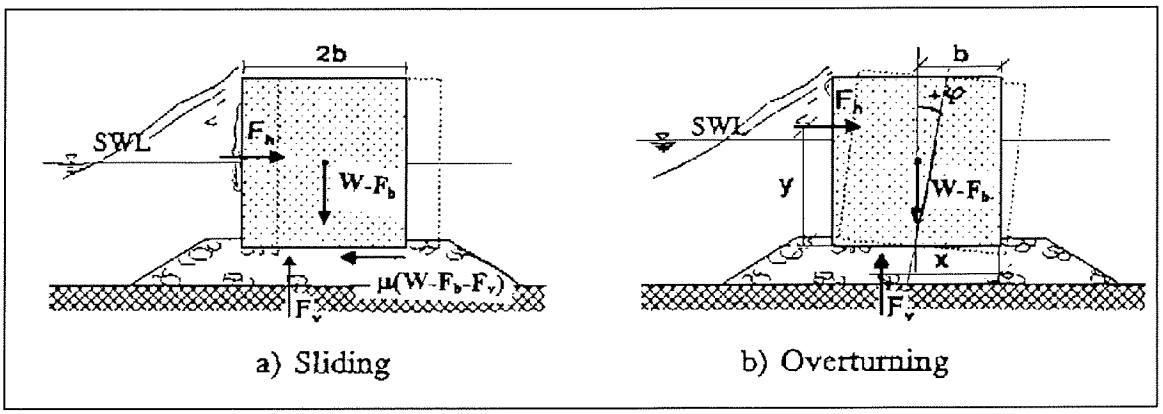

Figure 7-3 Overall failure modes [Oumeraci 1994]

7.2.1 Sliding

The bearing capacity for sliding between caisson and soil is,

$$F_v = \left(W - F_b\right) \cdot \tan\phi \qquad 7\text{-}16$$

with,

W	=	weight of caisson
F_b	=	buoyancy of caisson
ϕ	=	internal friction of soil

7.2.2 Overturning

According to the EUROCODE the maximum rotation force is reached at,

$$e = 0.3 \cdot B_c \qquad 7\text{-}17$$

with,

e	=	eccentricity of the vertical force
B_c	=	width of the caisson

This is a rough estimation. More accurate determination of the maximum rotation capacity can be made by the theory by Brinch Hansen [Verruijt 1993].

7.3 *Theory of Brinch Hansen*

With this theory the maximum bearing pressure of a strip foundation can be determined. A strip foundation shows good agreement with the foundation of a vertical breakwater.
The theory of Brinch Hansen has been the subject of many discussions. Although the theoretical base of this formula is weak, it can give a good approximation of the bearing pressure of the foundation. The theory has been derived for dry conditions, but can also be used for 'wet' conditions.

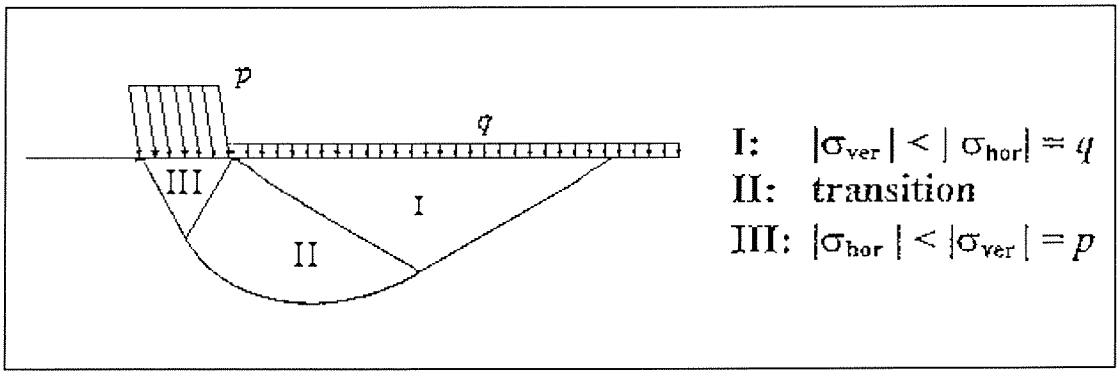

Figure 7-4 Definition sketch theory of Brinch Hansen [according to Verruijt 1993]

In the above sketch the resultant of the horizontal force (i.e. wave load) and the weight of the caisson is visulalised by the inclination of the pressure p.
To apply the theory of Brinch Hansen correctly the calculation of rotation capacity should be derived through the following sketch,

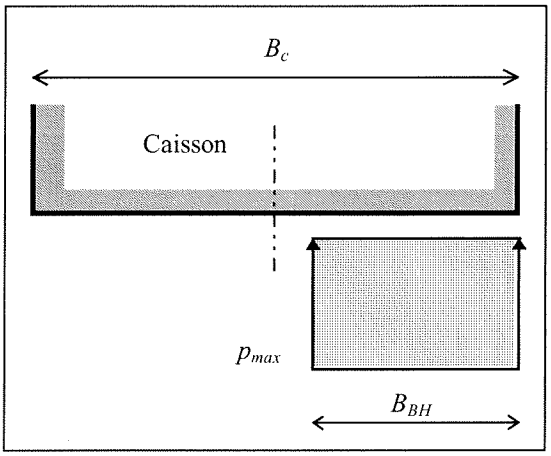

Figure 7-5 Sketch rotation pressure

The vertical equilibrium should of course always be respected, thus resulting in a value of B_{BH}.
The maximum rotation capacity is,

$$M_{\max} = \left(\tfrac{1}{2}B_c - \tfrac{1}{2}B_{BH}\right)\cdot\left(B_{BH}p_{\max}\right) \qquad 7\text{-}18$$

with,

M_{max}	=	maximum rotation capacity per unit length of caisson
B_c	=	width of caisson
B_{BH}	=	length of soil pressure, depending on vertical equilibrium

p_{max} = maximum soil pressure according to the theory of Brinch Hansen

7.3.1 Calculation of maximum bearing pressure (p_{max})

Brinch Hansen used the theory of Prandtl and defined the bearing pressure of a strip foundation (p). The formulae below are used to estimate the maximum soil bearing pressure.

$$p = i_c s_c c N_c + i_q s_q q N_q + i_\gamma s_\gamma \tfrac{1}{2} \gamma_s B_{eff} N_\gamma \qquad 7\text{-}19$$

with,

p	=	maximum bearing pressure of the foundation (per unit length of caisson)
i_c, i_q, i_γ	=	inclination factors, reduction related to the direction of the load
s_c, s_q, s_γ	=	reduction factors related of the shape of the foundation
N_q, N_c, N_γ	=	dimensionless constant
c	=	cohesion
q	=	pressure next to the foundation
γ_s	=	weight of soil (kN/m^3)
B_{eff}	=	effective width of the foundation (i.e. caisson)
e	=	eccentricity of the load
ϕ	=	internal friction of the soil

Inclination factors (i_c, i_q, i_γ)

$$i_c = -\frac{\frac{F_h}{B_{eff} L_{eff}}}{c_u + \frac{F_g}{B_{eff} L_{eff}} \cdot \tan\phi} F_h \qquad 7\text{-}20$$

$$i_q = i_c^2 \qquad 7\text{-}21$$

$$i_\gamma = i_c^3 \qquad 7\text{-}22$$

with,

B_{eff}	=	effective width of the foundation (caisson)
L_{eff}	=	effective length of the foundation (caisson)

Shape factors (s_c, s_q, s_γ)

$$s_c = 1 + 0.2 \cdot \frac{B_{eff}}{L_{eff}} \qquad 7\text{-}23$$

$$s_q = 1 + \frac{B_{eff}}{L_{eff}} \cdot \sin\phi \qquad 7\text{-}24$$

$$s_\gamma = 1 - 0.3 \cdot \frac{B_{eff}}{L_{eff}} \qquad 7\text{-}25$$

Dimensionless factors (N_c, N_q, N_γ)

$$N_q = \exp\left(\pi \cdot \tan\phi\right) \cdot \tan\left(\frac{\pi}{4} + \frac{\phi}{2}\right)^2 \qquad 7\text{-}26$$

$$N_c = \left(N_q - 1\right) \cdot \cot\left(\phi\right) \qquad 7\text{-}27$$

$$N_\gamma = 2 \cdot \left(N_q - 1\right) \cdot \tan\phi \qquad 7\text{-}28$$

7.3.2 Validity formula of Brinch Hansen for dynamic conditions

The formula of Brinch Hansen is derived for static loading. The formula can also be used for dynamic loading, when for all loading situations the following condition is fulfilled [Verruijt 1996],

$$\omega < \omega_0 \qquad 7\text{-}29$$

with,

ω = the radian frequency of motion of the structure

$$c_s = \sqrt{\frac{E_s}{\rho_s}} \qquad 7\text{-}30$$

$$R = \sqrt{\frac{B_c \cdot L_c}{\pi}} \qquad 7\text{-}31$$

$$\omega_0 = \frac{2 \cdot c_s}{R} \qquad 7\text{-}32$$

With the geometry of the Genoa Voltri breakwater and the (static) conditions for the subsoil filled in the equations above, this yields to,

$$\omega_0 = 49$$

and from calculations of the eigenfrequencies of the Genoa Voltri breakwater (about 1.2 and 4.5), the condition in equation above ($\omega < \omega_0$) is always fulfilled, ergo the formula of Brinch Hansen is valid during impact conditions.

7.4 Calculation of maximum soil pressure at failure

The formulae derived in previous paragraphs and chapters concerning soil pressures are used for the calculations in the next chapter. The maximum soil forces and sliding and rocking force are calculated in this paragraph.

Table 7-1 Subsoil conditions

	ϕ	c_u (Pa)	E(MPa)	ν	ρ_s/ρ_w
min	25	-	139	0.29	-
char	30	2	192	0.33	1.48
max	35	-	202	0.37	-

The Brinch Hansen formula of the previous paragraph is used in MathCad sheet "*Brinch Hansen.mcd*" (see annex). The values are presented in Table 7-2.

The subsoil conditions are visualised in Table 7-2 below. Note the difference in bearing pressure at increasing horizontal force.

Table 7-2 Maximum bearing pressure p_{max} with and without inclination

p_{max}	no inclination	horizontal force (by Goda's formulae)
effective width of foundation	$B_{eff} = 22.5\ m$	$B_{eff} = 16.4\ m$
$\phi = 31^0$	2059 kN/m^2	638 kN/m^2
$\phi = 33^0$	2844 kN/m^2	955 kN/m^2
$\phi = 35^0$	3947 kN/m^2	1423 kN/m^2

The effective width of the caisson (B_{eff}) decreases when the vertical impact pressure increases. In MathCad sheet "*Brinch Hansen.mcd*" (see annex Brinch Hansen.mcd) the vertical force is a reasonable equivalent of the impact pressure, resulting in a conservative value for p_{max}. The respective sliding and rocking force are given in table below.

Table 7-3 Maximum sliding and rocking force with inclination (Goda force)

	$F_{v,max}$	M_{max} (Nm)
B_{eff} (m)	16.4	16.4
$\phi = 31^0$	1.16×10^8	1.16×10^9
$\phi = 33^0$	1.25×10^8	1.41×10^9
$\phi = 35^0$	1.62×10^8	1.57×10^9

8. Derivation of computer model

The program software chosen to calculate the differential equations is MathCad. This program allows constants entered in physical shape as one would write it in a formula. This leads to an open and clear program listing, accessible for many readers.

In this chapter the verification of the dynamic model and the calculations of the wave impact loads are presented.

8.1 Calibration of the dynamic model

The calibration of a numerical model is essential for the latter evaluation of the outcome of the calculation. The verification of the dynamic model will be done with the prototype measurements of the Genoa Voltri breakwater carried out by Lamberti and Martinelli (1998).

8.1.1 Description of the prototype measurements

Three kinds of excitations were used, the vertical (type A) and horizontal hit (type B) of a sac, half filled with sand and weighing 2 tons, and the impact of a 100 ton tugboat (type C). 15 accelerometers were used for monitoring the caisson oscillations, while the last was placed on the hitting body in order to get information on the applied force. Almost no problem of overloading was found.
The sac fall was not completely free therefore the final speed of the sac was measured with the aid of a video camera. It varied between 5 and 10 m/sec. The speed of the tugboat was close to 0.3 m/s, and the impact force was evaluated by an accelerometer fixed to the tugboat. The three obtained signals (sway, heave and rolling) have been analysed in the frequency domain.

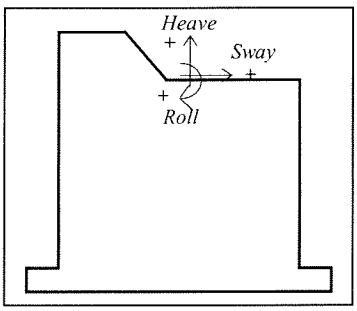

Figure 8-1 Sway, heave and roll

8.1.2 Description of the analysis

Due to the system dynamics the different tests enhance different modes of excitation. The various modes appear in each of the three signals.
The vertical fall of the sac excites mainly mode m3 and with progressively lower intensity mode m2 and m1. The sac hitting the caisson vertical excites mode m2, mode m1. The tugboat will excite mainly mode m1 and m2. Due to the co-ordinate system it is not convenient to define a centre of rotation far from the zone where the accelerometers are placed, since this would increase the noise in the signals and the accuracy of the measurements.
With these hypothesis the periods of oscillations have been interpreted, as shown in the following. It was possible to evaluate the higher centre of rotation

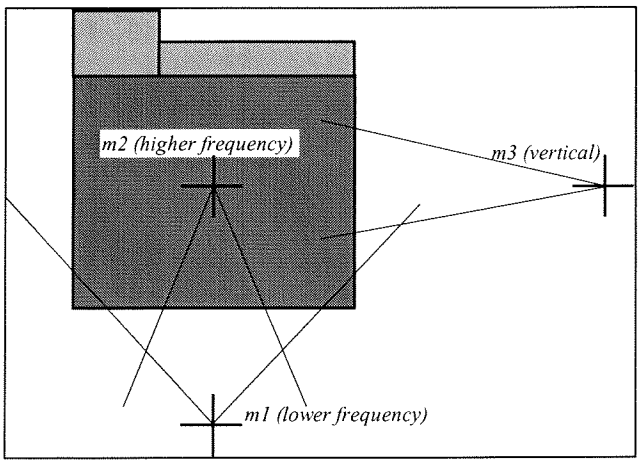

Figure 8-2 Scheme of modes of oscillations

8.1.3 Results of the prototype measurements

The natural frequencies of oscillation of vertical breakwater caissons in Voltri have been measured. They agree with previous values.
The rotation centres identified, show that only mode m2 has its centre within the caisson, whereas mode *m1* and *m2* centres are far outside the caisson.

The adjacent caissons were found to be excited as well particularly for mode *m1*. A large amount of energy is then subtracted from the central caisson by the wave propagating along the breakwater.

Table 8-1 The natural periods of oscillation

Test type	Sway signal (Hz)		Heave signal(Hz)	Roll signal(Hz)
	m1	*m2*	*m3*	*m2*
1C	1.4	2.3	-	2.3
2A	1.2	2.5	3.0	2.5
2B	1.4	2.7	-	-
2C	1.4	2.5	-	2.5
3A	1.8	3.6	4.3	3.6
3C	1.8	3.6	-	3.6
mean	1.5	2.87	3.65	2.9
stdev	0.24	0.58	0.92	0.64

With test type
A = vertical falling sac, excites mainly mode *m3*
B = horizontal hitting sac, excites mainly mode *m1* and *m2*
C = tugboat collision

8.1.4 Tug boat collision

The tugboat collision will be used for verifying the dynamic model. In order to do so the force applied by the tugboat and the response of the caisson is needed.

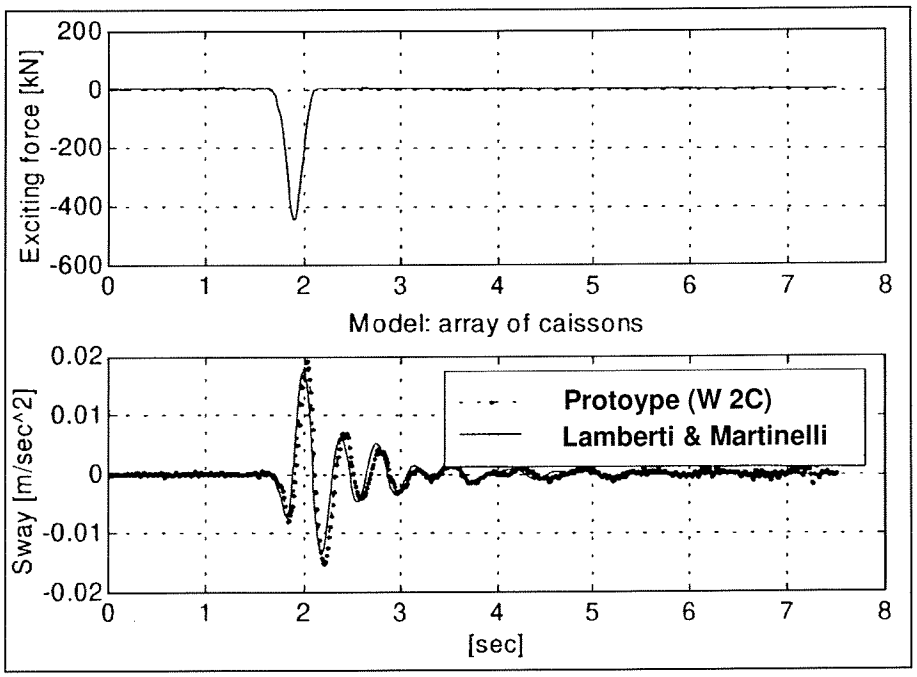

Figure 8-3 Tugboat excitation Genoa Voltri breakwater [Lamberti & Martinelli (1998)]

From this figure the following figures can be extracted,

maximum force = 450 kN
impact duration = 0.45 sec
maximum excitation = 0.018 m/s^2
minimum excitation = 0.013 m/s^2

Implementing the force from figure 8-3 in the dynamic model should result in a similar shape and about the same order of acceleration as the prototype measurements.

This is done by calculating the spring constants and the dashpots according to the previous chapter. The calibrating is done by choosing a damping parameter $D_{interlock}$ so that the shape and value of the response is similar to those in figure 8-3 above. The choice of parameter must not reach any absurd value. The probable values range from 0.1 (little interlocking) to 0.3 (high interlocking). It is probable that this value would be around 0.20.

By iterative calculations the value of the damping parameter $D_{interlock} = 0.14$ with an internal damping of 0.03.

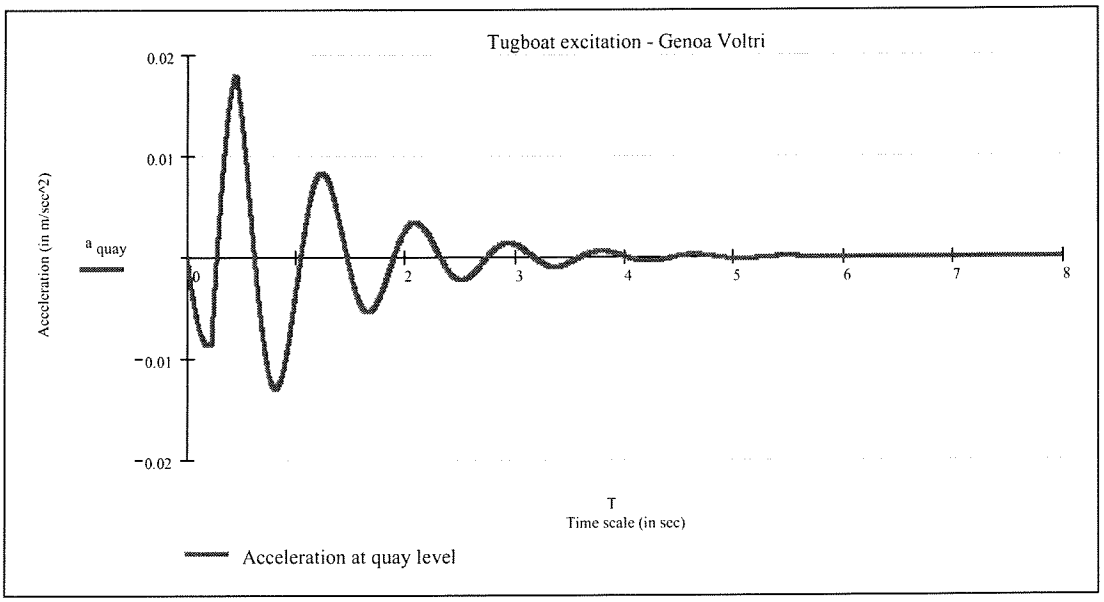

Figure 8-4 Calculation tugboat excitation Genoa Voltri breakwater

8.1.5 Conclusions

From figure 8-4 the conclusion can be drawn that the dynamic model is accurate in both figures as in shape of the excitation. The maximum value of acceleration measured in nature is 0.018 m/s^2, while the MathCad calculation comes up with the same value, 0.018 m/s^2. Also the minimum acceleration (3rd peak) obtained the same value, as in the measurements. Comparison in numbers is given in Table 8-2 below.

Table 8-2 Measured and calculated response to tugboat collision

	measured	calculated
maximum force (kN) (input)	450	-
impact duration (sec) (input)	0.45	-
maximum acceleration (m/s^2)	0.018	0.018
minimum acceleration (m/s^2)	0.013	0.014

Graphic comparison between the measured and calulated response of the dynamic model is visualised in Figure 8-5.

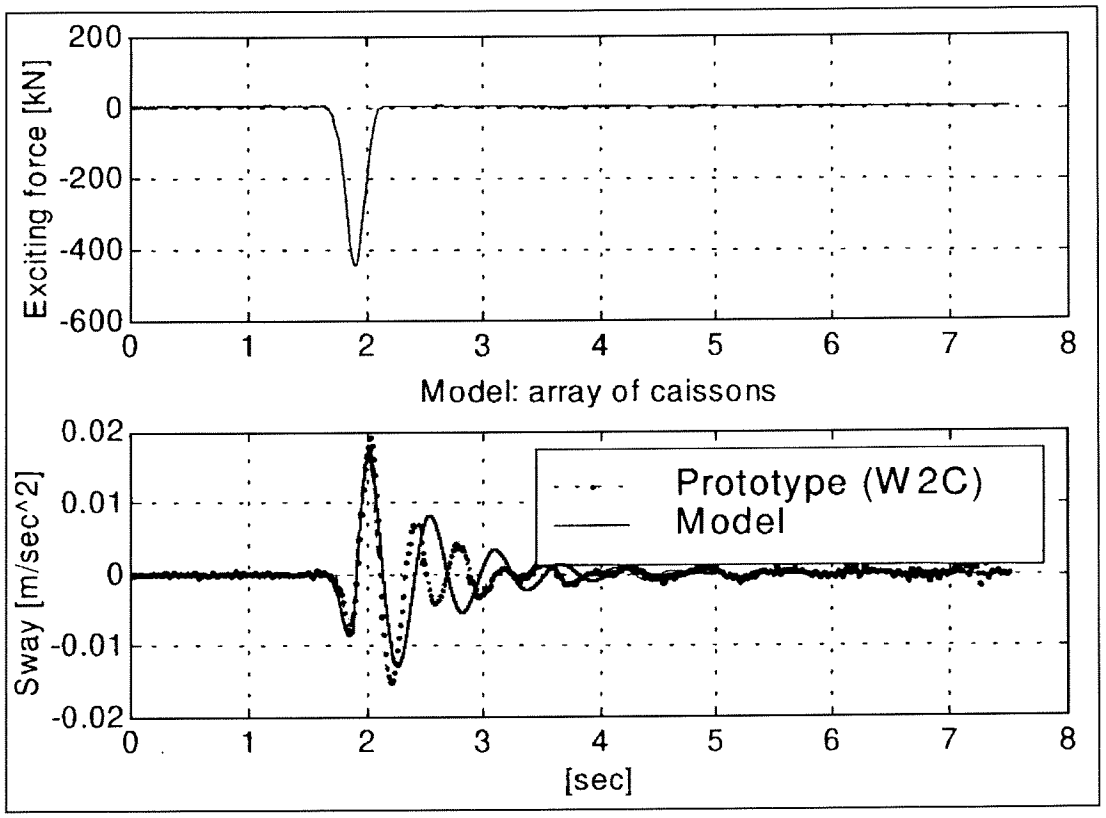

Figure 8-5 Comparison measurements and dynamic model

The acceleration calculated is longer in duration than the measured acceleration. This can be accredited to the fact that the dynamic model does not reckon with the interaction between caissons. The interaction between caissons results in higher energy loss and in a different way than represented with this model as the excitation propagates along the breakwater, therefore reducing the response of the caisson. The reason to this small discrepancy can be explained by not complete modelling of the interlocking phenomenon. Comparison measurements and dynamic model

Conclusions:

1. Good agreement of model as far as acceleration concerned
2. Good shape of response to tugboat collision

9. Calculation response to wave impact

The calculation of wave impact forces with the model derived in the previous chapter. The model is calibrated and can now be used for calculations of the response to wave impacts approximated by the formulae of Schmidt (two formulae) and Klammer, Oumeraci & Kortenhaus.

To be able to evaluate all the different calculations some standard agreements are made to make the evaluation process easier.

- The horizontal displacements are situated in the bottom plate of the caisson. This makes it easier to compare graphs and it also diminishes the possibility for errors. If the horizontal displacements are not situated in the bottom plate, than it is clearly presented at what point the displacement is given.
- The graph presents the data in the format amplitude (displacement or rotation) versus total impact duration. This is also the case with the KO&K (Klammer, Oumeraci & Kortenhaus) formula which uses the input of t_r (instead of t_d)
- The maximum value on the axis of the Excel-graphs will be equal. This makes it easier to compare several graphs.
- In the graph, horizontal lines will appear (referred to as *phi_plmax* and *x_plmax*). These lines represent the area of elastic-plastic behaviour. Above these lines the construction will have a permanent displacement.
- The formula derived by Klammer, Oumeraci and Kortenhaus is referred to as KO&K. The formula derived by Schmidt et al with constant momentum is referred to as Schmidt2.

In order to gain insight in the effect of wave impact loads on a vertical breakwater, the assumption is made that the **waves at the Genoa Voltri breakwater <u>will</u> break and therefore wave impact <u>do</u> occur.**

9.1 Response of the caisson under simple loadings

To gain more insight in the dynamic behaviour of the Genoa Voltri breakwater under wave impact load it is necessary to know what the computer model will do when a certain load scheme is applied to the structure. The properties of the model and its response can only be evaluated thoroughly if the response of the model to a simple force scheme is clearly understood. Therefore two simple force schemes have been applied to the structure.

The first is a constant force with different impact durations. The force is kept constant while the impact duration varies. This scheme is likely to show a maximum amplitude at the first eigenfrequency.

The second scheme is the approach of momentum conservation with different impact duration. The amount of momentum is kept constant while the impact duration will vary, in contrast to the constant force loading scheme where the amount of momentum increases with increasing impact durations. This loading scheme is likely to show a maximum at the smaller impact durations, for the force is much larger and thus will be the response. The response at the eigenfrequency will be small because the force is much smaller than at shorter impact durations.

In Figure 9-1 the response of both loading schemes constant force and momentum conservation are compared.

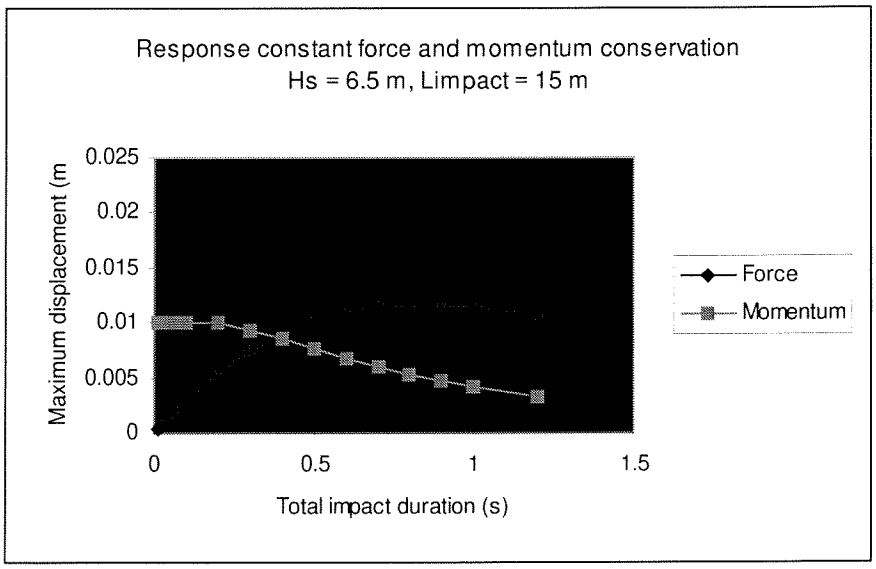

Figure 9-1 Comparison constant momentum and force

Loading scheme : Constant force

As expected, the highest response of the breakwater occurs at the eigenfrequency of the caisson (about 0.8 sec). The amplitude of the caisson is smaller at the shorter impact durations (about 0.1 sec). The reason for this is, the smaller amount of 'energy' (i.e. momentum) the force has when the impact duration (very) short. At longer impact durations (about 1.0 seconds) the amount of energy is large - and increasing. Nevertheless, the amplitude is decreasing from 1.0 to 1.2 seconds. The explanation is that the resonance will decrease as the impact duration differs increasingly from the eigenperiod.

Loading scheme : Constant momentum

The amplitude has a maximum at the short impact durations (about 0.1 sec). With increasing impact duration (longer) the amplitude decreases. There is no increase at impact duration around the eigenperiod (about 0.7 sec). This looks rather awkward, for we have seen with the constant force loading an increase of amplitude around the eigenperiod - not a decrease as observed here. It looks as if damping influences the resonance phenomenon at large scale. This is not true, as shown in the next graph (Figure 9-2).

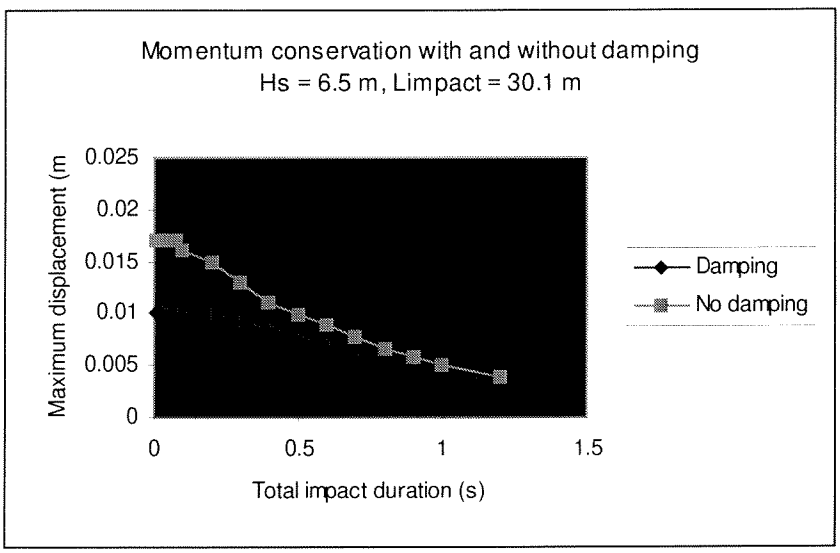

Figure 9-2 Comparison constant momentum with and without damping

Damping only influences the magnitude of the amplitude. The explanation for this behaviour of the computer model (and also in nature) is that the force dominates the amplitude. As the force is high at (very) short impact durations (about 0.1 sec) the amplitude is at its maximum. While the impact duration elongates, the force decreases, thus the amplitude of the caisson decreases.

Figure 9-1 and Figure 9-2 show the displacement as a function of the impact duration. The response of the rotation as a function of the impact durations shows a similar relation as the displacement.

9.2 Calculations of response of the Genoa Voltri breakwater

To gain insight in the response of the breakwater to different wave impacts, multiple impact durations were inserted in the computer model. The maximum horizontal excitation was then calculated and the data inserted in an Excel sheet.
After several runs the final result is the relation of the maximum horizontal displacement versus the impact duration.

To evaluate the calculation results in this stage the boundary between elastic and plastic behaviour of the soil is placed within the graph, resulting in the figure below.

The length of impact on the caisson is given by L_{impact}, approximately 15 meters. The calculation will start by applying the wave impact on the full length of the caisson. The following calculations the reduction of the length of the impact is applied.

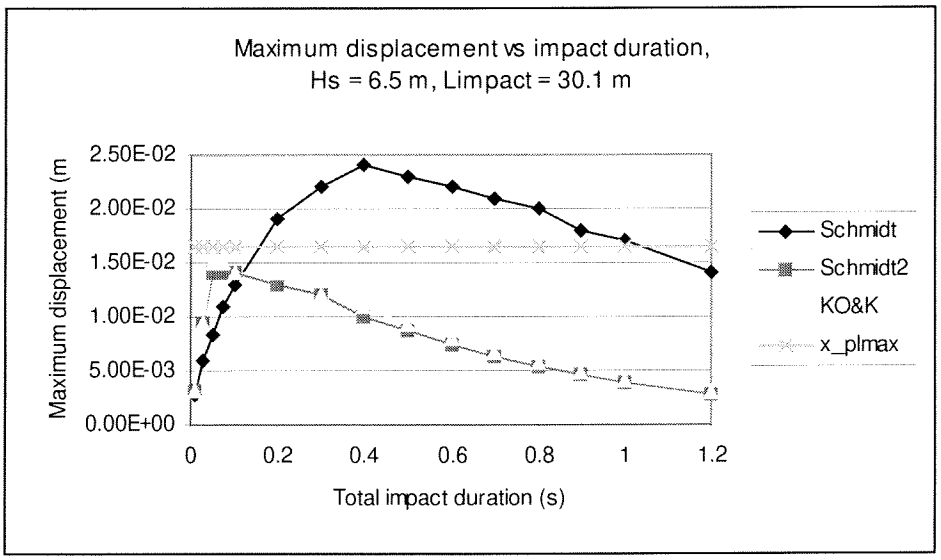

Figure 9-3 Displacement vs impact duration, L_{impact} = 30m

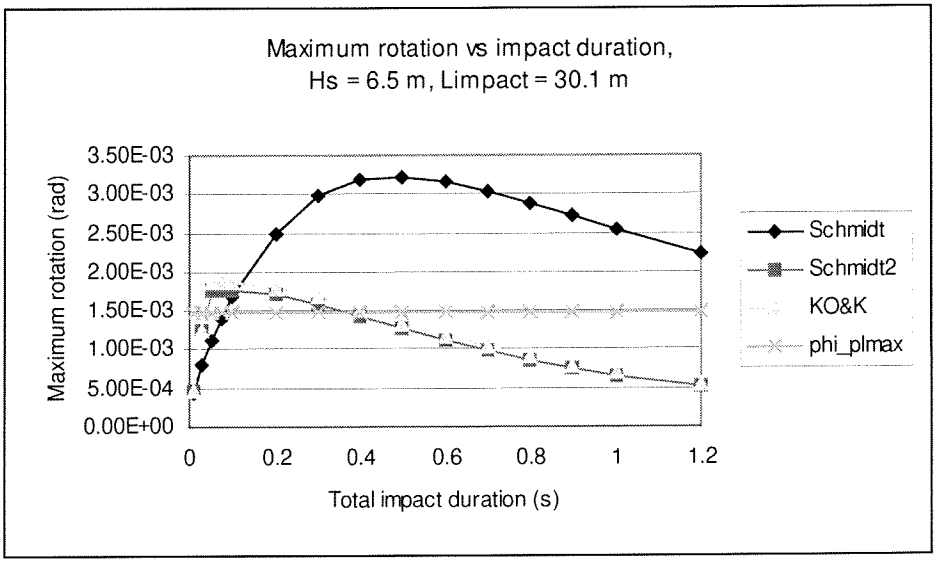

Figure 9-4 Rotation vs impact duration, L_{impact} = 30m

First observation of results :

- The response has its maximum around the eigenperiod (formulae Schmidt) and at around much shorter impact durations (Schmidft2 and KO&K). The reason of the high amplitude at shorter impact duration is the theory of constant momentum, as concluded from the simple loading schemes of constant momentum and constant force.
- Exceeding upper limit soil resistance for sliding and rotation. Little displacements and larger rotations expected according to this computer model.

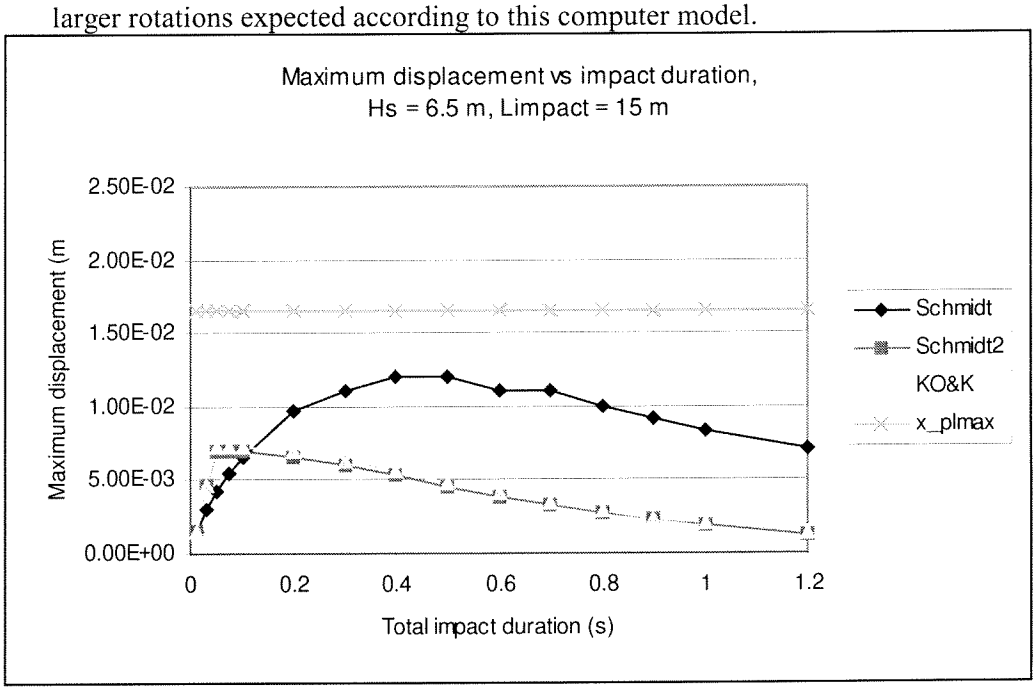

Figure 9-5 Displacement vs impact duration, L_{impact} = 15 m

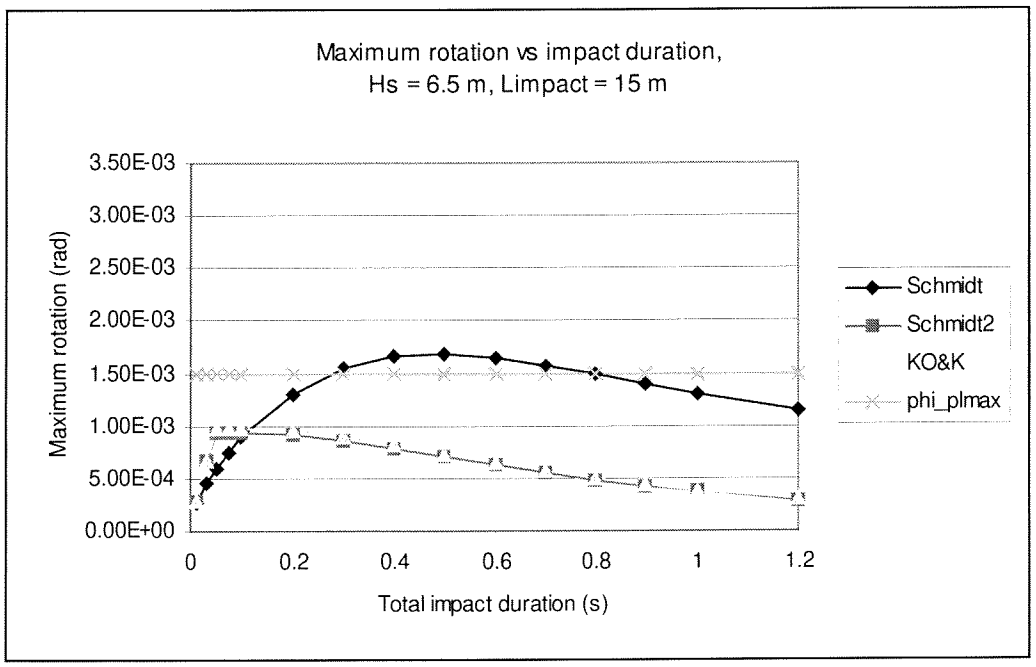

Figure 9-6 Rotation vs impact duration, L_{impact} = 15 m

First observation of results :

- Not exceeding upper limit soil resistance for sliding and rotation.
- Differences between formulae (all three) similar to those at $L_{impact} = 30.1m$.
- Substantial resistance for sliding. Little resistance for rotation. The construction "tends to go through its knees".

9.2.1 General conclusions

Based upon the first results of the computer model the following (general) observations can be made:

1. Resistance of construction for sliding is much larger than for rotation.
2. The place (at what t_d) of the maximum amplitude differs between the three formulae. The formulae based upon the theory of constant momentum (Schmidt2 and KO&K) shows a maximum at short impact durations (about 0.2s), while the formula of Schmidt shows a maximum around the eigenperiod of the construction (about 0.8 s).

Ad 1. Resistance for rotation failure

Based on the calculations, the resistance of construction for sliding is much larger than for rotation. In nature this is not the case, for failure by rotation is always preceded or accompanied by sliding. Several failures of vertical breakwaters in the past show a (horizontal) sliding of the caisson and no rotation, other than in combination with sliding. The calculations made by H.A.T. Vink [1997] show that the caisson tends to "go through its knees" rather than sliding. The computer model derived for this study shows a similar phenomenon. A different approximation of the rubble mound foundation should show a larger resistance for rotation of the caisson, thus showing more coherence with the phenomenon observed in nature.

Ad 2. place of maximum amplitude
According to the input of the simplified loading scheme (constant momentum) the maximum amplitude of the formulae based upon the constant momentum (Schmidt2 and KO&K) will show a maximum at the shorter impact durations. The amount of momentum determines the maximum response. Therefore, when the amount of momentum is known, we can estimate the maximum response of the caisson.
The maximum amplitude of the Schmidt et al formula is at the eigenperiod of the structure (0.8 s). According to the simplified loading scheme of constant force, this is easy understood.

Further investigation will be needed at the subjects of:

1. Resistance for rotation
2. Constant momentum

9.3 Calculation of resistance for rotation.

The observation above about the resistance for rotation of the caisson is assumed to be not normative for failure. Therefore a rather rough approximation is applied to the Genoa Voltri breakwater. The rubblemound foundation is assumed be strong enough the withstand rotational and sliding forces. The caisson and the rubblemound foundation will therefore be schematised as a rigid body. In figure 9-7 a sketch is drawn to schematised the modelling.

Sketch	Description	Approximations
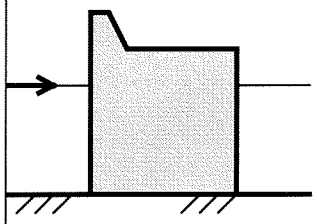	Caisson placed directly on sub-soil	• Conservative modelling of soil properties • Low resistance for rotation
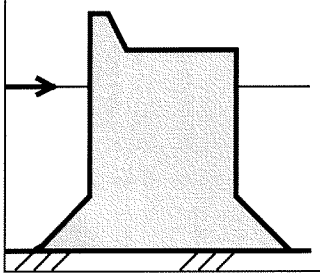	Caisson and rubblemound foundation schematized as rigid body	• Better modeling of soil forces • Rotation forces better modelled • Rigid body as whole doesn't exist in nature

Figure 9-7 Sketch modelling soil and caisson properties

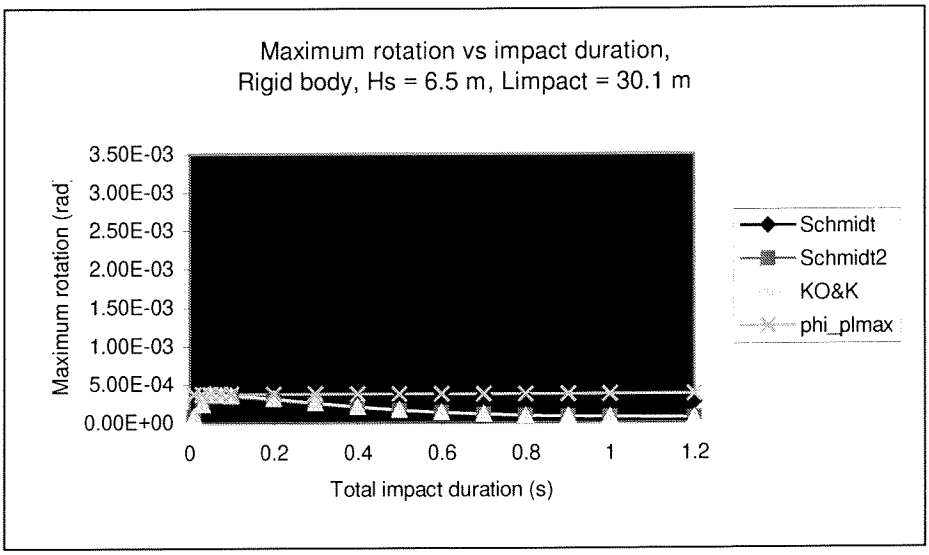

Figure 9-8 Rotation vs impact duration, caisson with rubblemound foundation

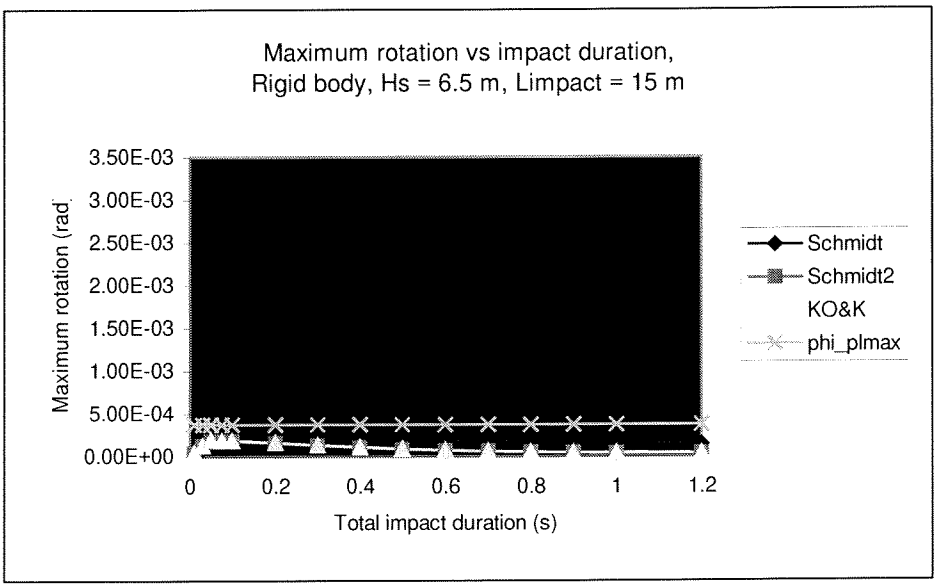

Figure 9-9 Rotation vs impact duration, caisson with rubblemound foundation

The resistance for rotation is substantial when applying the reduction of $L_{impact} = 15\ m$.

9.4 Theory of momentum conservation

The wave impacts upon a vertical structure like the Genoa Voltri breakwater have a higher peak at the shorter impact durations, while at the longer impact durations the impact force is lower. This phenomenon seems to justify the assumption that the momentum of a wave impact is constant. The vertical wall has to stop or reflect the same amount of water at both impacts (at shorter and longer impact durations).
The theory of constant momentum is examined with a dataset acquired from the LWI dataset through Pieter van Gelder.

From the variables the force and the time can be calculated with dimension. The momentum of the wave impact is calculated and presented in a graph for evaluation.

$$t_d = t_d^* \cdot \sqrt{\frac{d_{eff}}{g}} \qquad 9\text{-}33$$

$$F_h = \rho_w g H_b^2 \cdot F_h^* \qquad 9\text{-}34$$

with,
t^*_d = dimensionless impact duration
F^*_h = dimensionless impact force

Analogue with t_r .

The momentum will be calculated with the following formula. Note that the momentum does not depend on t_r .

$$I_{tot} = \tfrac{1}{2} F_{h\max} \cdot t_d \qquad 9\text{-}35$$

with,
F_{hmax} = maximum horizontal impact force

For examining purposes the dataset is printed on axis t_d versus I_h (see Figure 9-10).

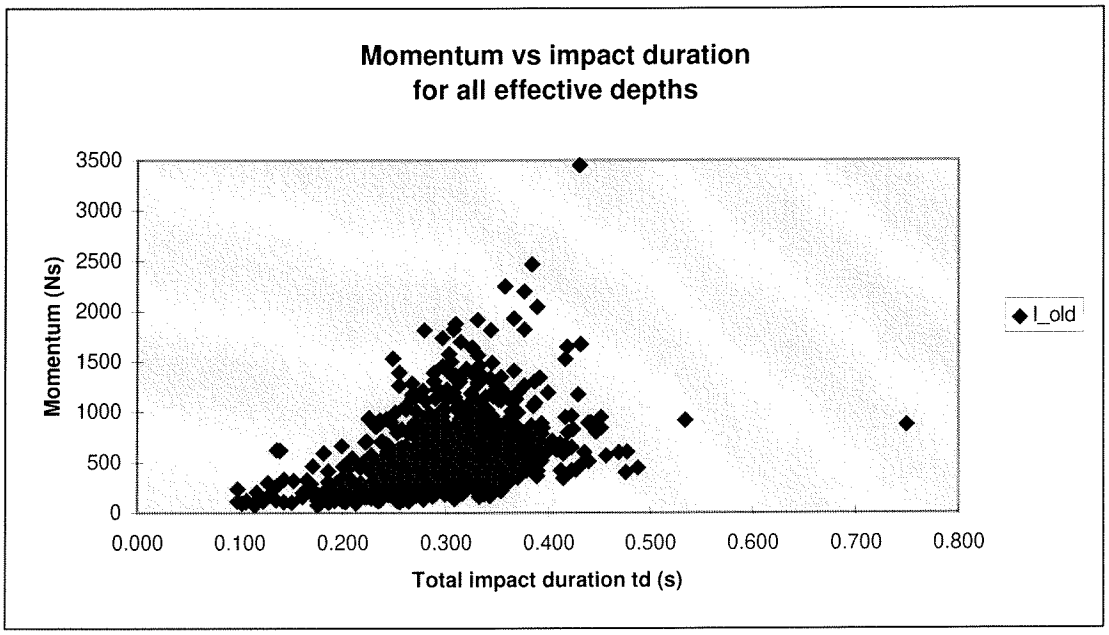

Figure 9-10 Momentum scattered dataset LWI 1-2

At first the scatter of the data seem to be rather wide. A closer look will reveal an average of momentum at about 500 Ns. Also the momentum seems to increase at increasing impact duration. In Figure 9-11 the distribution of the dataset is shown.

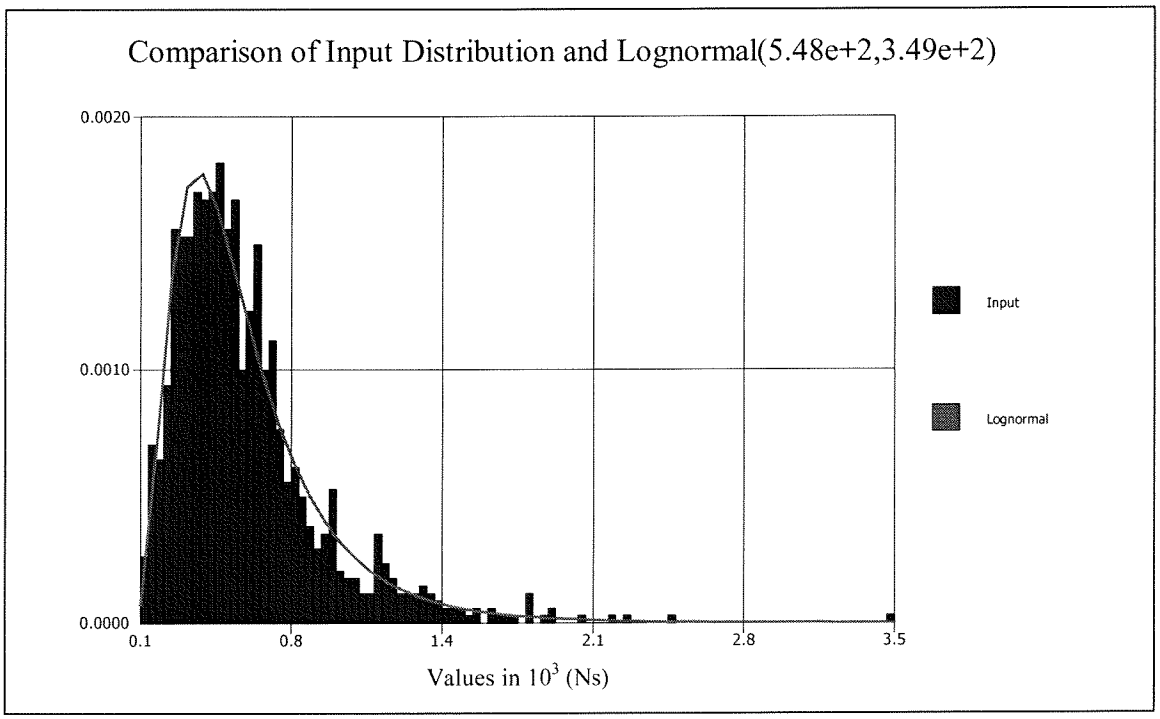

Figure 9-11 Distribution of momentum of dataset, all effective depths

The statistics of the distribution of the dataset is shown in Table 9-1. The dataset is a collection from several effective depths, ranging from 0.06 m to 0.62 m. The largest amount of data-points is at $d_{eff} = 0.43\ m$. In the Table 9-1 also the statistics of the data at $d_{eff} = 0.43\ m$ is given.

Table 9-1 Statistics LWI dataset (note d_{eff}!)

	t_d (s)	I_{old} (Ns)	I_{new} (Ns)	t_d (s)	I_{old} (Ns)	I_{new} (Ns)
Average	0.283	511	541	0.304	535	568
Stdev	0.096	360	384	0.061	321	347
Kurtosis	3.25	6.82	5.72	4.49	4.10	3.98
Skewness	-1.49	1.80	1.72	0.14	1.70	1.69
d_{eff} (m)	**all**	**all**	**all**	**0.43**	**0.43**	**0.43**

From the dataset it can be concluded that the total dataset represents the set with $d_{eff} = 0.43\ m$ rather well, i.e. there is no significant difference.

The next table shows that the momentum is not constant. In fact the total amount of momentum impinging on a vertical wall increases, when the impact duration increases.

Table 9-2 Increase of total momentum with increasing impact duration

t_d (s) =	0.00 - 0.20		0.21 - 0.30		0.31 - 0.40		0.41 - xx	
	I_{old}	I_{new}	I_{old}	I_{new}	I_{old}	I_{new}	I_{old}	I_{new}
Average	**231**	**248**	**470**	**499**	**616**	**653**	**837**	**875**
Stdev	139	144	288	311	344	369	545	562
Kurtosis	2.77	2.22	2.74	2.61	4.85	4.58	14.59	11.68
Skewness	1.67	1.53	1.50	1.46	1.94	1.90	3.38	3.03

The data set shows a remarkable phenomenon. The impacts at short impact durations are absent in the dataset. This is awkward, for the wave impact is likely to occur at short impact durations.
The second observation is that the impact rise time in proportion to the total impact duration is small. Expected values of 0.3 to 0.65 are not reached in the dataset. The average is about 0.15 s (with standard deviation of 0.09 s). The reason could be in the definition of the total impact duration. An example of a force time diagram is given in the figure below. The definition of the time impact duration can be made in many ways.

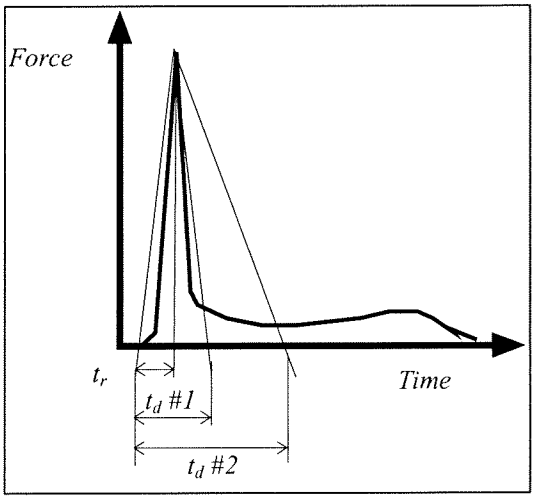

Figure 9-12 Definition of total impact duration

Important is to realise that the wave impact is schematised as a triangular load. The impact duration t_r is rather simple, from zero to maximum impact force. The total impact duration is more difficult to determine. At what time is the impact force ended as impulsive load and started as a quasi-static load?

In the dataset the total impact duration is defined as start of impact force until the lowest force after the peak (t_d *#2*). When defining the wave impact load as above the wave impact load scheme as a triangular force is not correct, for the impact load in nature has a smaller momentum as the schematised load.
Also when schematising the impact load as t_d *#2* the absence of impact loads at short impact durations is clear. The impact loads are longer than when defining the impact loads as t_d *#1*.

To show the difference between the t_d from the dataset and another t_d (calculated from $t_r/0.3$), compare the graph below with Figure 9-10. Note that the scales at the axis are similar.

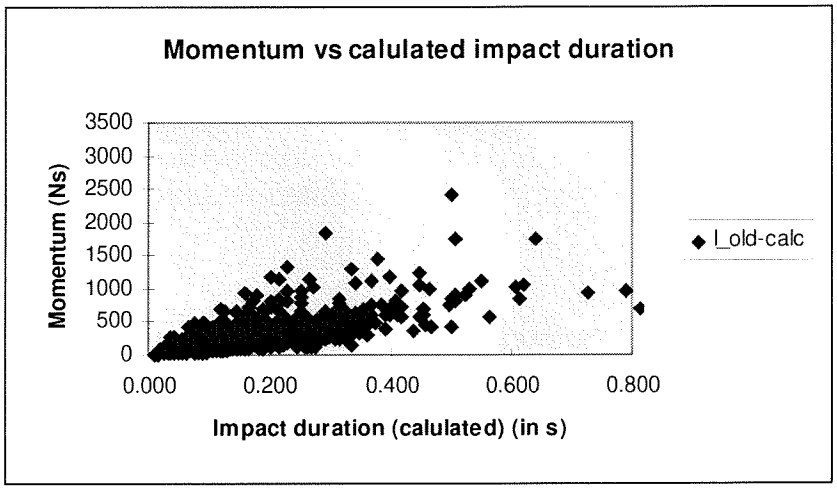

Figure 9-13 Momentum vs calculated total impact duration

9.4.1 Conclusions dataset

In search of a resemblance with the theory of constant momentum, the dataset LWI 1-2 was used. The graphs, distributions and statistical values have given enough matter to draw the following conclusions.

According to the dataset:

1. The total amount of momentum increases at increasing impact duration. The increase (decrease) of momentum is substantial.
2. There are little or no impact forces (and momentum) at short impact durations (<0.15 s). This can be accounted for the definition of total impact duration, that results in very large impact durations.
3. The impact rise time in proportion to the total impact duration is small (about 0.15 s), not at all in the range of the expected 0.3 s to 0.65 s.

General conclusions:

1. The importance of correct defining of the total impact duration, especially when the schematised triangular impact load is used, is essential for the evaluation of impact forces and momentum.
2. The theory of constant momentum seems not to be justified according to the dataset LWI 1-2. The dataset shows an increase of momentum at increasing impact duration.

10. Conclusions and recommendations

This chapter deals with the final conclusions, most important results and recommendations of this graduation study. Throughout the whole report interim conclusions and recommendations have been drawn from:

1. A study of current used formulae
2. Investigation of the time duration of wave impacts on a vertical breakwater
3. Calculation of the response of the Genoa Voltri breakwater to wave impacts

10.1 Results

In this section the results of previous chapters are summed up. The results are presented in 'Response of the Genoa Voltri breakwater', 'LWI-dataset' and 'Wave impact load', and will be used to draw the final conclusions in the next section.

10.1.1 Response of the Genoa Voltri breakwater

The response of the Genoa Voltri breakwater to wave impacts have been calculated with a spring-dashpot model. The calibration of the model has been done with full-scale measurements of the response to a tugboat impact. See chapter 6 and 8.
The wave impact loads are estimated with modern formulae which differ the wave impact to impact duration (t_d) and maximum impact force ($F_{h,max}$). The results are presented in chapter 9.

- **Maximum response**

According to the input of the loading scheme (triangular force diagram) the maximum amplitude of the formulae based upon the theory of momentum conservation (Schmidt2 and KO&K) will have its maximum at very short impact duration.
The amount of momentum determines the maximum response at short impact duration. Therefore, in theory, when the amount of momentum is known, we can estimate the maximum response of the caisson. This applies only when the theory of momentum conservation is applicable. In nature full-scale effects such as aeration will influence the magnitude and the duration of the impact, and thus reducing the applicability of the theory of momentum conservation. The results of the evaluation of the LWI-dataset show that the theory of momentum conservation is not applicable.
The maximum amplitude of the Schmidt et al formula is around the Eigenperiod of the structure (about 0.6 s). The formula of Schmidt et al is purely based upon a datafit of model tests.

- **Resistance for rotation failure**

Based on the estimations of the computer model, the resistance of construction for sliding is much larger than for rotation. In nature this is not the case, for failure by rotation is always preceded or accompanied by sliding. Several failures of vertical breakwaters in the past show a (horizontal) sliding of the caisson and no rotation, other than in combination with sliding. The calculations show that the caisson tends to "go through its knees" rather than sliding. A different approximation of the rubble mound foundation shows a larger resistance for rotation of the caisson, thus showing more agreement with the phenomenon observed in nature.

- **Wave breaking at Genoa Voltri breakwater**

There is no wave breaking in front of the Genoa Voltri breakwater. Prediction of impacts [Calabrese & Allsop 1997] and formulae for wave breaking [Miche, CUR 169] show that incoming waves shall not break. The water in front of the Genoa Voltri breakwater is too deep.

10.1.2 LWI 1-2 dataset

- **Conservation of momentum**

The total amount of momentum increases at increasing impact duration. The increase (decrease) of momentum is substantial. Therefore it can be concluded that the theory of conservation of momentum is not applicable according to the dataset.

- **Impact duration**

There are little or no impact forces (and momentum) at short impact duration (<100 msec). Also the impact rise time in proportion to the total impact duration is small (about $0.15 \times t_d$), not at all in the range of the expected 0.3 to $0.65 \times t_d$ [Schmidt 1992]. This can be accounted for an incorrect used definition of total impact duration, which results in very long impact duration.
When defining the total impact duration, the duration is not allowed to elongate by definition without carefully research why that definition should be used and if that definition is justifiable. The danger of the use of such a wrong definition is that when applying a simple triangular load upon a vertical breakwater, the user runs the risk of overestimating the wave impact load in a very conservative way, resulting in a very expensive breakwater. A better way to evaluate the (measured) impact duration is shown in the Figure 10-1.

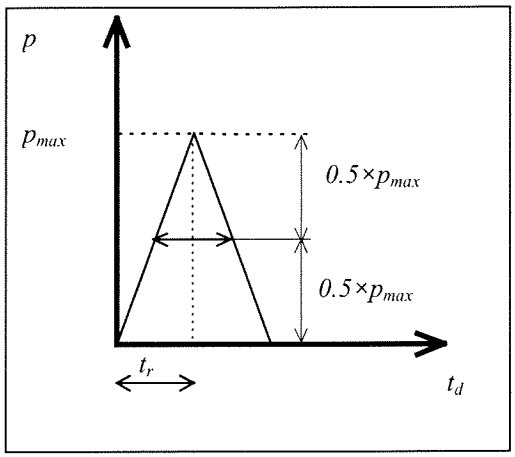

Figure 10-1 Suggested definition of impact duration T½

10.1.3 Wave impact load

The wave impact consists of two variables: the maximum impact load and the impact duration (t_r and t_d). The impact duration is very important to the maximum reponse of the vertical breakwater, for when the impact duration (t_d) is similar to the Eigenfrequency of the structure the reponse will reach a maximum.

The duration of the impact pressure at a vertical breakwater is much shorter than assumed in the latest formulae (Schmidt et al and KO&K). The impact duration is about 20 to 100 msec, with an average of about 20-40 msec.

The results of full-scale measurements of bow flare slamming and wave impact at the Dieppe breakwater [Bagnold 1939] are given below;

- The analogy of the bow flare impact and the wave impacts on a vertical wall is justified, for the full-scale measurements of bow-flare slamming and the full-scale measurements at Dieppe [Bagnold 1939] show large similarity in maximum pressure and impact duration.

- The duration of the impact pressure at a vertical breakwater is much shorter than assumed in the latest formulae (Schmidt et al and KO&K). The impact duration is about 20 to 100 msec, with an average of about 20-40 msec.

- The maximum impact pressure is about 500 to 650 kPa.

- The scatter of maximum impact pressure found at wedge tests (model scale) and bottom slamming tests (also at model scale) show large scatter. Therefore is justified to reduce the width of the wave impact. The high impact pressures do occur, but are local.

10.2 Final conclusions

The objective of this graduation project is:

"To gain more insight in the time duration of wave impacts and investigate whether these wave impacts have a significant influence on the overall stability of the vertical breakwater."

To answer the first question we have to take a look at the results of the evaluation of the full-scale measurements of bow flare slamming and wave impact on a vertical wall at Dieppe. The duration of the impact pressure at a vertical breakwater is much shorter than assumed in the latest formulae (Schmidt et al and KO&K). The impact duration is about 20 to 100 msec, with an average of about 20-40 msec.

To answer the second question we have to look at the response graphs of chapter 9, which show the maximum response of the Genoa Voltri breakwater to the wave impact load of Schmidt and Klammer, Oumeraci and Kortenhaus. These formulae don't have any limitation of impact pressure above an impact duration of 100 msec. According to the answer of the first question (impact duration) we see that the impact duration is shorter than 100 msec, therefore the response of the breakwater above 100 msec is highly unlikely to occur.

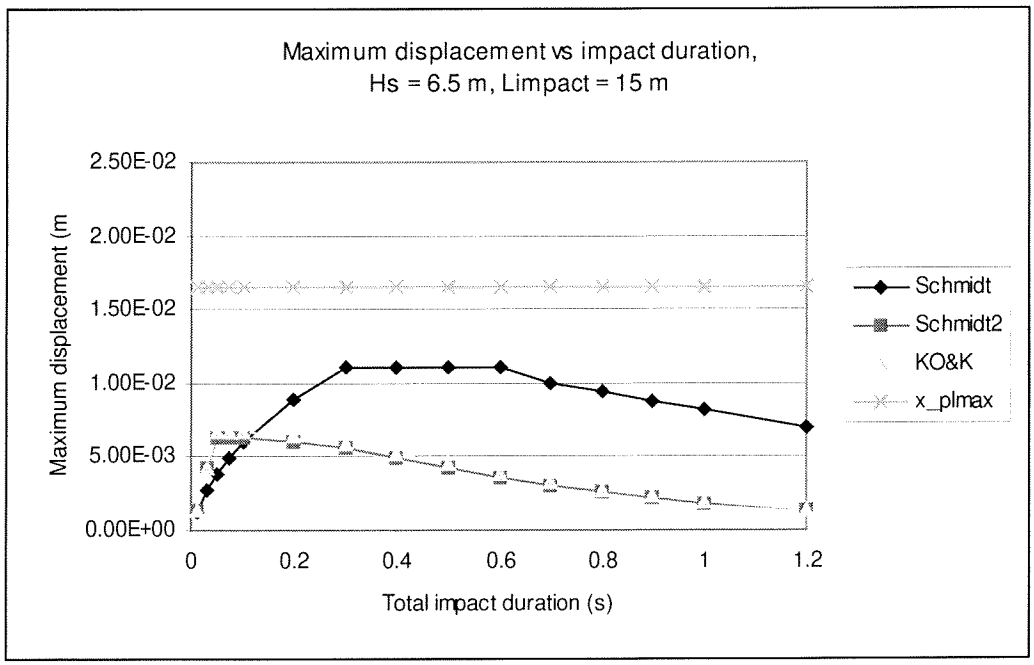

Figure 10-2 Displacement vs impact duration, Limpact = 15 m

As is visualised in Figure 10-2 we can see that the formula of Schmidt, which is not based upon the theory of momentum conservation has its maximum, has its maximum response at the Eigenfrequency of the caisson. Therefore, knowing that the wave impacts don't occur at impact duration above 100 msec, the wave impacts won't influence the overall stability of the vertical breakwaters.

As is visualised in Figure 10-2 we can see that the formulae based upon the theory of momentum conservation (i.e. formulae of Schmidt2 and Klammer, Oumeraci and Kortenhaus) have their maximum response at short impact duration (i.e. about 100 msec). The response of the Genoa Voltri breakwater is not limited by the impact duration, but by the maximum force applied in the dynamic model. As can be seen in Figure 10-2 the maximum reponse is far below the maximum allowed displacement.
The maximum impact pressure is about 500 to 650 kPa, as could be concluded from full-scale measurements at a vertical breakwater (Dieppe) and bow flare impacts (see chapter 5). This impact pressure doesn't result in response higher than given by the formulae of Schmidt2 and KO&K.
Further the impact width (L_{impact}) can reduce the applied force on the caisson.

Therefore the conclusion can be drawn that the wave impacts are not important for the stability of the Genoa Voltri breakwater, and similar breakwaters in general.

10.3 Recommendations

The recommendations for future research are,

1. Research for scattering of wave impacts (i.e. width of impact, L_{impact}) should be made, for the scattering of wave impact is very large and therefore the width of wave impact (L_{impact}) could be reduced. It is likely that the reduction of impact width is enough to make the impact force too little to have any influence on the overall stability of the breakwater.
2. A better and logical definition of wave impact duration should be made, regarding the modelling of the impact load (triangular shape).
3. The possibility of interlocking of the caissons should be further examined, for the interlocking of the caissons increases the resistance of overall stability.
4. Research for local effects, like the double wave impact peak and air entrapped wave impact, should not be made, awaiting the research for scattering of wave impact load and a better definition of wave impact duration.

Bibliography

Bagnold, R.A. *"Interim report on wave pressure research"* , 1939

Beukelman, W. *"Slamming on forced oscillating wadges at forward speed. Part I: test results"* - Report No. 888, 1991

Curtin, W.G., Shaw, G., Parkinson, G.I., Golding, J.M. *"Structural Foundation Designer's Manual"*, Page 187-197, 1995

Gelder, van P. *"Analysis of wave impact data on vertical breakwaters"* Delft Workshop, 1998

Gerritsma, J.*"Bewegingen en Sturen I, Golven"* (Motion and Steering I, Waves) lecture notes, mt 513 (in dutch) report nr. 473-K , 1994

Japan Shipbuilding Reserach Association, *"Full scale measurement of wave loads and structural response of large ore carrier"* (in Japanese), SR 124, Report 140, 1971

Japan Shipbuilding Reserach Association, *"Full scale measurement of wave loads and structural response of large ore carrier"* (in Japanese), SR 124, Report 152, 1972

Lamberti and Martinelli *"Prototype measurements of the dynamic response of caisson breakwaters"*, 1998

Mizoguchi, S. and Tanizawa, K. *"Impact wave loads due to slamming - A review"* , Ship Technology research, 1996

Nakashima, S., *"Full scale measurement of wave loads on bow flare of large tanker"*, Shipbuilding Engineering 5, 1973

Norwegian Geotechnical Institute, De Groot, Andersen, Burcharth, Ibsen,Kortenhaus, Lundgren, Magda, Oumeraci, Richwien *"Foundation design of vertical breakwaters"* , publication nr. 198, volume 1 (of 2), 1996

Richart, Hall and Woods *"Vibrations of soil and foundations"*, [RHW 1970], 1970

Ochi, M.K., Abramson, H.N., Band, E.G.U., Kawakami, M., Nagai, T., Olsen, H., Schenzle, P., Sluijs, van M.F. *"Slamming and impact"* Report committee II.3, 6th International Ship Structures Congress, 1976

PIANC *"Identification and evaluation of design tools"* draft February 1996, PIANC PTCII, 1996

Radev, D. *"Slamming on forced oscillating wadges at forward speed. Part I: Slamming simulation on penetrating wedges at forward speed"* Report No. 890, 1991

Schulz, K.P. *"Effect of air enclosure on impact load reduction"*, 1992

Suhara, T., Hiyama, H.and Koga, Y. *"Shock pressure due to impact of water jet and response of elastic plates"* Japan Soc. Nav. Arch., 46, (in Japanese), 1973

Tanizawa, K.and Yue, D.K.P. *"Numerical computation of the plunging wave impact"* Soc. Nav. Arch. Japan, 218, (in Japanese), 1992

Verruijt, A. Prof. dr ir *"Offshore Soil Mechanics"*, lecture notes, 1994

Verruijt, A. Prof. dr ir *"Grondmechanica"* (in Dutch) lecture notes B 28, 1996

Vink, H.A.T. *"Wave impacts on vertical breakwaters"*, graduation rapport, 1997

Vulovich, R., Hirayama, T., Toki, N. and Mizuno, H. *"Characteristics of hull stresses measured on a large containership in rough seas"* SNAME Transactions, 1989

Walkden, M.J.A., Hewson, P.J., Bullock, G.N. *"Scaling"* , 1997

Watanabe, I. *"Effects of the three-dimensionality of ship hull on the wave impact pressure"* Journal of the Society of Naval Architects of Japan, 1987